6-1966

The Design and Construction of a Visco Seal Test Facility

Charles Franklin Bowman
University of Tennessee - Knoxville

To the Graduate Council:

I am submitting herewith a thesis written by Charles Franklin Bowman entitled "The Design and Construction of a Visco Seal Test Facility." I have examined the final electronic copy of this thesis for form and content and recommend that it be accepted in partial fulfillment of the requirements for the degree of Master of Science, with a major in Mechanical Engineering.

William K. Stair, Major Professor

We have read this thesis and recommend its acceptance:

Lida K. Barnett, R. L. Maxwell, J. F. Bailey

Accepted for the Council:
Carolyn R. Hodges

Vice Provost and Dean of the Graduate School

(Original signatures are on file with official student records.)

To the Graduate Council:

I am submitting herewith a thesis written by Charles Franklin Bowman entitled "The Design and Construction of a Visco Seal Test Facility." I recommend that it be accepted for nine quarter hours of credit in partial fulfillment of the requirements for the degree of Master of Science, with a major in Mechanical Engineering.

Major Professor

We have read this thesis and recommend its acceptance:

Accepted for the Council:

Dean of the Graduate School

THE DESIGN AND CONSTRUCTION OF A VISCO SEAL TEST FACILITY

A Thesis

Presented to

the Graduate Council of

University of Tennessee

In Partial Fulfillment

of the Requirements for the Degree

Master of Science

by

Charles Franklin Bowman

June 1966

ACKNOWLEDGMENT

The author would like to express his appreciation to Professor William K. Stair for his guidance and assistance in the preparation of this thesis. The assistance of Robert H. Hale, an active participant in this project, is gratefully acknowledged. Sincere appreciation is also extended to my wife, Nancy P. Bowman, for her assistance in the preparation of this thesis for publication. The work described in this thesis was supported in part by the National Aeronautics and Space Administration under Grant NSG-587.

TABLE OF CONTENTS

LIST OF TABLES

LIST OF FIGURES

FIGURE PAGE

LIST OF SYMBOLS

Symbol	Description	Units
English Alphabet		
A	Area	$inch^2$
a	Axial length across land	inch
b	Axial length across grooves	inch
c	Clearance	inch
D	Major screw diameter	inch
F	Body force	pound
h	Groove depth	inch
L	Effective seal length	inch
p	Pressure	p.s.i.
q	Power loss	Btu./second
R	Major screw radius	inch
Re	Reynolds number	dimensionless
t	Time, $\tan\alpha$	second, dimensionless
U	Surface velocity	inch/second
u	Velocity in the η direction	inch/second
v	Velocity in the ξ direction	inch/second
w	Velocity in the z direction	inch/second
x	Displacement, coordinate	inch, dimensionless
y	Coordinate	dimensionless
z	Coordinate	dimensionless

LIST OF SYMBOLS (Continued)

Symbol	Description	Units
Greek Alphabet		
α	Helix angle	degrees
β	(h + c)/c, active arc	dimensionless degrees
γ	b/(a + b)	dimensionless
η	Coordinate	dimensionless
Λ	Sealing coefficient	dimensionless
μ	Viscosity, coefficient of friction	pound-second/inch^2, dimensionless
ξ	Coordinate	dimensionless
ρ	Density	pound-second^2/inch^4
τ	Shear stress	p.s.i.
Φ	Dissipation function	dimensionless
ϕ'	Dissipation function for Couette flow	dimensionless
ϕ''	Dissipation function for Poisseuille flow	dimensionless
Ψ	Sealing coefficient	dimensionless
Subscripts		
A	Asanuma	
c	Clearance	
g	Groove	
L	Laminar	
M&M	McGrew and McHugh	

LIST OF SYMBOLS (Continued)

Symbol	Description	Units
o	Of the plate	
p	Relative to the plate	
r	Land (major screw radius)	
S	Stair	
s	Relative to the surface	
T	Turbulent	
x	In the x direction	
y	In the y direction	
z	In the z direction	
η	In the η direction	
ξ	In the ξ direction	

LIST OF SYMBOLS (Continued)

Symbol	Description	Units
Greek Alphabet		
α	Helix angle	degrees
β	$(h + c)/c$, active arc	dimensionless degrees
γ	$b/(a + b)$	dimensionless
δ	Beam deflection, displacement of sleeve axis	inch, inch
ϵ	Strain	inch/inch
η	Coordinate	dimensionless
θ	Pad location angle, slope of beam	degrees degrees
Λ	Sealing coefficient	dimensionless
μ	Viscosity, coefficient of friction	pound-second/inch^2 dimensionless
ξ	Coordinate	dimensionless
π		dimensionless
ρ	Density	pound-second^2/inch^4
σ	Stress	p.s.i.
τ	Shear stress	p.s.i.
Φ	Dissipation function	dimensionless
ϕ'	Dissipation function for Couette flow	dimensionless
ϕ''	Dissipation function for Poisseuille flow	dimensionless
ψ	Sealing coefficient	dimensionless
Ψ	Angle of contact	degrees

LIST OF SYMBOLS (Continued)

Symbol	Description
Subscripts	
A	Asanuma, aluminum
c	clearance
g	Groove
H	Horizontal
HB	High-speed belt
L	Laminar
LB	Low-speed belt
M&M	McGrew and McHugh
o	Of the plate
P	Pad
p	Relative to the plate
R	Recess
r	Land (major screw radius)
S	Stair, steel
s	Relative to the surface
SE	Effective sill
T	Total
V	Vertical
x	In the x direction
y	In the y direction
z	In the z direction

LIST OF SYMBOLS (Continued)

Symbol	Description
η	In the η direction
ξ	In the ξ direction

INTRODUCTION

The visco seal is a device that provides a means of sealing a rotating shaft passing through a bulkhead wall, thereby establishing a pressure gradient across the wall. The operation of the visco seal (also called threaded seal, spiral groove seal, and viscosity pump) is based on a momentum exchange principle through viscous shear.

Consider two flat plates separated by a liquid (Figure 1). As the plate moves across the liquid, it transmits momentum to the molecules of liquid adjacent to the plate. These molecules in turn collide with other molecules, which continue the process of collision in which each molecule conveys to the next molecule less momentum than was transmitted to it. As a result, the velocity of the molecules in contact with the moving plate is equal to that of the plate, and the velocity of molecules at the stationary surface is zero. For Newtonian fluids the velocity of the fluid between the two surfaces has been experimentally found to be directly proportional to the distance from the fluid element to the stationary surface when the flow is laminar and no pressure gradient is present (see Figure 1).

The momentum which impels the molecules to motion must be transmitted from the plate, and if no external force is applied to the plate its motion will eventually cease when all its momentum is transmitted to the fluid. It is clear, therefore, that the fluid exerts a force on the plate, and this force per unit area of the plate is known as viscous shear. Within certain limits shear in rigid bodies is proportional to

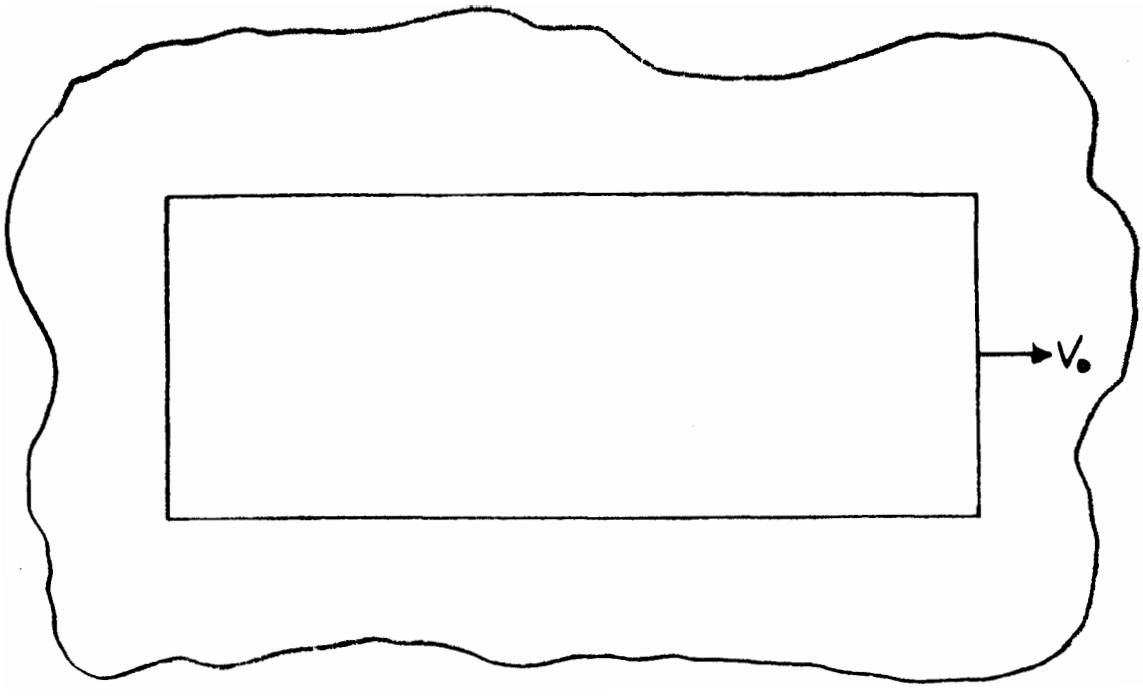

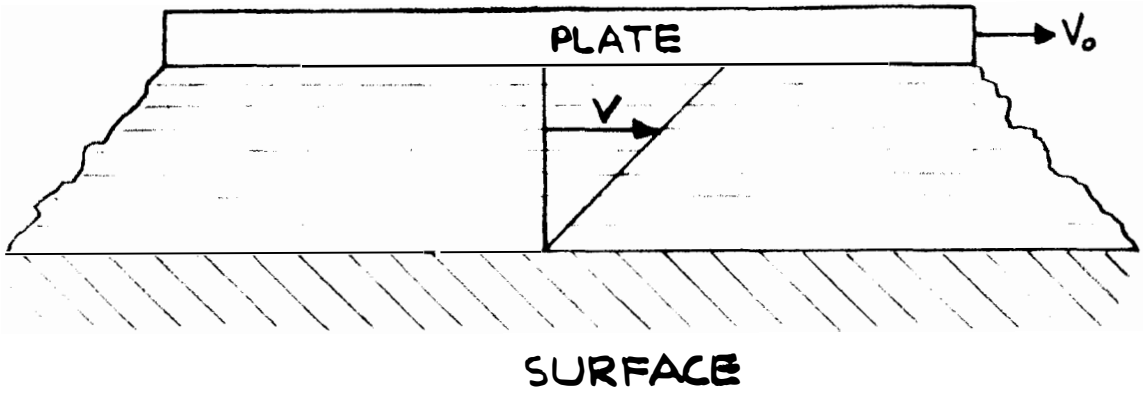

V_o - VELOCITY OF PLATE
V - VELOCITY OF FLUID

Figure 1. Velocity profile for moving flat plate.

the deformation of the body under either static or dynamic loading. The shear within a fluid, however, exists only under dynamic conditions, and the shear stress for Newtonian fluids is proportional to the rate of deformation of the fluid:

$$\tau = \mu \frac{dv}{dX} \tag{1}$$

The constant of proportionality is called the viscosity of the fluid. In order for the plate to continue to move across the fluid at a constant velocity it must be acted upon by a force in the direction of the motion V_o, which is equal in magnitude to the viscous shear times the area of the plate.

Consider now a plate which has raised grooves on the side in contact with the liquid (see Figure 2) and is assumed infinite in the direction of motion V_o. As the plate moves, momentum is transferred to the fluid causing it to move with a certain velocity. Since very little of the liquid can pass between the fixed surface and the raised or "land" part of a groove on the plate, the greatest part of the fluid travels up the root of the groove and passes out from under the plate at the top edge.

The plate and surface shown in Figure 2 may be approximated by a threaded shaft and a smooth cylindrical cavity (see Figure 3) if the diameter of the shaft is large in comparison to the distance between the plate and surface. As the shaft rotates, the fluid between the shaft and cylinder walls is forced up the shaft and out the end at the process side in a motion similar to that shown in Figure 2. If

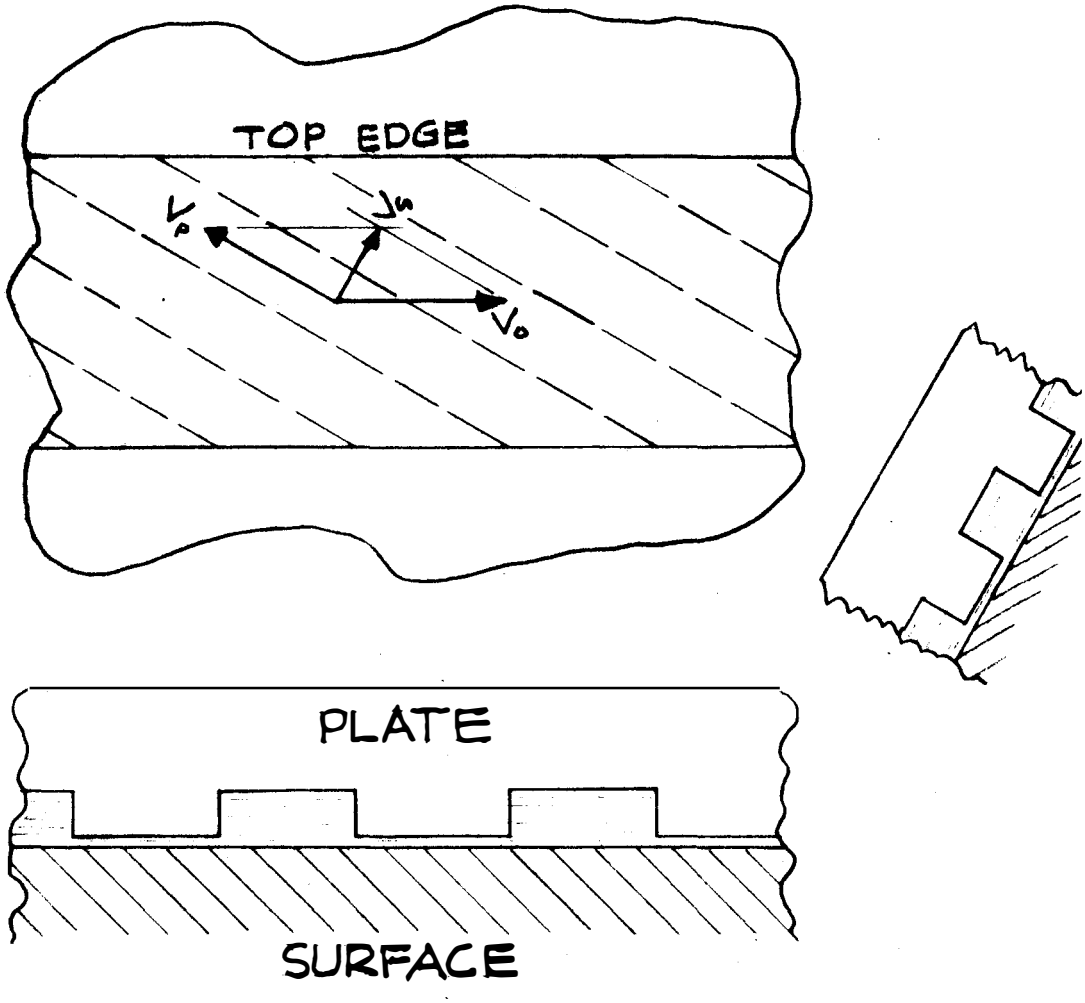

V_s - VELOCITY OF FLUID RELATIVE TO THE FIXED SURFACE

V_p - VELOCITY OF FLUID RELATIVE TO THE MOVING SURFACE

Figure 2. Grooved flat plate

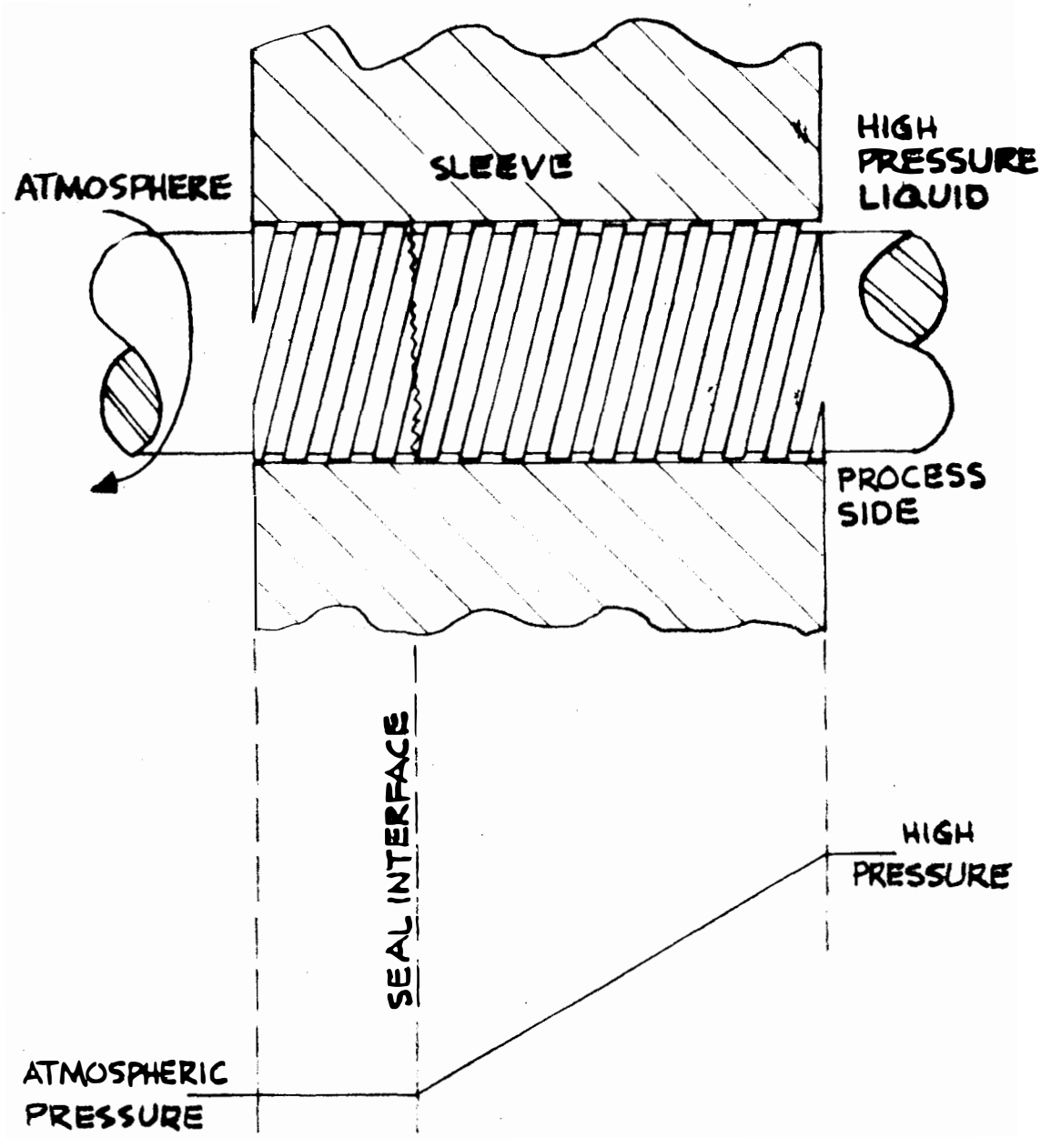

Figure 3. Single-directed visco seal.

pressure exerted on the fluid at the end of the shaft will not allow the fluid to escape at the end, a pressure gradient is established which ranges from the high pressure at the process end of the shaft to atmospheric pressure at the other end. If the rotation of the shaft generates sufficient pressure in the fluid to equal the fluid pressure at the process end, no sealant fluid is lost out the atmospheric end, and a seal is provided. It should be noted that power is dissipated when the shaft speed is held constant due to the torque required to overcome the viscous shear.

The visco seal is often designed with two oppositely directed grooves between which the sealant is injected (see Figure 4). By this arrangement, one side of the seal undergoes a pressure drop from that at the sealant inlet to the high-pressure side of the bulkhead, and the other side of the seal undergoes a pressure drop from that at the sealant inlet to the low-pressure side of the bulkhead. The pressure developed by the seal at the sealant inlet must, therefore, be greater than the pressure on either side of the bulkhead.

The visco seal has a long life, provides virtually perfect sealing, and requires very little make-up sealant fluid. It is applicable in many instances where a gas under pressure is prone to leak down a shaft extending out of a pressurized area. An example of this situation is when a space vehicle must maintain an ambient cabin pressure with various rotating shafts projecting into a vacuum. Another example is in gas- or liquid-cooled reactors, where long maintenance-free

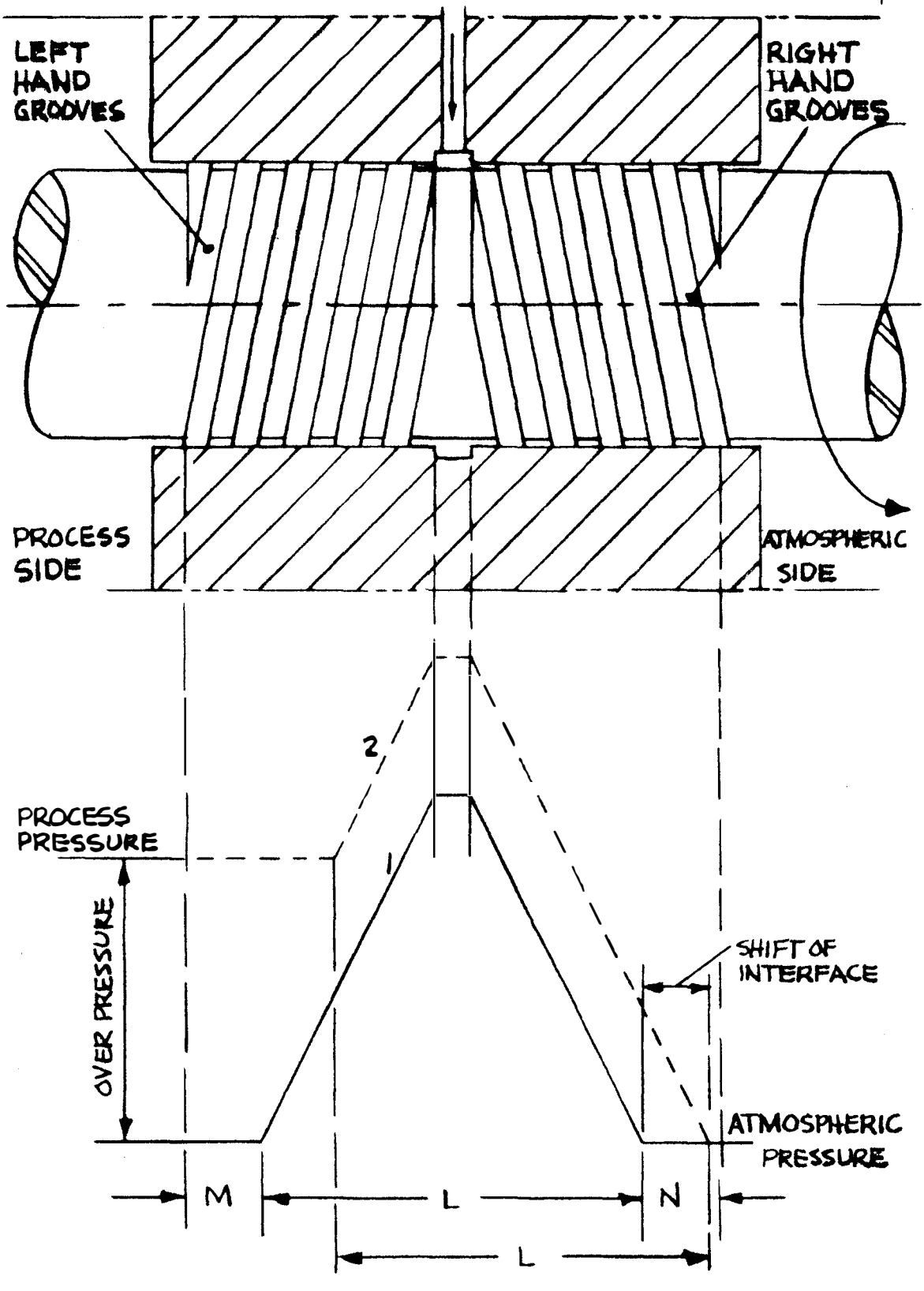

Figure 4. Double-grooved visco seal.

life is important. The visco seal is also applicable in gas turbines, where very high shaft speeds may not permit long-term utilization of mechanical seals.

There are several disadvantages inherent to the visco seal. The simplified seal is effective only when the shaft is rotating and rotating in the proper direction. The visco seal, like some other types of seals, sometimes requires an auxiliary sealant system. Proper design may compensate for these disadvantages or eliminate them completely.

CHAPTER I. SURVEY OF LITERATURE

A survey of the literature patterned after a more comprehensive work by Stair (1)* is presented in this chapter. In addition, literature published since the report by Stair is also surveyed.

A screw viscosity pump capable of maintaining pressures of 1000 pounds per square inch (hereafter designated p.s.i.) was exhibited in 1920 by Sir John Dewrance. After seeing this model, Rowell and Finlayson (2,3) presented an analysis of a screw viscosity pump for laminar flow. They developed an equation representing the flow rate from the pump as a function of the thread dimensions, length of the threaded section, relative surface velocity, and fluid viscosity. The most important simplifying assumption made was that the clearance between shaft and sleeve was zero. The pressure developed for a given shaft and speed was found to be greatest at the shut-off head. While the problem of energy dissipation due to viscous friction was not discussed, the use of a cooling jacket was considered an essential part of the pump for maximum pressure development.

In 1951 Asanuma (4) presented a theoretical study of the visco seal with an approach somewhat similar to that of Rowell and Finlayson, except for less restrictive assumptions. Asanuma's equation for laminar flow is

$$\Delta p = S\frac{6\mu VL}{c} . \qquad (2)$$

The factor S in Asanuma's equation is dependent on screw thread geometry.

*Numbers in parentheses refer to similarly numbered references in LIST OF REFERENCES.

In Asanuma's analysis he shows that the theoretical seal performance under laminar conditions could be maximized by selecting the screw thread geometry as follows:

1. The width of the thread should be as narrow as possible.
2. The ratio of groove width to depth (a/h) should be five to ten.
3. The value of β should be between six and eleven.
4. The helical angle of the screw thread should be 10 to 20 degrees.

In 1955 Boon, Honingh, and Van Rijssen (5) published an article in which a general discussion on dynamic shaft seals was presented. Although the possibilities of the visco seal had been suggested by Rowell and Finlayson, Asanuma and Boon were perhaps the first to consider the problem both analytically and experimentally. It appears that the work of Asanuma and Boon may have been done simultaneously and independently.

Figure 4 shows the basic seal studied by Boon (5). The sealing fluid fills the clearance space and grooves for a distance L, the distance M is filled with the system fluid, and the distance N is filled with ambient air. The pressure distribution indicated by curve 1 (solid line) is obtained when the system pressure is equal to atmospheric pressure. When the system pressure is increased, the pressure distribution indicated by curve 2 (dashed line) is obtained. Note that the interfaces between the sealing fluid and the system fluid and between the atmosphere and the sealing fluid move axially. Boon reports that pressure gradients of 20 atmospheres/centimeter (746 p.s.i./inch) were experimentally

attained with ease even though the experiments did not fully conform to the theoretical equations. One of the disadvantages of the seal shown in Figure 4 is its inability to seal when the shaft is at rest. To overcome this shortcoming, the seal shown in Figure 5 was designed. The rotor A is driven by the shaft, with an elastomeric seal E used to prevent leakage between the shaft and rotor. Rather than being of a single diameter, the rotor is made larger in diameter on the process side (assuming that the process is pressurized). This variation in diameter provides a sealing shoulder at F that contacts the stator B when the speed, and consequently the pressure at C, is reduced below a certain value. Tests were conducted with oils having viscosities of 70 centistokes and higher with radial clearances between the stator and rotor of 15 to 20 microns (0.0006 to 0.0008 inch). At room temperature and maximum system gas pressure of 20 atmospheres (hereafter designated as atm.), 294 p.s.i. absolute, the seal provided complete shutoff against gas leakage while operating at 1500 revolutions per minute (hereafter designated as r.p.m.) and when stationary. The maximum shaft surface velocity employed was 22.9 ft. per second (45 mm. shaft at 2950 r.p.m.). Boon observed that the pressure developed by the visco seal can be increased by:

1. Increasing the seal length.
2. Decreasing the clearance between rotor and stator.
3. Decreasing the depth of the grooves.
4. Increasing the viscosity of the sealing fluid.

He also observed that loss of sealing fluid was not serious and continuous makeup was unnecessary; the leakage due to diffusion was negligible.

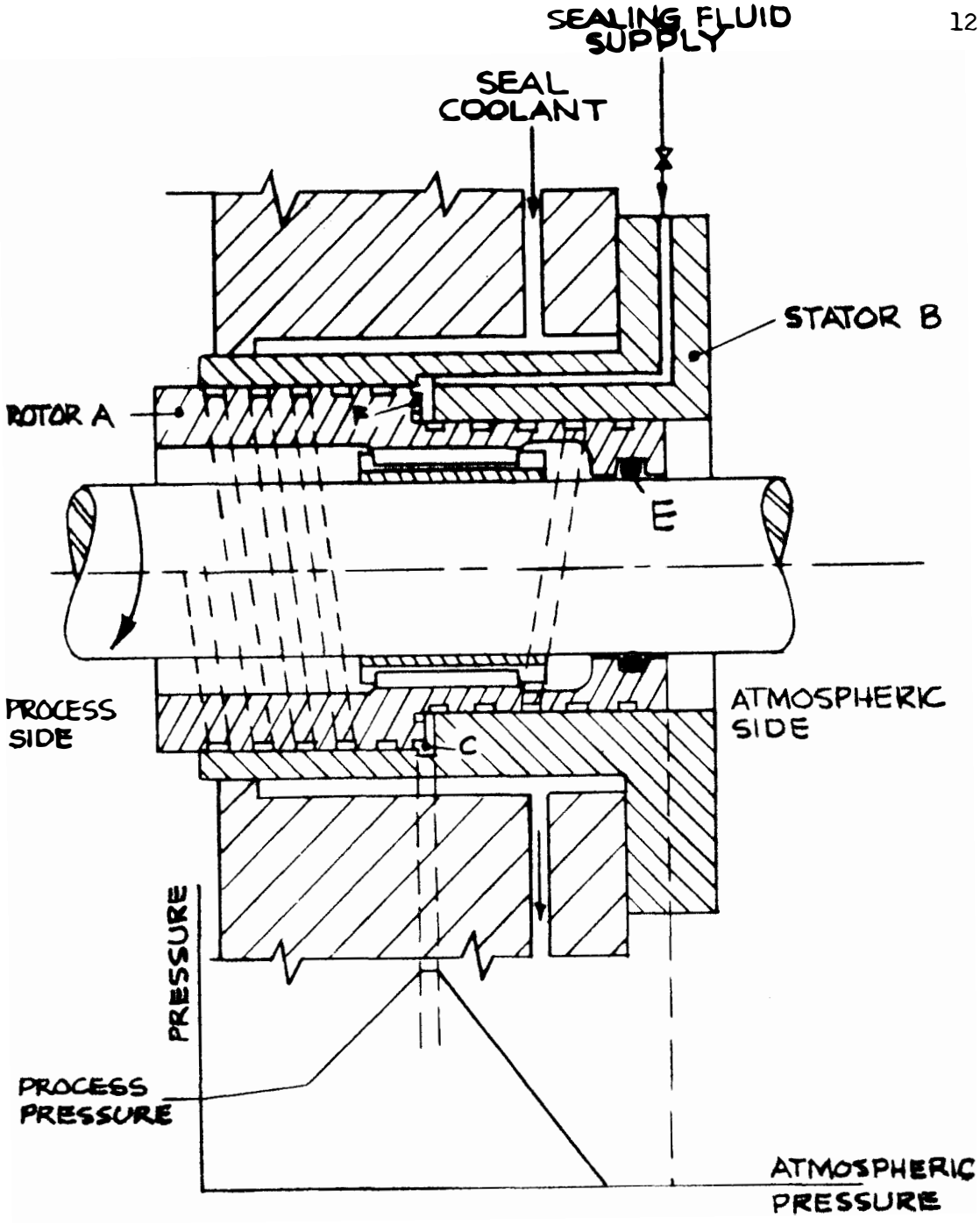

Figure 5. Visco Seal for static and dynamic sealing.

Boon (5) commented further that the visco seal would not be suitable for high-temperature use because the sealing action depends on the viscosity of the sealing fluid. It is important to note that the conclusions drawn by Boon (5) are essentially in agreement with those which may be reached on the basis of the work done by Rowell and Finlayson (2,3) and those made by Asanuma (4).

The experimental results of tests run on the seal similar to the one in Figure 4 were the basis for a thesis by Van Hoek (6). Van Hoek chose, rather than square grooves, peculiar "V-"shaped grooves.

In 1956, Frössel (7) presented a study on the visco seal in the laminar and turbulent flow regions as a result of research on seals for high-speed applications. His equation for laminar flow sealing capacity was

$$\Delta p = C_1\left(\frac{\mu U L}{h^2}\right), \tag{3}$$

where C_1 is an empirical coefficient depending on the ratio (h/c), the form of the thread, and the screw thread geometry. Frössel reasoned that C_1 would be zero for helix angles of zero and 90 degrees and would reach a maximum at some intermediate angle. Table I gives the values of the coefficient C_1 as given in the work by Frössel (7). Frössel observed that the grooves could be on either the shaft or the sleeve and the result would be the same. His solution to the problem of sealing a stationary shaft in conjunction with a visco seal was to employ an elastomeric lip-type seal which would unseat and become inoperative due to centrifugal force when the shaft was turning. The conclusions reached by Frössel, which are the result of extensive

TABLE I

VALUES OF THE COEFFICIENT C_1 FOR EQUATION (3), ACCORDING TO FROSSEL

	Helix Angle – α							
	0	5	10	12	15	20	25	90
Metric thread with a pitch of 1 mm., a thread height of 0.7 mm., and h/c = 14	0	14	25	27	24	16	11	0
Metric thread with a pitch of 0.5 mm., a thread height of 0.3 mm., and h/c = 6	0	3	5	6	7	7	6	0

experimental work but very limited analysis, were, for the most part, similar to those by Rowell and Finlayson, Asanuma, and Boon.

In 1959 Boon and Tal (8) presented a detailed analysis of the visco seal under laminar flow conditions. Their equation for sealing head under laminar flow conditions was developed as

$$\Delta p = \frac{2\mu UL}{C_2 c^2} , \tag{4}$$

where C_2 is a dimensionless coefficient that was theoretically derived using commonly accepted simplifying assumptions regarding flow (see page 19) to be a function of screw thread geometry (α, β, and γ) alone. Boon and Tal indicate that the theoretical minimum value for C_2 is 3.65333 when the form parameter values are

α = 15 degrees, 40.5 minutes;

β = 3.65333;

γ = 0.5.

Substituting the minimum value of C_2 into Equation (4),

$$\Delta p_{(max)} = 0.54706 \frac{\mu UL}{c^2} . \tag{5}$$

Boon and Tal define the optimum construction as that requiring the minimum power to seal a given pressure. Usually the values of diameter, speed, and required pressure are known and μ, L, U, and the screw thread geometry may be adjusted in order to make the power requirement as low as possible. Their expression for power dissipation is

$$q = \frac{C_3}{C_2} \frac{2\pi DL\mu U^2}{c^2} , \tag{6}$$

where C_3 is a dimensionless coefficient which has been theoretically derived as a function of screw thread geometry (α, β, and γ) alone. Boon and Tal indicate that the minimum power requirement cannot be attained in a practical seal; however, the value can be made low by appropriate choice of screw thread form parameters. Boon and Tal acknowledge that their study was based on the assumption of laminar flow but indicate that the seal could possibly be operated in the turbulent region, although they undertook no tests to confirm this speculation.

Asanuma (9) extended the theoretical studies of an earlier paper (4) and reported on extensive testing of various thread forms used in a visco seal. The equation for the sealing pressure is the same as Equation (2). A dimensionless theoretical expression for the factor S was derived for square threads as a function of the screw thread geometry alone. It was reported that the triangular thread was more suitable than either the square or semicircular grooves. The theoretically derived and experimentally verified dimensional relationships for the groove design as reported by Asanuma are as follows:

1. The clearance must be as small as possible, but it is usually proscribed by the fit-quality available in fabrication. That is, the ratio R/c should take values between 32 and 2400. (Note that normal bearing R/c ratios will fall within this range.)

2. The value of γ should be approximately 0.5.
3. The groove width (b) should be five to twenty times the groove depth (h).
4. The value of β should be approximately six.
5. The helix angle should be approximately 10 to 11 degrees.

Asanuma observed that multithreaded screws provide the same sealing performance as single-threaded screws. Asanuma also observed (as did Frössel) that the performance of the plain shaft within a grooved sleeve was the same as a grooved shaft within a plain sleeve.

In 1964, McGrew and McHugh (10) presented an analytical and experimental study of the visco seal in both laminar and turbulent operation. In this theoretical study for operation in the laminar region, which was patterned after a paper by Zotov (11), McGrew and McHugh presented the equation for sealing pressure as

$$\Delta p = \Psi_L \frac{\mu U L}{c^2} \quad , \tag{7}$$

where Ψ_L, a dimensionless laminar sealing coefficient, is a function of screw thread geometry alone. The equation is

$$\Psi_L = \frac{6\beta_0^2(1+\beta_0)^{-1}}{\tan\alpha\left[1 + \frac{E\beta_0^3}{\gamma(1-\gamma)\sin\alpha}\right]} \tag{8}$$

The sealing coefficient is a function of eccentricity, as indicated by the factor E, which is called the eccentricity

correction factor and which was reported to vary theoretically from 1.0 to 2.5 as the eccentricity varies from 0 to 1. McGrew and McHugh did not measure eccentricity; therefore, the values of E were not confirmed experimentally. McGrew and McHugh solved for the optimum form parameters, which they found to be:

α = 21.6 degrees;

β = 3.78;

γ = 0.5

By assuming concentricity, the sealing coefficient was computed from Equation (8), and the equation McGrew and McHugh developed for maximum sealing is

$$\Delta p_{(max)} = 0.61 \frac{\mu U L}{c^2} \quad . \tag{9}$$

In the analytical study of the visco seal in the turbulent region McGrew and McHugh did not consider the leakage flow across the land; their approach was to demonstrate the form of the turbulent sealing equation and then to evaluate the constants experimentally. The equation was given as

$$\Psi_T = K_1 + K_2 Re^n \tag{10}$$

where K_1, K_2, and n are constants. McGrew and McHugh observed a large increase in the sealing coefficient when the flow became turbulent. The two investigators also observed seal breakdown in both laminar and turbulent flow and commented that seal breakdown may be affected significantly by fluid surface tension.

In January of 1965 Stair (13) presented a theoretical analysis of the visco seal for the concentric laminar case similar to the analysis by Boon and Tal (8). The seal investigated by Stair is shown in Figure 6. Stair made the following simplifying assumptions:

1. The sealant is a Newtonian fluid with negligible change in density.
2. The flow is steady-state and incompressible.
3. The velocity in z direction is negligible with negligible pressure change in the z direction.
4. The body forces are small in comparison to viscous forces.
5. Both the groove and the land of the thread are assumed infinite flat plates in the ξ and η directions.

The equations of motion and continuity for laminar flow may be written as (assumption 1):

$$\rho \frac{Du}{Dt} = F_\xi - \frac{\partial P}{\partial \xi} + \mu \nabla^2 u \ ;$$

$$\rho \frac{Dv}{Dt} = F_\eta - \frac{\partial P}{\partial \eta} + \mu \nabla^2 v \ ; \qquad (11)$$

$$\rho \frac{Dw}{Dt} = F_z - \frac{\partial P}{\partial z} + \mu \nabla^2 w \ ;$$

$$\frac{\partial u}{\partial \xi} + \frac{\partial v}{\partial \eta} + \frac{\partial w}{\partial z} = 0 \ . \qquad (12)$$

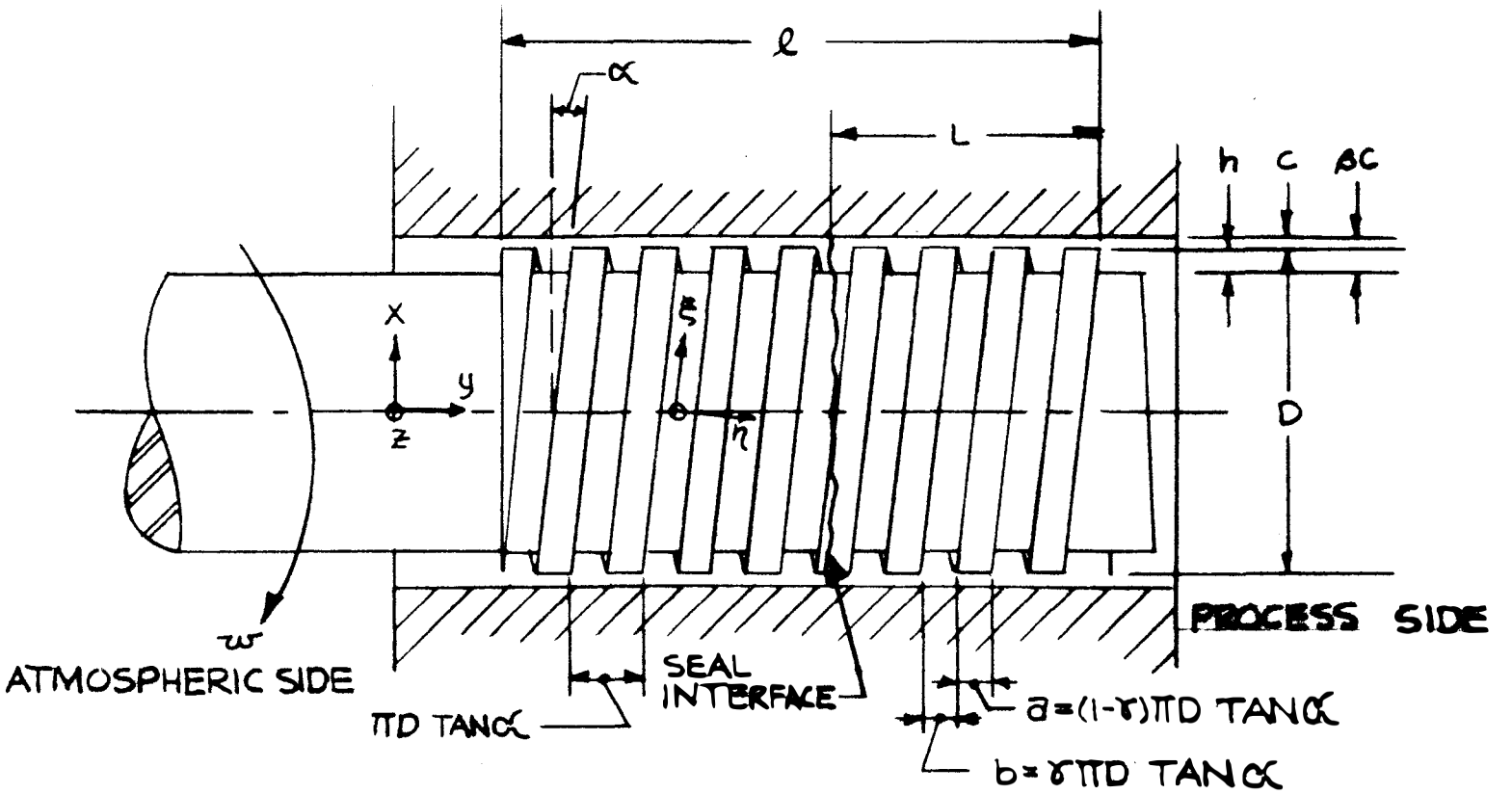

Figure 6. Visco seal.

By considering assumptions 2, 3, and 4, the equations may be reduced to

$$\frac{\partial^2 u}{\partial z^2} = \frac{1}{\mu}\frac{\partial P}{\partial \xi} \tag{13}$$

$$\frac{\partial^2 v}{\partial z^2} = \frac{1}{\mu}\frac{\partial P}{\partial \eta} \tag{14}$$

Integrating Equations (13) and (14),

$$u = \frac{1}{2\mu}\frac{\partial P}{\partial \xi} z^2 + C_1 z + C_2; \tag{15}$$

$$v = \frac{1}{2\mu}\frac{\partial P}{\partial \eta} z^2 + C_3 z + C_4 \ . \tag{16}$$

The velocities in the region of the grooves and in the region of the lands may be determined by noting the following boundary conditions:

Along the lands	Across the lands
$u_r = U\cos\alpha$ at $z = 0$	$v_r = -U\sin\alpha$ at $z = 0$
$u_r = 0$ at $z = h_r$	$v_r = 0$ at $z = h_r$

Along the grooves	Across the grooves
$u_g = U\cos\alpha$ at $z = 0$	$v_g = -U\sin\alpha$ at $z = 0$
$u_g = 0$ at $z = h_g$	$v_g = 0$ at $z = h_g$

The velocity components along the lands and grooves may be identified. By deriving an equation for the net flow in the seal and setting the flow equal to zero and collecting the resulting equation into dimensionless groups a sealing coefficient,

$$\Lambda = \frac{6\mu UL}{\Delta p c^2} = \frac{\beta^3(1 + t^2) + \gamma t^2(1 - \gamma)(\beta^3 - 1)^2}{\gamma t(1 - \gamma)(\beta^3 - 1)(\beta - 1)} \tag{17}$$

may be defined. By writing the equations for the time rate of

energy dissipation in the sealant by viscous action per unit volume of flow in the ξ and η directions and integrating over the appropriate volumes, an expression for the power loss in the visco seal may be written as:

$$q = \frac{\mu\pi DLU^2}{c}\left\{(1 - \gamma + \frac{\gamma}{\beta}) + 3\left[\frac{t^2\gamma(1-\gamma)(\beta-1)^2(1-\gamma+\gamma\beta^3)}{\beta^3(1+t^2) + t^2\gamma(1-\gamma)(\beta^3-1)^2}\right]\right\} . \quad (18)$$

Equation (18) may be written as:

$$q = \Phi\frac{\mu\pi DLU^2}{c} \quad (19)$$

where Φ, dissipation function, corresponding to the bracketed term of Equation (18), is a function of screw thread geometry. If

$$\Phi = \phi' + \phi'' , \quad (20)$$

where

$$\phi' = 1 - \gamma + \frac{\gamma}{\beta} , \quad (21)$$

and

$$\phi'' = 3\left[\frac{t^2\gamma(1-\gamma)(\beta-1)^2(1-\gamma+\gamma\beta^3)}{\beta^3(1+t^2) + t^2\gamma(1-\gamma)(\beta^3-1)^2}\right] , \quad (22)$$

then ϕ' represents the loss due to Couette flow and is independent of the angle α. The ϕ'' term represents the loss due to Poiseuille flow and depends upon α, β, and γ.

It has been suggested by McGrew and McHugh (10) that Φ'', due to Poiseuille flow, was small in comparison with ϕ' and

could be neglected. This approach assumes that the power loss can be written as:

$$\bar{q} = \mu UA \frac{\partial V_x}{\partial z} \cdot \tag{23}$$

The velocity gradients are taken as U/h_r over the land area A_r and $\frac{U}{h_g}$ over the groove area A_g. Thus,

$$\bar{q} = \mu U \frac{UA_r}{h_r} + \frac{UA_g}{h_g} \tag{24}$$

Since

$$A_r = (1 - \gamma)\pi DL \tag{25}$$

and

$$A_g = \gamma \pi DL \, , \tag{26}$$

then

$$\bar{q} = \frac{\mu \pi DLU^2}{c} \left(1 - \gamma + \frac{\gamma}{\beta}\right) \tag{27}$$

or

$$\bar{q} = \phi' \frac{\mu \pi DLU^2}{c} \cdot \tag{28}$$

The order of magnitude of the ϕ'' component of the power loss is, for some screw thread configurations, the same as that of ϕ', and the smaller error occurs with visco seals having low values of α and γ, while the more significant errors occur with larger values of α and γ. Since the larger values of α and γ are of the most interest for practical seals, the simplified evaluation of the dissipation function appears to be questionable.

It is the opinion of the investigators involved in this study that the approach as presented by Stair (13) is the best theoretical approximation to the actual characteristics of laminar flow in the visco seal. It should be noted that all of the theoretical derivations surveyed assume concentricity and laminar flow with the exception of the work by McGrew and McHugh, who attempted to predict (1) the range of an eccentricity factor E and (2) the form of the equation for the sealing coefficient in turbulent flow. No attempt was made in any of the experimental studies surveyed to measure the actual eccentricity during operation.

Although all of the investigators discussed in this chapter report what each one concluded to be the optimum thread geometry (i.e., the geometry at which the sealing coefficient is at a minimum), these geometries were not in agreement.

Table II shows the values of the sealing coefficient as reported by Stair (13), McGrew and McHugh (10), and Asanuma (9). It should be noted that since the equation for sealing coefficient as reported by Asanuma is a function of the clearance and the shaft diameter, the values for Asanuma's sealing coefficient in Table II were computed with the clearance assumed equal to 0.002 inch and the shaft diameter assumed equal to 1.250 inch. The values shown in Table II have all been converted to the

TABLE II

A COMPARISON OF SEALING COEFFICIENTS

α	γ	β	Λ_s	$\Lambda_{M\&M}$	Λ_A
8	0.3	3	19.8	26.8	28.3
8	0.3	5	13.0	13.6	15.9
8	0.3	7	13.8	12.6	15.7
8	0.5	3	16.8	22.6	24.2
8	0.5	5	11.6	11.9	14.2
8	0.5	7	12.9	11.5	14.7
8	0.7	3	19.7	26.8	28.7
8	0.7	5	13.0	13.6	16.2
8	0.7	7	13.8	12.6	16.0
14	0.3	3	13.5	16.7	19.0
14	0.3	5	12.9	11.3	15.1
14	0.3	7	17.9	14.4	19.7
14	0.5	3	11.9	14.3	16.6
14	0.5	5	12.1	10.3	14.1
14	0.5	7	17.4	13.8	19.0
14	0.7	3	13.5	16.7	19.1
14	0.7	5	12.9	11.3	15.2
14	0.7	7	17.9	14.4	19.8
20	0.3	3	12.4	13.3	16.6
20	0.3	5	15.0	11.9	17.4
20	0.3	7	23.2	18.2	25.9
20	0.5	3	11.2	11.5	14.8
20	0.5	5	14.4	11.2	16.6
20	0.5	7	22.8	17.7	25.4
20	0.7	3	12.4	13.3	16.7
20	0.7	5	15.0	11.9	17.5
20	0.7	7	23.2	18.2	25.9

Λ_s – Based on Boon and Tal theory
M&M – Based on McGrew and McHugh theory
Λ_A – Based on Asanuma theory

definition for sealing coefficient as defined by:

$$\Lambda = \frac{6\mu UL}{\Delta pc^2} ,$$

where Λ is dimensionless. Table III shows the equations derived by the investigators and written in a common nomenclature. Figures 7 through 11 show graphically the results of a computer program for the solution of the equations for the sealing coefficient and dissipation function derived by Stair (13). Also shown in Figures 7 through 10 are the values for the sealing coefficient for a value of $\gamma = 0.5$ as determined from the equations by McGrew and McHugh (10) and Asanuma (9). In addition, the values for the dissipation function as determined from the equations by McGrew and McHugh are shown in Figure 11.

TABLE III.

DESCRIBING EQUATIONS

INVESTIGATOR	EQUATION
Stair	$\Lambda_S = \dfrac{\beta^3(1+t^2)+\gamma t^2(1-\gamma)(\beta^3-1)^2}{\gamma t(1-\gamma)(\beta^3-1)(\beta-1)}$
McGrew and McHugh	$\Lambda_{M\&M} = \dfrac{\beta t^2(\beta-1)^3\gamma(1-\gamma)+\beta(1+t^2)}{t\gamma(\beta-1)^2(1-\gamma)}$
Asanuma	$\Lambda_A = \dfrac{\beta^3\gamma(1-\gamma)t^2K_2+t^2+1}{\beta\gamma(1-\gamma)tK_1}$ $K_1 = (1-\frac{1}{\beta})^2 - \frac{8\beta^2}{\pi^4}\left(\frac{c}{a}\right)\sum_{n=1}^{\infty}\left\{\frac{1}{n^4}\sin\frac{n\pi}{\beta}\left[\cos n\pi\beta-(-1)^n\right]\tanh\frac{n\pi}{2\beta}\left(\frac{a}{c}\right)\right\}$ $K_2 = \frac{(\beta-1)^2(\beta+2)}{\beta^3} - \frac{24}{\pi^4}\left(\frac{c}{a}\right)\sum_{n=1}^{\infty}\left\{\frac{1}{n^4}\sin\frac{n\pi}{\beta}\left[\cos n\pi\beta-(-1)^n\right]\tanh\frac{n\pi}{2\beta}\left(\frac{a}{c}\right)\right\}$ $-\frac{48}{\pi^5}\beta\left(\frac{c}{a}\right)\sum_{n=1}^{\infty}\left\{\frac{1}{n^5}\left[\cos\frac{n\pi}{\beta}-(-1)^n\right]^2\tanh\frac{n\pi}{2\beta}\left(\frac{a}{c}\right)\right\}$
Stair	$\Phi = 1-\gamma+\frac{\gamma}{\beta}+3\left\{\dfrac{t^2\gamma(1-\gamma)(\beta-1)^2(1-\gamma+\gamma\beta^3)}{\beta^3(1+t^2)+t^2\gamma(1-\gamma)(\beta^3-1)^2}\right\}$
McGrew and McHugh	$\Phi' = 1-\gamma+\frac{\gamma}{\beta}$

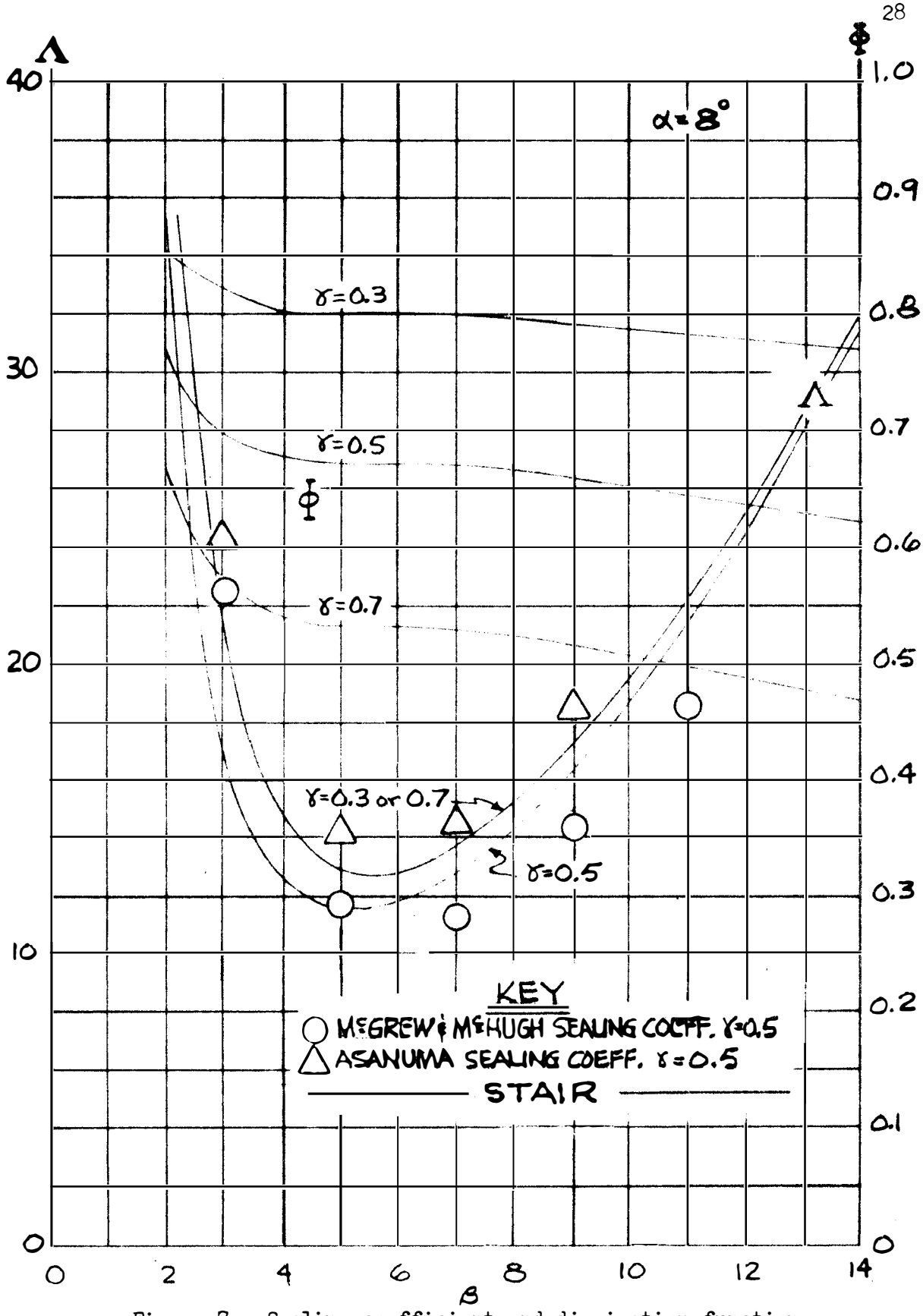

Figure 7. Sealing coefficient and dissipation function.

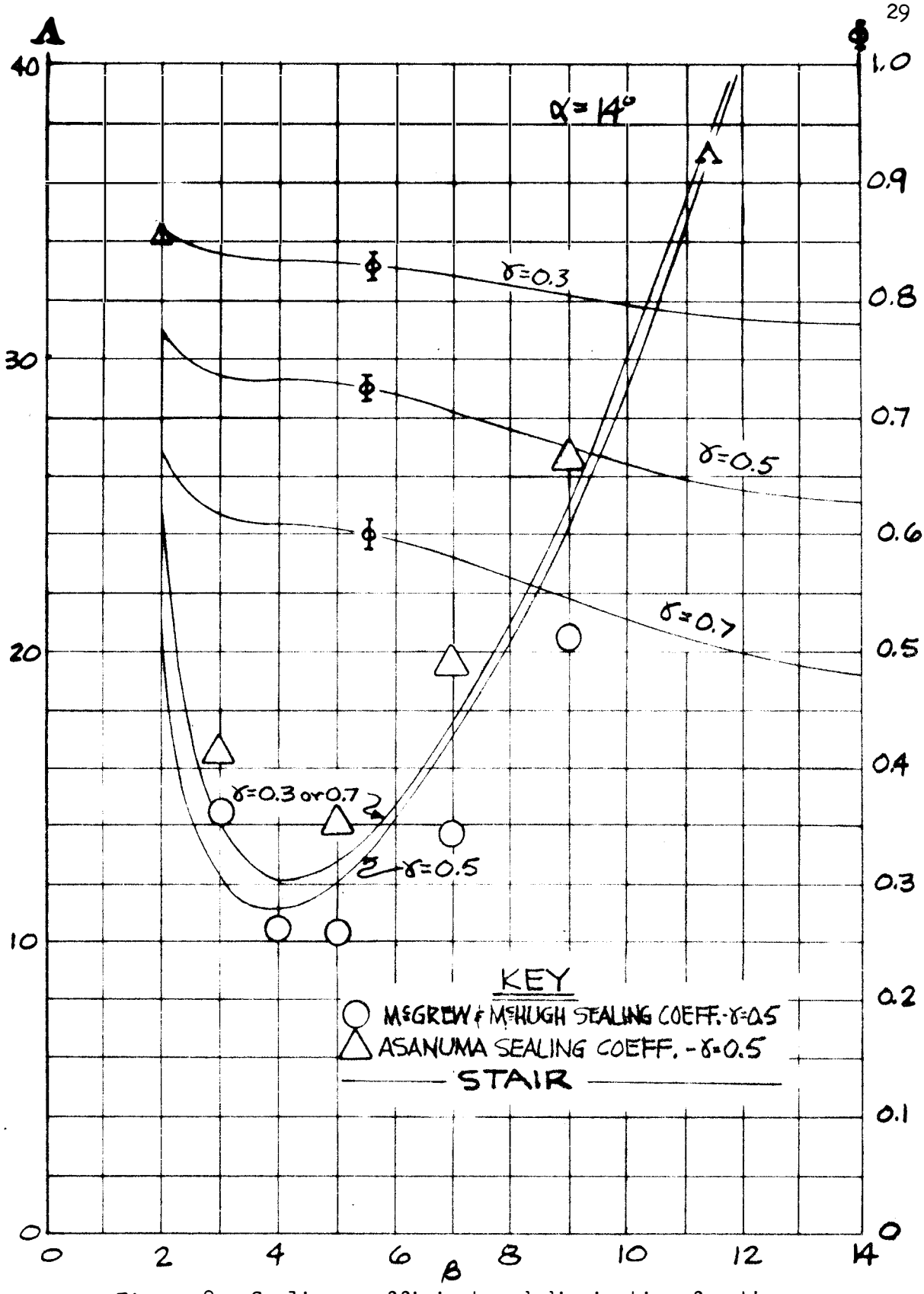

Figure 8. Sealing coefficient and dissipation function.

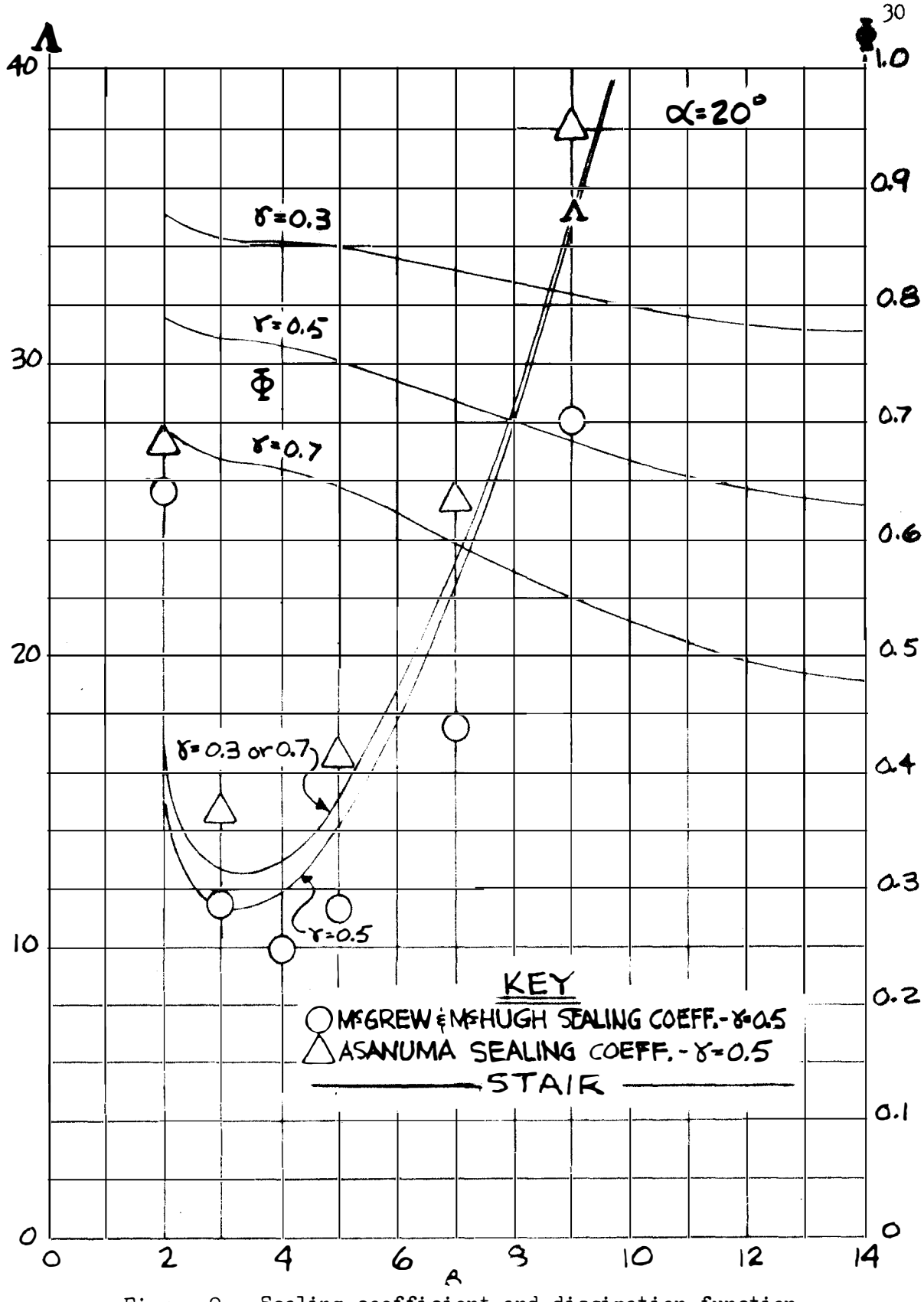

Figure 9. Sealing coefficient and dissipation function.

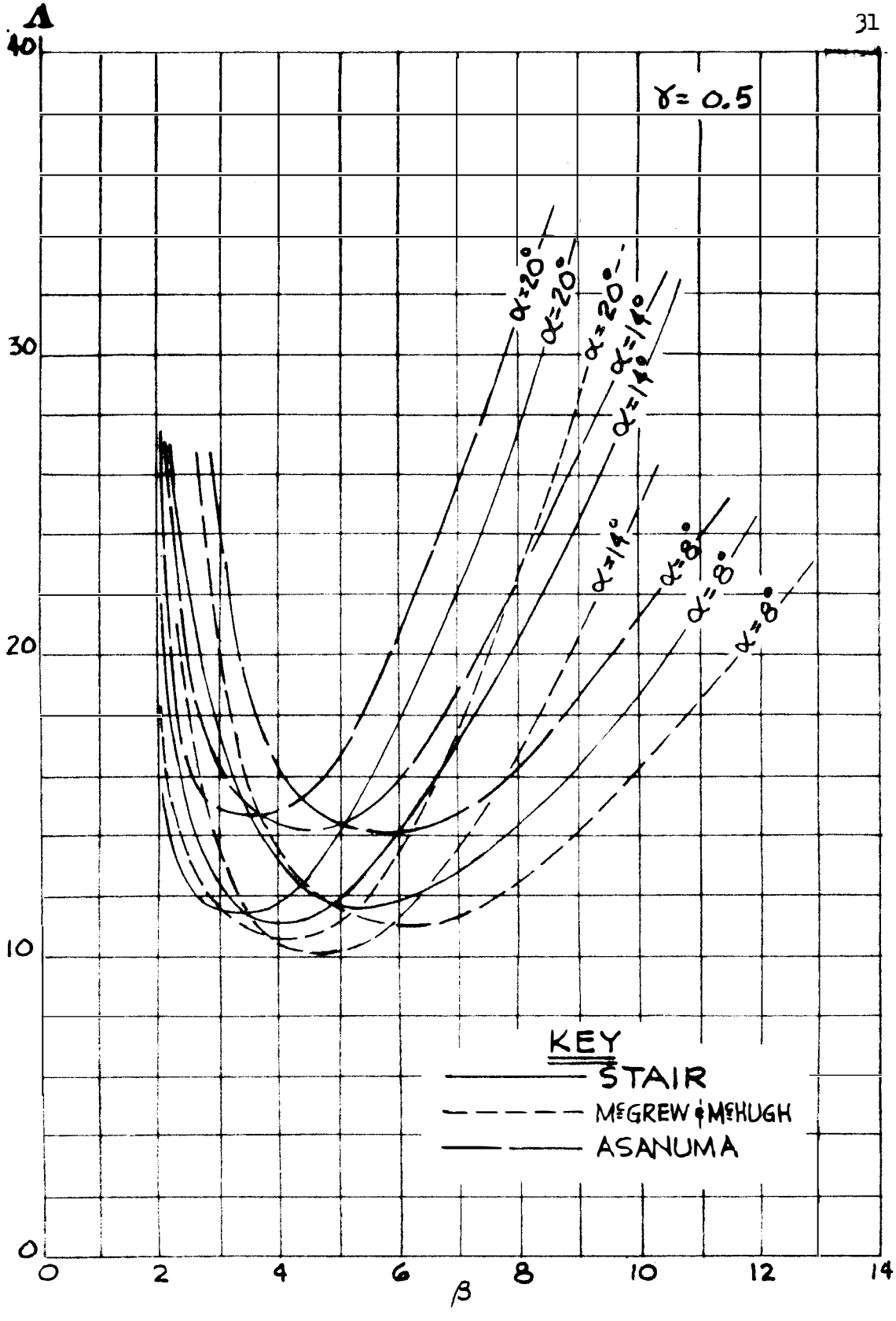

Figure 10. Sealing Coefficient.

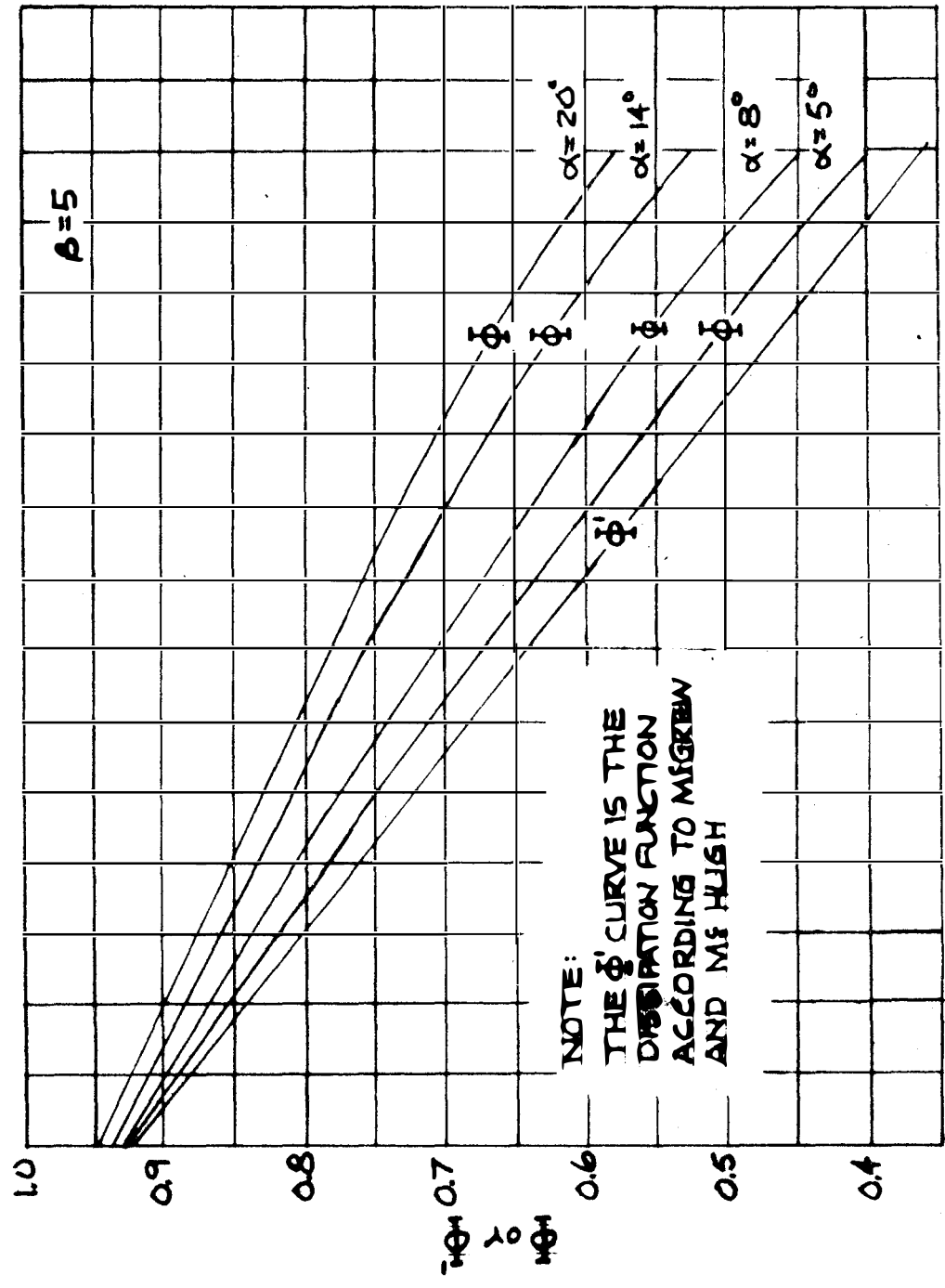

Figure 11. Dissipation function.

CHAPTER II. PRELIMINARY DESIGNS

This chapter is composed of three parts:

1. Presentation of the operational capabilities desired in the proposed visco seal tester.
2. Discussion of test facilities constructed and operated by other investigators.
3. Presentation of three proposed designs in preliminary form, and discussion of the reasons for selecting the third design.

One of the most important requirements of the proposed tester is the ability to experimentally verify the equations developed by the investigators and presented in Chapter I. The test facility must be capable of varying as many of the independent variables in these equations as feasible without extensive modification of the tester. With the exception of the shaft diameter D, all of the variables in Equations (17) and (18) may be varied easily within certain limits. For this reason the shaft diameter is held constant at 1.25 inch. The length of the threaded shaft and thus the maximum seal length L is limited by such factors as dynamic inbalance and dynamic shaft whip considerations. The radial clearance c is limited by the precision of fabrication methods available. The surface velocity U is confined within the range of the drive mechanism. The sealant viscosity may be varied with little difficulty.

Since both the sealing coefficient and the dissipation function should be minimized, a compromise form parameter would probably lie within the limits:

$$0.3 < \gamma < 0.7$$

$$2 < \beta < 14$$

$$8 \text{ degrees} < \alpha < 20 \text{ degrees}$$

It should be noted that small values of β are progressively less precise because very small values of screw thread depth h are limited in their precision to available fabrication methods.

Although a complete experiment design will not be presented, a few remarks regarding the approach in the investigation of the three variables in the ranges indicated should be made. Each variable is to be investigated at three levels. A complete classical experiment would require twenty-seven tests at each sealant fluid viscosity. The investigators, however, decided upon a fractional factorial experiment in which only one-third of the tests (nine tests) are run with the variables confounded in a modified latin square. Figure 12 shows the latin square employed for the tests. Additional information concerning the latin square is provided by Schenck (19).

In addition to the study of the validity of the equations presented by Stair (13), the tester must enable the investigators to undertake a number of other important studies. Although the equations by Stair assume concentric operation, in the practical case the shaft is almost certain to be eccentric, and McGrew and

	$\alpha = \alpha_1$	$\alpha = \alpha_2$	$\alpha = \alpha_3$
$\gamma = \gamma_1$	$\beta = \beta_1$	$\beta = \beta_2$	$\beta = \beta_3$
$\gamma = \gamma_2$	$\beta = \beta_3$	$\beta = \beta_1$	$\beta = \beta_2$
$\gamma = \gamma_3$	$\beta = \beta_2$	$\beta = \beta_3$	$\beta = \beta_1$

Figure 12. Experiment design.

McHugh have suggested that eccentricity is significant. A study to determine the effects of eccentricity is therefore proposed. Although square threads were used in the analysis by Stair, the merit of this or any other type of thread geometry is uncertain, and a study of screw thread geometry is also proposed. As has been stated, the equations by Stair are valid only for laminar flow. Although very little work has been done on thoeretical equations for the sealing coefficient and power dissipation in the turbulent region, the test facilities should be capable of exploring this region.

Upon surveying the requirements of the test facilities, a number of problems were envisioned. It has been noted that the seal eccentricity may be significant. In order to locate the center of the shaft with respect to the center of the sleeve (i.e., eccentricity), the radial clearance must be determined within certain limits of precision while the shaft is rotating. This clearance must be measured in two planes normal to the centerline of the shaft some distance apart, and in each plane the clearance must be measured at two locations, preferably 90 degrees apart, in order to completely locate the centerline of the shaft with respect to the centerline of the sleeve. The clearance must be measured without allowing any object to come in contact with the rotating shaft. The precision of the measurement of the clearance is generally conceded to be the greatest source of error.

Another major problem anticipated in the design of the required test facilities is that of power dissipation measurement. In order to measure the power dissipated per unit time, the torque transmitted to the sleeve through viscous shear from the shaft must be measured. The problem of measuring torque that may be applied to the sleeve is elementary, but distinguishing between torque due to viscous shear and torque due to other effects such as bearing friction, which may be on the same order of magnitude as viscous torque, is a more difficult problem.

In Chapter I it was noted that a number of investigators have developed theoretical equations for predicting the sealing coefficient and dissipation function. Some of these investigators also designed, constructed, and operated test facilities to evaluate the equations developed. The test facilities operated by Asanuma, Van Hoek, and McGrew and McHugh will be examined.

The test apparatus used by Asanuma (see Figure 13) in a second and more significant investigation (9) was constructed so that the threaded shaft could be tested as both a seal and a pump. The single-grooved shaft is held in a vertical position by a radial-ball bearing at the top of the shaft. The grooved portion of the shaft is partially surrounded by a sleeve supported by a radial-ball bearing at the bottom of the sleeve and a thrust-ball bearing near the center of the grooved section of the shaft. The grooved shaft is driven by a 1/4-horsepower motor through a pulley positioned above the top bearing. The sealant

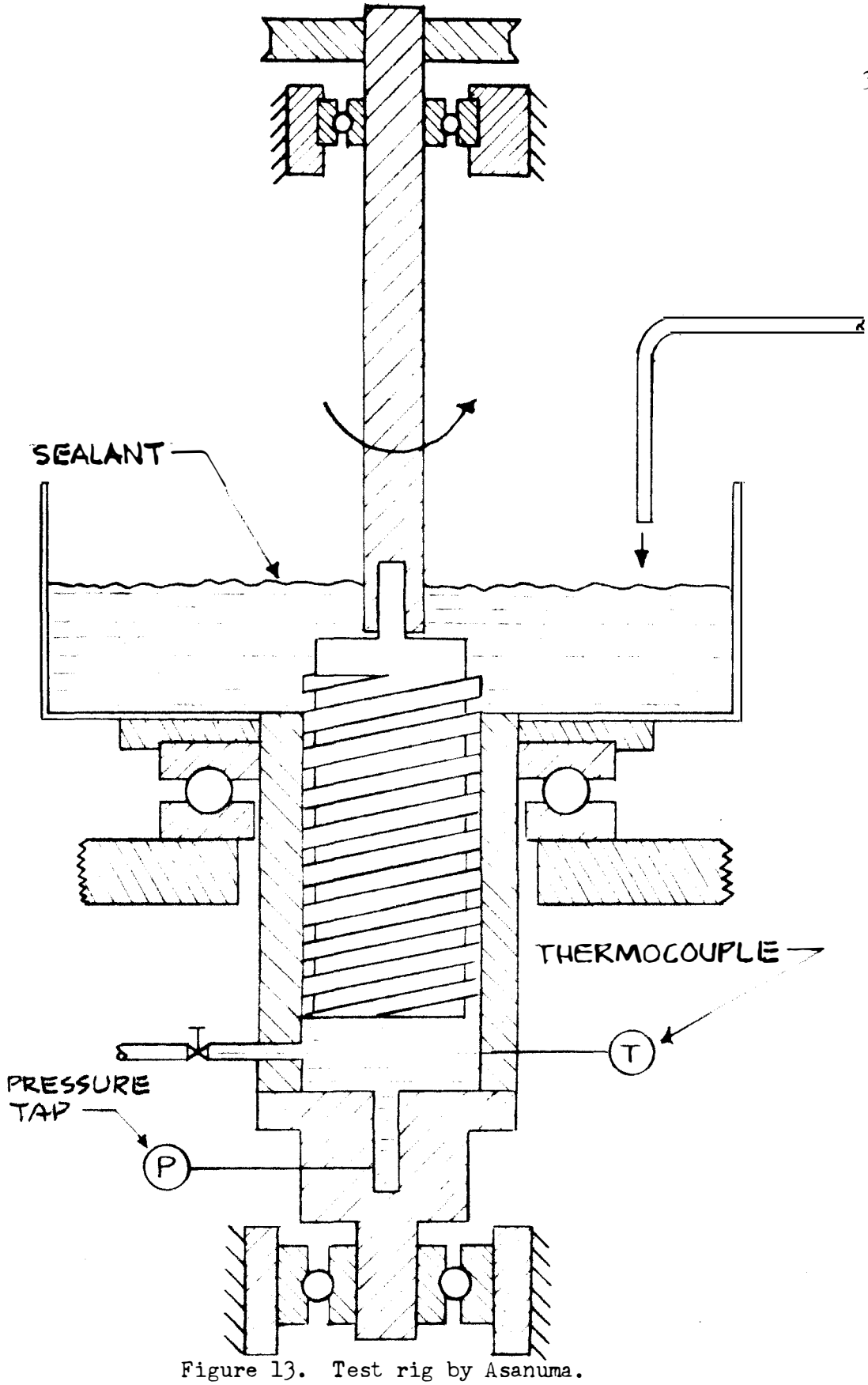

Figure 13. Test rig by Asanuma.

is introduced into the grooves at the top of the sleeve from a pan. The temperature of the oil may be measured in the pan and at the bottom of the sleeve. The maximum sealing pressure (discharge pressure when testing a visco pump) is measured by a manometer at the bottom of the sleeve. An oil outlet (closed when testing a seal) is located at the bottom of the sleeve. It should be noted that Asanuma did not develop an equation for power loss and made no attempt to measure the torque on the sleeve due to viscous shear.

The test facility constructed (6) by Van Hoek (see Figure 14) was designed to investigate double-grooved seals. In Van Hoek's test screw Number 2 the sealant is injected under pressure between the two sections, which are threaded in opposite directions. No attempt was made to make the sleeve free-floating or to measure the power loss due to viscous friction. However, the sleeve is mounted with an O-ring connection to the stand, which can be adjusted for alignment purposes. The sleeve is water-cooled to maintain a constant sealant temperature and viscosity.

Perhaps the most effective test facility was constructed by McGrew and McHugh (10) in which a single-grooved shaft was surrounded by a water-cooled sleeve. Sealant was introduced into the grooves under pressure through a hole in the sleeve, and a torque arm connected to the sleeve contacted a strain-gage beam to record the torques imposed on the sleeve. As has been stated,

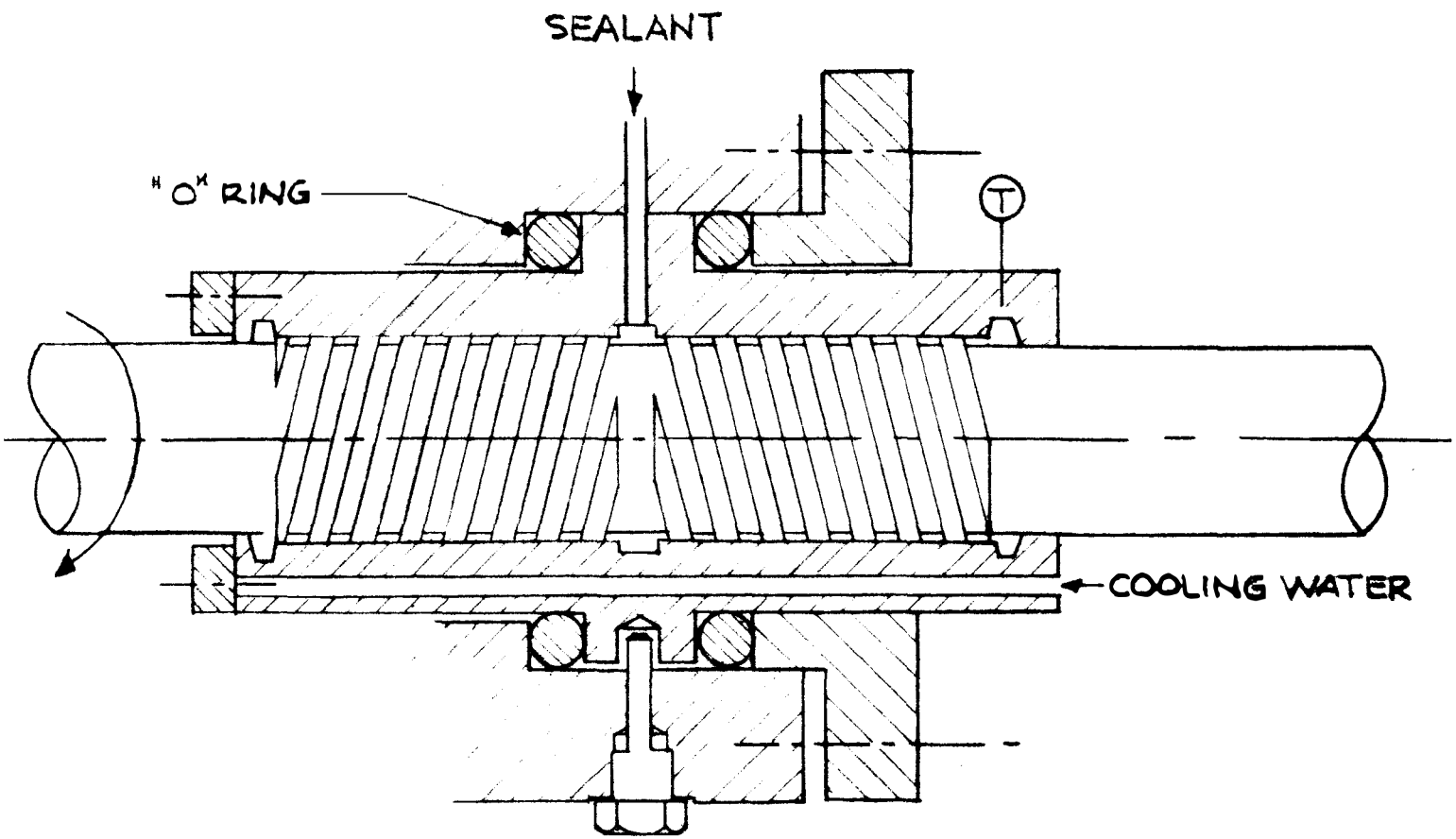

Figure 14. Test rig by Van Hoek.

one of the major design problems is to be able to distinguish between the sum of the torques on the sleeve and torque due to viscous shear. McGrew and McHugh attempted to solve this problem by making all torques on the sleeve negligible except that due to viscous shear. At first they attempted to free-float the sleeve on the shaft on the theory that the seal would support the sleeve in a nearly concentric position with hydrodynamic pressure. This arrangement proved to be unstable, however, and was abandoned. Figure 15 illustrates the final approach of McGrew and McHugh; they mounted the sleeve on ball bearings, on the assumption that the torque on the sleeve due to static friction of the ball bearings would be small in comparison to the torque due to viscous shear. This was not the case, however, and McGrew and McHugh were unable to precisely determine the power loss. It should also be noted that McGrew and McHugh did not measure the eccentricity.

At the beginning of this study, a number of preliminary design proposals were considered. Three of these proposals, including the proposed design which was adopted, are discussed here along with a short discussion of the relative merits of each proposal.

In the first design, the problem of constructing a free-floating sleeve (with which McGrew and McHugh had difficulty) is circumvented by suggesting that a thermodynamic analysis be made

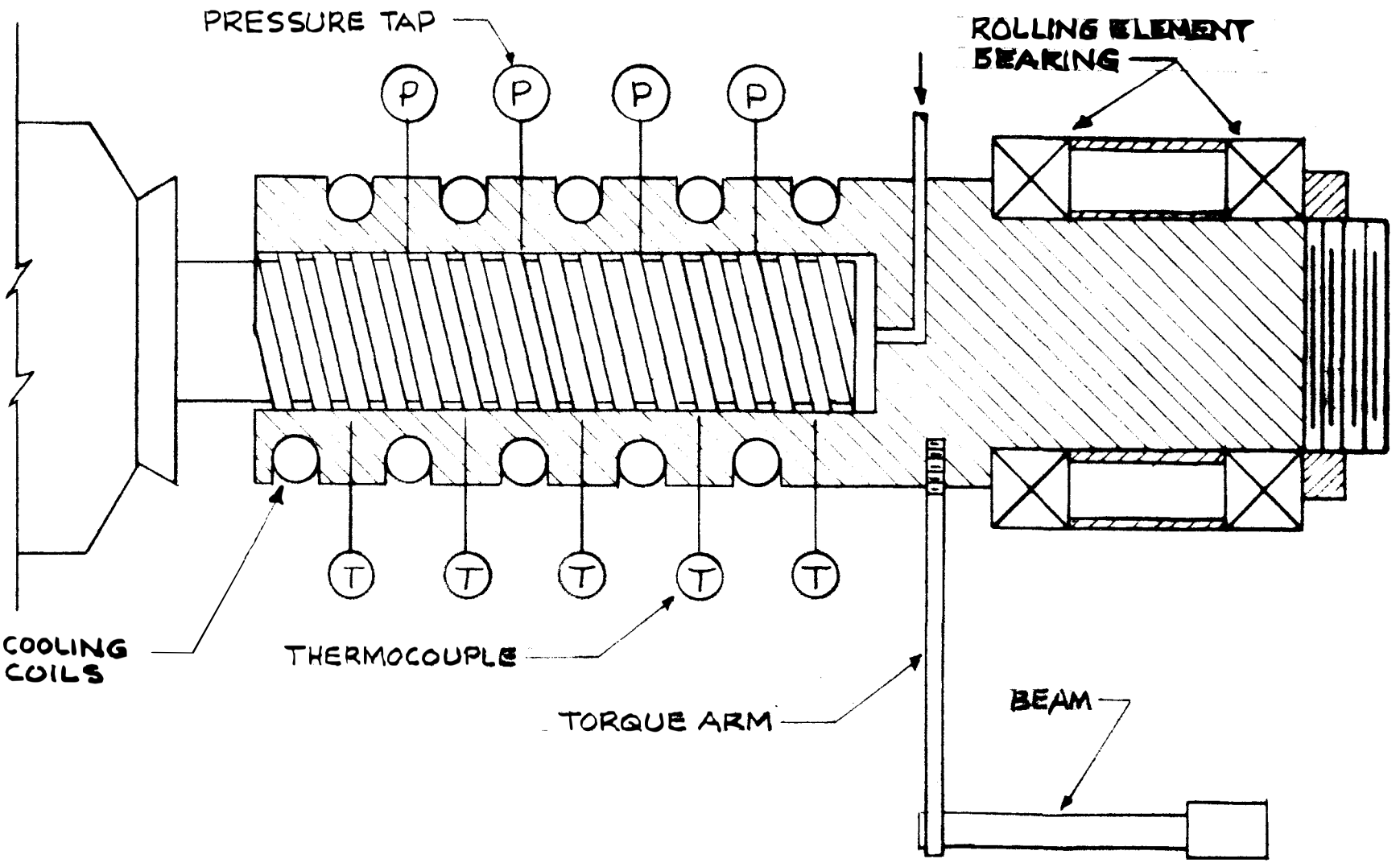

Figure 15. Test Rig by McGrew and McHugh.

(see Figure 16). This idea was never given serious consideration, since the cost of a calorimetry analysis would be relatively high if the desired limits of precision were maintained. Such an approach might be resorted to, however, as a check on the order of magnitude of the power loss. Figure 16 shows four induction probes located at right angles and in two planes. These probes, manufactured by the Bently Scientific Company, are capable of measuring the distance between two surfaces through an induction principle without requiring contact between the two surfaces. This approach to the eccentricity measurement problem is common to all three preliminary designs.

In the second proposal (see Figure 17) the problem of measuring power loss is resolved by using hydrostatic radial bearings to free-float the sleeve. At this point, it will suffice to say that the hydrostatic bearing suspends the sleeve in a film of oil in which (unlike ball bearings) the friction torque imposed on the sleeve due to the bearing approaches zero. Eight hydrostatic pads (four are shown) are located at 90-degree intervals in two planes, and each pad is supplied with lubricant under presssure. In this design a double-grooved shaft is mounted on two ball bearings and surrounded by the sleeve, which is supported by the hydrostatic bearings. Sealant is introduced under pressure between the threaded sections, and clearances are measured by induction probes. Cooling passages

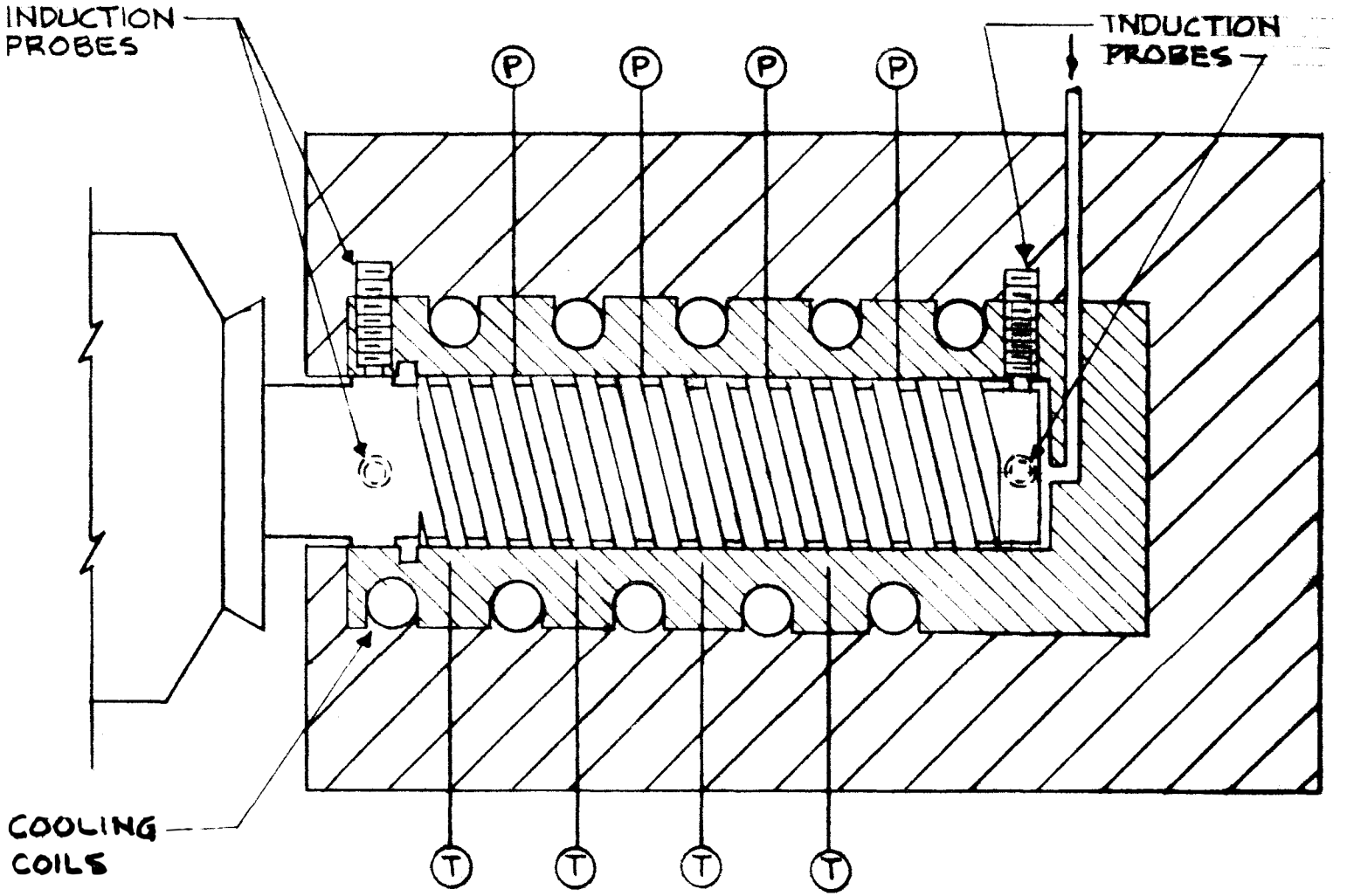

Figure 16. Proposed Test Rig No. 1.

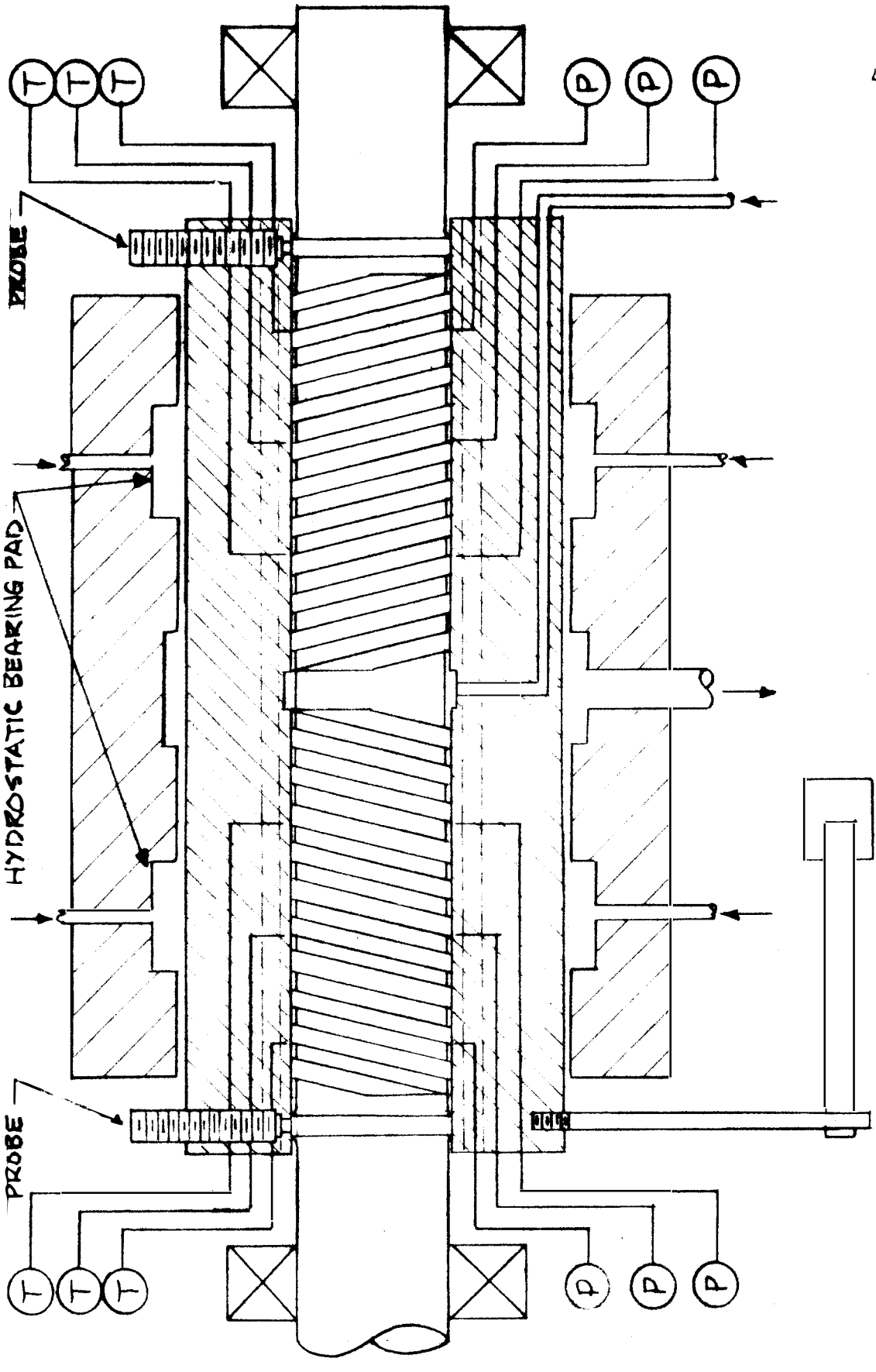

Figure 17. Proposed Test Rig No. 2.

are located parallel to the axis around the sleeve. To permit assembly the sleeve must be constructed in two longitudinal halves fitted together.

The outstanding advantage contained in this design is its ability to measure the torque due to viscous shear within small limits of precision. By free-floating the shaft and using flexible connections, the initial torques on the sleeve are made constant, and the change in torque for a given shaft speed is due to viscous shear alone. In addition, the double-grooved feature of the design eliminates the axial thrust due to pressure development inherent to the single-grooved design. This design is highly versatile in application. It may be used not only to verify theoretical equations, but also to study the effects of eccentricity and turbulent operation and to study the load-carrying ability of the visco seal. Perhaps the most important disadvantage to this design is the test sleeve, which would require complicated and expensive machining operations to fabricate.

After consideration of several alternative proposals, the design shown in Figure 18 as a full-scale elevation view was selected. A single-grooved shaft, driven through a high-speed spindle, is surrounded by a sleeve as shown. Hydrostatic bearings and induction probes are employed as in previous designs discussed. Sealant under pressure is injected into the sleeve, and the pressure and temperature of the sealant

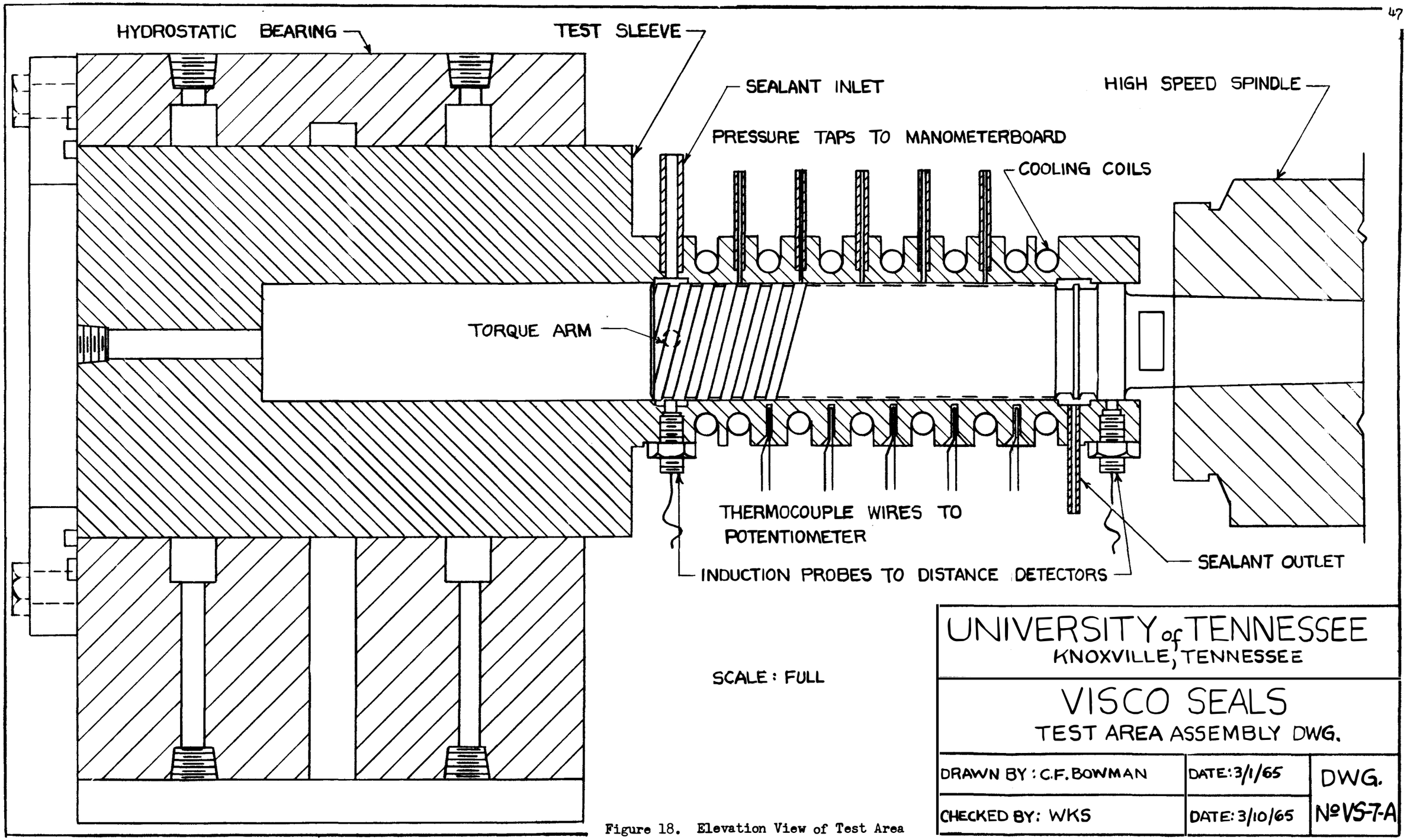

SCALE : FULL

UNIVERSITY of TENNESSEE KNOXVILLE, TENNESSEE		
VISCO SEALS TEST AREA ASSEMBLY DWG.		
DRAWN BY : C.F. BOWMAN	DATE: 3/1/65	DWG.
CHECKED BY: WKS	DATE: 3/10/65	Nº VS-7-A

Figure 18. Elevation View of Test Area

are measured along the sleeve. Cooling coils are wrapped around the sleeve along the section surrounding the shaft. The torque arm contacts a strain-gage beam to indicate torque acting on the sleeve. The axial pressure force is carried by a hydrostatic thrust plate at the end of the bearing block.

The design shown in Figure 18 is capable of measuring torque due to viscous shear and eccentricity within acceptable limits of precision and is capable of operation in the turbulent region. In addition, it may be used to study effects of sealant diffusion into a vacuum by replacing the test spindle with a double-groove spindle of equal total length, injecting the sealant through the middle pressure tap, and evacuating the cavity in the sleeve. This design is not conducive to studies of the load-carrying capacity of the visco seal.

CHAPTER III. FINAL DESIGN

This chapter presents the final design of the test facility. Figure 18 shows a cut section through the middle of the test area as an elevation view. The three major parts comprising the test area are the test spindle (see Figure 19), the hydrostatic bearing housing (see Figure 29, page 81), and the test sleeve (see Figure 30, page 82). The clearance between the test spindle and the test sleeve may be varied by changing the test spindle; the radial clearance between the test sleeve and the hydrostatic bearing is six mils at room temperature. The portion of the test spindle mating with the high-speed spindle is burnished with MoS_2 to prevent seizure of the two parts.

A complete schematic flow diagram of the systems serving the test facility is shown in Figure 24 in the Appendix, page 76. The hydrostatic bearing system is shown in the lower left corner of Figure 24. Oil returning from the bearing is collected in a sump tank. The main pump draws the oil out of the sump through a filter and heat exchanger and pumps it at a pressure of 1000 p.s.i. through a final filter and a gate valve and into the manifold block. Part of the oil returns directly to the sump tank through a relief valve that regulates the discharge pressure. From the manifold the oil flows through eight lines, which pass through flow control valves before delivering the oil to the eight pads in the two hydrostatic

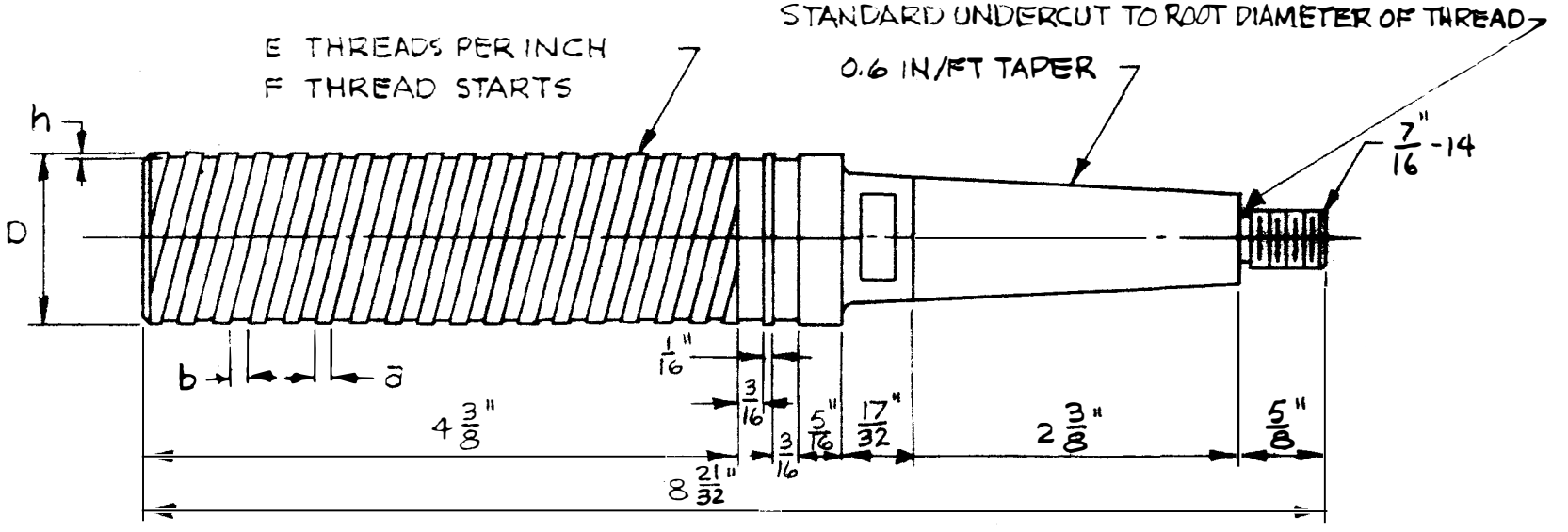

SPINDLE No.	DIMENSIONS						SPINDLE No.	DIMENSIONS					
	a	b	h	D	E	F		a	b	h	D	E	F
1	0.0934	0.1596	0.0101	1.2440	3.82	4	3B	0.0828	0.0842	0.0116	1.2408	5.90	4
2	0.1176	0.0494	0.0116	1.2465	5.90	"	4B	0.0514	0.1156	0.0101	"	5.90	"
3	0.0828	0.0842	0.0137	1.2461	5.90	"	5	0.1585	0.0607	0.0179	1.2455	4.52	2
4	0.0514	0.1156	0.0128	"	5.90	"	6	0.1070	0.1083	0.0180	"	3.82	"
2B	0.1176	0.0494	0.0092	1.2420	5.90	"	7	0.1083	0.1600	"	"	4.50	"

Figure 19. Test Spindle.

radial bearings. A pressure switch located on the manifold stops the test spindle if the oil pressure drops below a proscribed amount.

The sealant supply tank provides the test sleeve with sealant at a controlled pressure. A pressure gage and a relief valve are located on the sealant tank to indicate approximate sealant supply pressure and to provide a safety backup for the pressure regulators, respectively.

The pressures developed in the seal are measured through five equally spaced twenty-five mil pressure taps leading through flexible tubing to three-way valves. For lower pressures manometers are used, and for higher pressures bourdon tube pressure gages are employed.

The temperature distribution is determined by five equally spaced thermocouples.

The torque is measured by a strain-gage beam and an SR-4 indicator. A microswitch turns off the spindle drive motor if the torque on the sleeve causes the beam to deflect more than a proscribed amount.

The clearance indication system consists of four induction-type clearance probes attached to the test sleeve. Each probe is connected to a distance detector powered by a common direct-current power supply unit. The detector output is monitored by vacuum tube voltmeters.

Cooling of the seal is provided by a 1/4-inch cooling coil wrapped around the test sleeve and soldered in place.

The test spindle is driven by a two-horsepower thymotrol controlled direct-current motor. The power is transmitted through two precision spindles that step up the speed by a factor of ten. The high-speed spindle is lubricated by an oil mist system that must become operative before the motor will start. An optical tachometer measures the speed of either the high- or low-speed spindle, from which the speed of the test spindle may be computed.

The visco seal tester consists of a test stand upon which most of the component parts are located; an oil stand, which supplies the hydrostatic bearings with oil at approximately 1000 p.s.i. and constant temperature; and the instrumentation and control stand. The assembled visco seal test stand is shown in Figures 25 and 26 in the Appendix, pages 77 and 78; the assembled oil stand is shown in Figure 33, page 85; and the assembled control stand is shown in Figure 38, page 90. No flexible lines are shown on any assembly drawings. Parts lists are shown with each assembly drawing, and the make and model of all purchased items are given in Table IV.

Of the eight systems that service the test area, the most involved is the hydrostatic bearing system. Justification of the decision to employ hydrostatic bearings is simple; there is no more direct nor more economical way to achieve the desired results. The

TABLE IV

MAKE AND MODEL OF PURCHASED ITEMS

Commercially available item number	Manufacturer	Model number
1	Apco	10In2
2	Robertshaw-Fulton Controls Company	Unknown
3	Robertshaw-Fulton Controls Company	Unknown
4	U.S. Gauge	19583
5	U.S. Gauge	18636
6	Unknown	Unknown
7	Unknown	Unknown
8	Bently Scientific Company	D-152
9	General Electric Company	5CD187E203
10	Globe Woven Belting Company	No. 200 Apache
11	Microswitch Corporation	BZE-7RQT2
12	Whitnon Manufacturing Company	B257D
13	Illinois Testing Laboratories, Inc.	139818
14	Whitnon Manufacturing Company	B257DUTI
15	C. A. Norgren Company	10-015-004
16	C. A. Norgren Company	701-200-11
17	Jackes-Evans Manufacturing Company	B2P2
18	C. A. Norgren Company	12-001-012
19	Hewlett-Packard Company	506A
20	American Brake Shoe Company	FC0423102
21	Unknown	Unknown
22	Unknown	Unknown
23	U.S. Navy Surplus	307795
24	Meletron	302-155
25	Circle Seal	5159T-6T-300
26	Unknown	Unknown
27	Vacco Valve Company	NV-6P-402-2M
28	U.S. Motor	310579
29	American Brake Shoe Company	B5939
30	American Brake Shoe Company	35-11707-X
31	Bendix Aviation Corporation	5-S-13460-16-D-0
32	Vacco Valve Company	NVA-6P-404-2M
33	U.S. Gauge	18913
34	Bendix Aviation Corporation	Unknown
35	Budd Company	P-350
36	Bently Scientific Company	E-30

TABLE IV (Continued)

Commercially available item number	Manufacturer	Model number
37	Rubicon Company	67122
38	Unknown	Unknown
39	Hewlett-Packard	522B
40	Lewis Engineering Company	10 S 18
41	Electronic Instrument Company	221
42	Unknown	Unknown
43	General Electric Company	CR2943A200A
44	Westinghouse Corporation	32063-B
45	Cutler-Hammer	Unknown
46	General Electric Company	9T51Y107
47	General Electric Company	9T51Y32
48	Westinghouse Corporation	NP45824-A
49	General Electric Company	Unknown
50	Hallowell	Unknown

power a given visco seal dissipates must be determined, and only two readily feasible methods are known to the author by which this determination may be accomplished. The first method, the calorimetry analysis, was rejected on the basis of excessive instrumentation and operation costs to achieve the desired precision; therefore, the method of free-floating the sleeve is the most likely alternative. Design calculations for the selected bearing geometry (see Figure 29, page 81 in the Appendix) for both the hydrostatic radial and thrust bearing are shown in a report by Stair (14).

The sealant is supplied under pressure at 0 to 75 p.s.i. gage. The sealant supply tank stores approximately one gallon of sealant and is pressurized by compressed nitrogen. The pressure in the nitrogen cylinder is approximately 2000 p.s.i. gage and is reduced through two pressure regulators connected in series. The second pressure regulator is used to adjust the sealant supply pressure.

To reduce the limits of precision on the pressure indication system an arrangement was devised to measure low pressures in the seal with manometers in inches of sealant and to switch to Bourdon tube pressure gages to measure higher pressures.

Thermocouples were inserted in the test sleeve thirty mils radially from the seal, and the temperature of the sealant is assumed to be equal to the temperature recorded.

An interesting problem encountered was: how may the distance between two close surfaces be measured without allowing any mechanical contact between the two surfaces. It is clear that since the sleeve

must be free-floating, no torque on the sleeve due to the contact friction associated with a dial gage indicator can be tolerated. In general, three types of systems are proposed for the solution of this problem (15). The first is the optical system, which is quite accurate but was rejected for this confined application because it is awkward to use. The second is the capacitance system, which works on the principle of an inverse function between the capacitance in a circuit and the proximity of the two surfaces to each other. This system was rejected because the presence of the sealant between the two surfaces introduces a variable dielectric and this affects the capacitance in the circuit. The third system is the inductance system, which was the one selected. The inductance system operates on the principle of an inverse function between the inductance in a circuit and the proximity of the two surfaces to each other. Unlike the capacitance, the inductance in a circuit is not significantly affected by the presence of sealant between the sleeve and the test spindle.

The cooling coils were located close to the test spindle-sleeve interface to provide the maximum control over the temperature of the sealant.

The drive motor selected has an operation range between 300 and 2500 r.p.m., but by interchanging the pulleys on the high-speed spindle and the low-speed spindle the test spindle may be operated at either 2 1/2 or 10 times the motor speed (subject to the horsepower limitations on the drive motor). The direct-current

drive motor and all pulleys are balanced to minimize vibration of the test stand. The belting selected is designed for high-speed applications in the range required for this study.

CHAPTER IV. STARTUP AND ANALYSIS

In this chapter, problems encountered during startup and operation of the visco seal tester are presented along with changes necessary to overcome those difficulties. A portion of the data obtained is presented and compared with test results of other investigators.

There were three major problems encountered in the startup of the hydrostatic bearing system. The first problem was the inability of the oil to return from the hydrostatic bearings to the sump tank by gravity flow at the flow rate required by the bearings. To solve this problem, a small vane pump unit was placed on the floor under the test stand and connected into the line between the hydrostatic bearings and the sump tank to pump the oil back to the oil stand. A gate valve was positioned in the line between this small return pump and the sump tank to regulate the flow of the oil back to the sump in order to make the flow to and from the test stand equal and to prevent the vane pump from pumping air into the sump tank. To facilitate the adjustments necessary to equalize the flow rate to and from the test stand, a small sump pan was placed on the test stand just below the hole in the test stand table top. This small sump collects the oil before its return to the large sump tank on the oil stand through the small return pump unit.

Figure 40 (see page 92 in the Appendix) shows the return pump and motor unit used, the small sump, and a revised schematic diagram of the part of the system that was changed. In addition, the drainage system away from the bearing block on the test stand was not adequate for the flow rate required. Therefore, a small dam was placed around the bearing block to allow the bearing oil to drain through the table top into the small sump. A drawing of this dam is also shown on Figure 40.

The second problem encountered in the hydrostatic bearing system was an excess of air bubbles in the oil, as indicated by "air hammer" in the pump. An extension was installed on the oil return line to dump the oil into the sump tank at the opposite end of the tank from the point where the oil discharges from the tank into the heat exchanger. By this arrangement, the oil was given more time to settle, and the noise in the pump was diminished considerably.

At one point the test sleeve began to show signs of lack of freedom. Upon removing the test sleeve from within the hydrostatic bearing block, a large quantity of small particles were discovered between the test sleeve and the hydrostatic bearing surface. Examination of the final filter on the discharge side of the oil pump revealed extensive damage. This third problem was caused, in the opinion of the investigators, by operational procedure. During shutdown it had been customary to simply shut off the oil pump drive motor after shutting off the test spindle drive motor. This procedure

left the lines on the discharge side of the pump empty (see Figure 24 in the Appendix, page 76). When the oil pump was restarted a sudden surge of oil at a high pressure passed through the filter, causing its eventual failure. A new procedure was initiated in which during shutdown the gate valve in the line to the manifold is closed before the oil pump drive motor is shut off, forcing the oil through the relief valve during the last few seconds of operation. Oil is therefore left in the line between the pump and the relief valve. During startup the pump motor is started before the gate valve is re-opened, eliminating the surge on the filter.

One final point should be made concerning the hydrostatic bearing system. The bearing block was designed to be positioned concentric with the test spindle at room temperature, so that the test sleeve would be positioned concentric with the test spindle when the oil flow rate through each pad was approximately equal. At operating temperature, however, the bearing oil heats up the hydrostatic bearing block and thermal growth takes place, positioning the centerline of the hydrostatic bearing slightly higher than that of the test spindle. Therefore, in order for the test sleeve to be positioned concentric with the test spindle, it must be positioned in an eccentric position relative to the hydrostatic bearing block when the bearing oil is at operating temperature.

One of the most important systems as far as data output is concerned is the pressure indication system. It is the pressure gradient, or the plot of sealant pressure versus seal length, which given an indication of the effective seal length, and the slope of this line indicates the increment of pressure per increment of seal length of which the given seal geometry is capable under the given conditions. It is important, therefore, that the limits of precision on the pressure indication system be as small as possible. The investigators felt that the pressure system as designed did not provide small enough limits of precision. One major error that became obvious during operation was that no method was provided by which the lines to the pressure gages could be bled to eliminate bubbles in the lines. During the early operation of the tester, violent bubbling of air into the pressure line was observed. This phenomenon, although not fully understood, is attributed to a combination of an air ingestion effect (16) and the circulation of air trapped in the sleeve. The bleed lines were provided, but they did not solve all of the problems which the air bubbling created. No matter how much the lines to the pressure gages were bled, air continued to be trapped in the lines, making the gage elevation corrections inaccurate. Air bubbles also became lodged in the plastic tubing that served as the manometers and were removed only with extreme difficulty. In addition, pressure loss due to the sealant passing through one valve and several feet of tubing

before it reached the manometer board contributed to the error in the manometer readings. It was the opinion of the investigators that the combination of all of the problems encountered in the use of the pressure indication system as designed made that system unacceptable and a new pressure indication system was designed and constructed. The new system was designed with as little tubing between the pressure taps and the pressure indicator as possible and with a bleed line located in such a manner as to eliminate as many bubbles from the system as possible. In addition, the pressure indicators were located on the same elevation as the centerline of the test spindle to eliminate the need for elevation correction.

Figure 41 in the Appendix (page 93) shows the new pressure indication system. Six mercury manometers and three pressure gages are located on a stand at the same elevation as the test spindle. The seal- and supply pressure and the first two pressure taps are read either on a gage or a mercury manometer, and the pressures at the last three pressure taps are measured on mercury or water manometers. This stand is located beside the test stand, and sealant flows through the flexible plastic tubing from the pressure taps on the test sleeve to a tee above the sleeve. Out of one side of the tee extends the flexible tubing to the pressure indicators; out of the other side of the tee extends the bleed line. Gate valves in both the lines to the pressure indicators and the bleed lines may be set to route the sealant through either line. When the lines to the pressure indicators are first filled with water, air bubbles may be bled out of the lines from the test sleeve to the

tees to eliminate most of the bubbles in the system. This system is considerably more accurate than the previous system and has operated satisfactorily.

As has been stated, one major source of bubbling was believed to be the circulation of air trapped in the sleeve. In a later alteration, the bubbling due to air entrapment was successfully eliminated by drilling a hole in the test sleeve for a bleed line at the top of the cavity. Only a slight amount of bubbling in taps Number 4 and 5, except for operation in the turbulent range, was observed thereafter.

Some difficulty was experienced in obtaining precise torque readings, but the difficulty was overcome by altering the procedure rather than the equipment. In the initial procedure, a zero was recorded at zero speed and the strain was read at each speed after manually lifting the torque arm and allowing it to settle on the beam. A zero was again taken at the end of each series of runs, and the two zeros were not often in agreement. By the revised procedure, a zero is read at the beginning of each run after vibrating the test stand, a strain is read at the speed for that run after the test stand has again been vibrated, the test spindle is stopped after each run, and the table is again vibrated and another zero strain read. The initial and final zero strains are averaged together to establish a working zero strain. The zero is observed to increase a slight amount with each increase in speed. At no time is the torque arm lifted from the beam. That the revised procedure is considerably more accurate is obvious when the difference in the data spread before and after its initiation is observed.

Figures 20 through 23 show data points obtained during the "shakedown" operation of the tester employing a seal with approximately the same screw thread geometry as used by McGrew and McHugh.

Screw Thread Geometry Tested	Screw Thread Geometry Tested by McGrew and McHugh
α = 14.5 degrees	α = 14.5 degrees
β = 3.38	β = 3.86
γ = 0.631	γ = 0.625

Water was the sealant used, and a radial clearance of 0.0035 inch was selected. The computed theoretical sealing coefficient and dissipation function for laminar flow with this screw thread geometry are 11.373 and 0.622, respectively. The experimental data were obtained by operating the test spindle at various speeds while measuring the dynamic torque on the sleeve (to compute power dissipation), the average temperature of the sealant (to compute the viscosity), the operating speed, the distance between the test sleeve wall and the test spindle at the probe locations (to compute the eccentricity), and the sealant pressure at locations along the shaft. A value for dp/dL was obtained by plotting a pressure profile, drawing the best linear fit, and computing a $\Delta p/\Delta L$ based on the intercepts of the curve. From the raw data thus obtained, the value for the sealing coefficient and dissipation function were obtained from Equations (17) and (19), and a value for the Reynolds number as defined by

$$Re_c = \frac{Uc\rho}{\mu} \tag{29}$$

was computed at each speed.

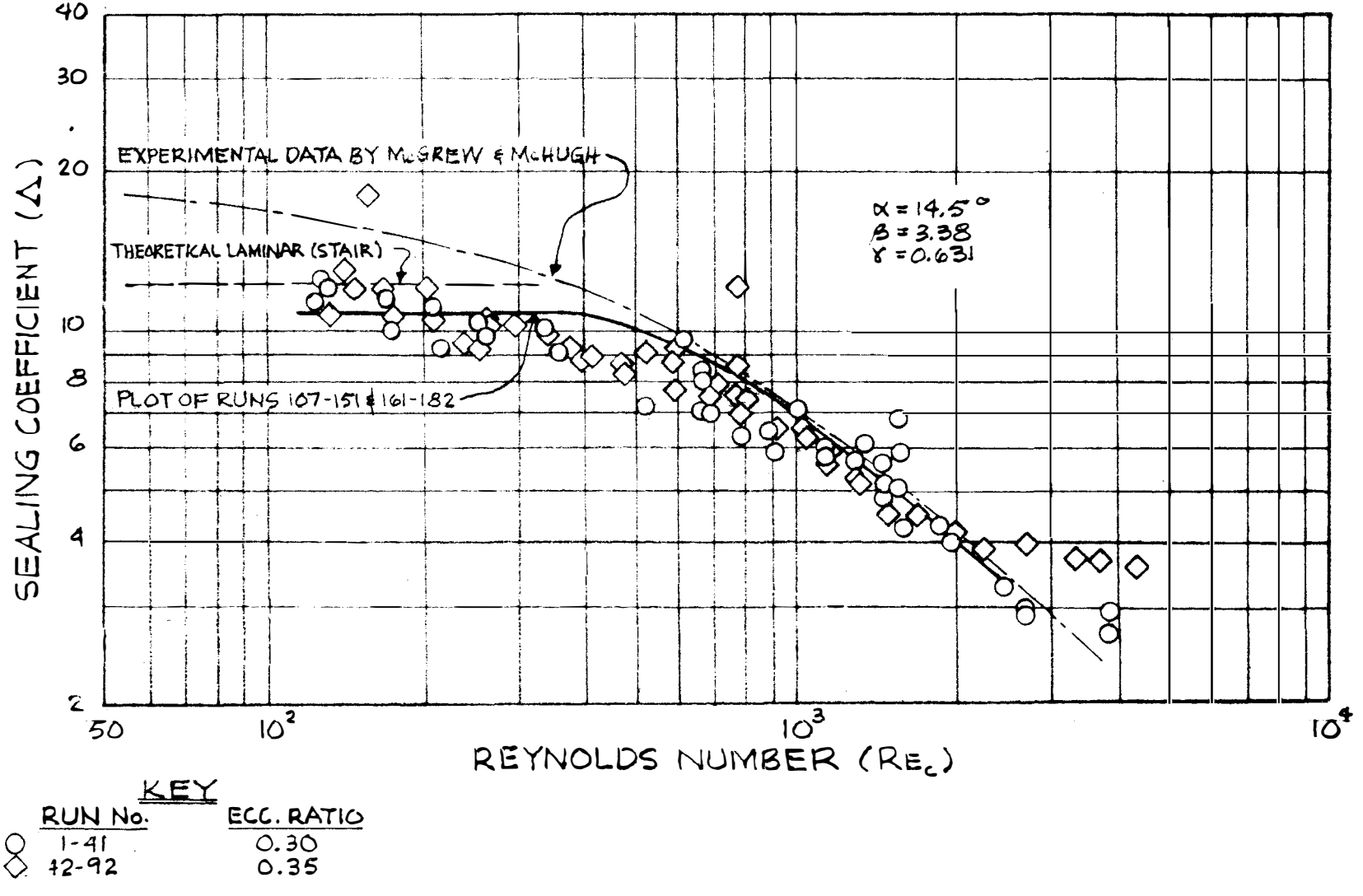

Figure 20. Sealing Coefficient versus Reynolds Number.

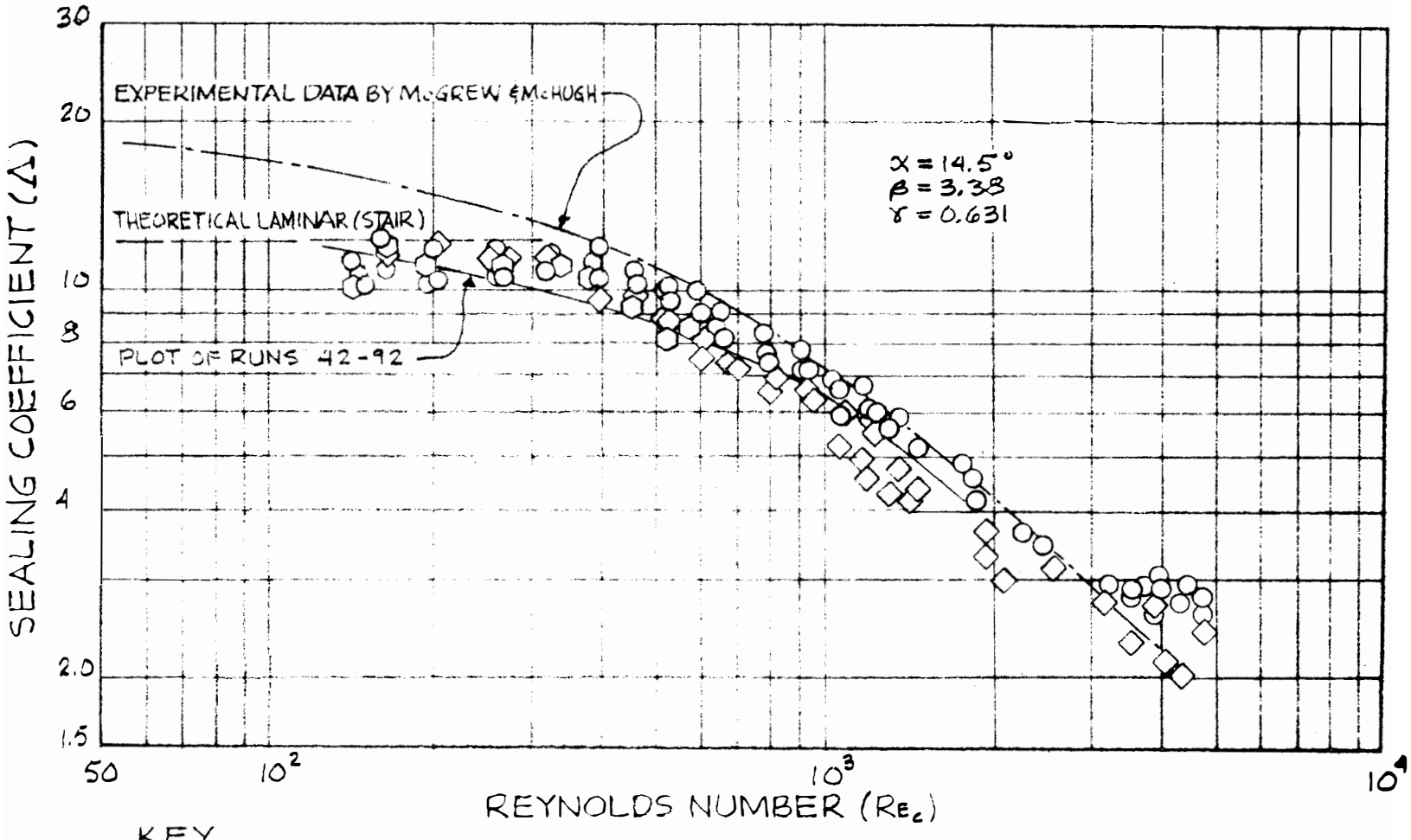

Figure 21. Sealing Coefficient versus Reynolds Number.

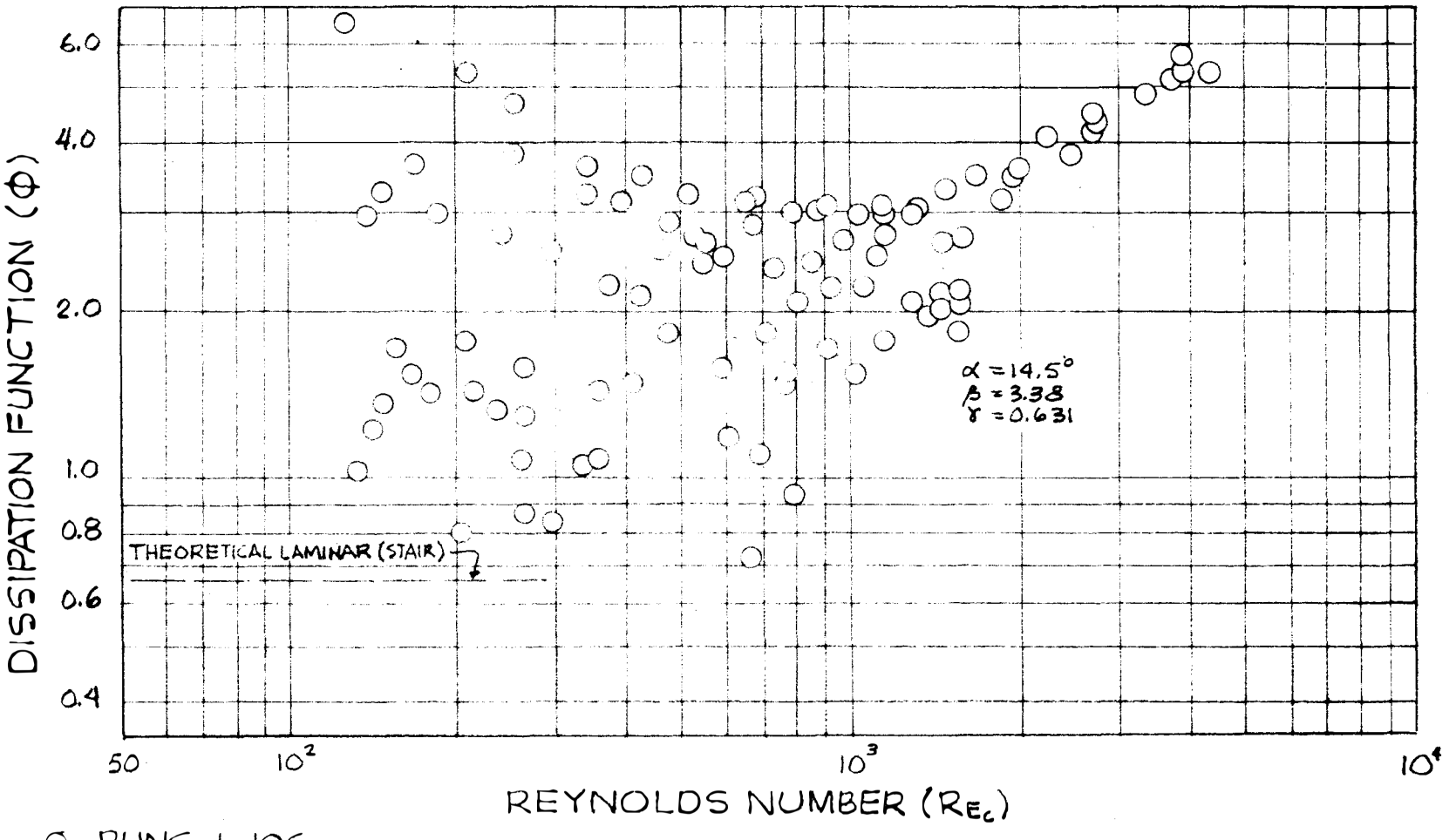

Figure 22. Dissipation Function versus Reynolds Number.

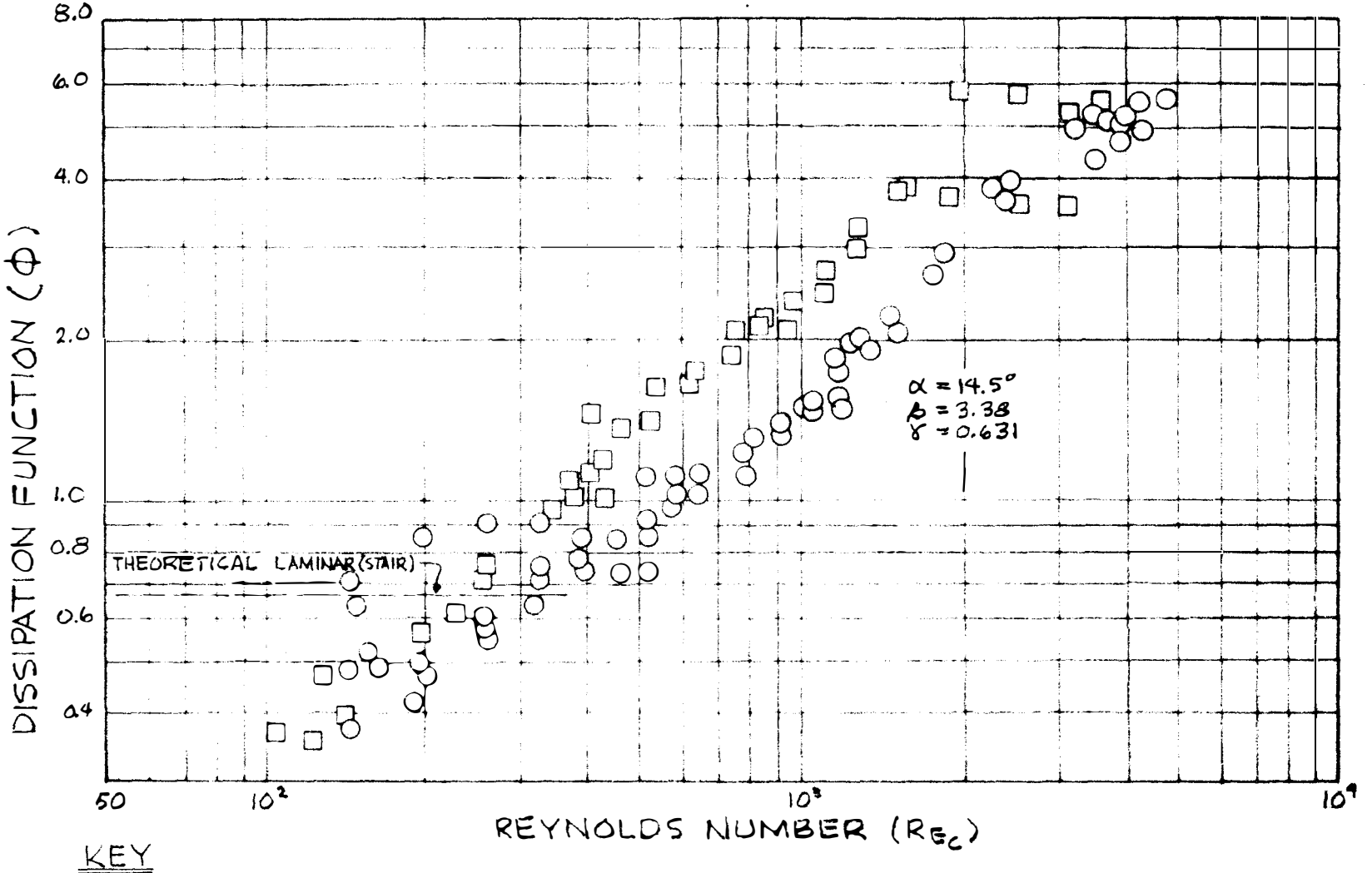

KEY

RUN NO.	ECC. RATIO
○ 107-182	0.15
□ 183-226	0.60

Figure 23. Dissipation Function versus Reynolds Number.

Consider Figure 20, in which are shown circles (runs 1 through 41) that were recorded using the original pressure system and diamonds (runs 42 through 92) that were recorded using the revised pressure system. The revised pressure system produces data that have less spread than the data produced by the original system. During runs 1 through 92 large numbers of bubbles were observed in the manometer lines during the transition from laminar to turbulent flow due to the air entrapment in the sleeve. In runs 107 through 151 and runs 161 through 182 (circled points) an insignificant number of bubbles were observed in the system in the lower turbulent region.

The data in runs 183 through 226 were taken as the seal operated in an eccentric position. Contrary to the conclusion drawn by McGrew and McHugh (10), experimental evidence indicates that the effect of eccentricity in the laminar region appears to be negligible. Eccentric operation in the turbulent region was observed to increase air ingestion and to decrease the value of the sealing coefficient. The data in runs 152 through 160 were taken after the tester had been idle for several days with water in the sleeve. Upon operation, a large quantity of bubbles were observed in the system in the laminar region. Oil was rubbed on the screw, and the bubbling ceased. The investigators concluded that the water had wetted the seal during the long period of inoperation, allowing an increase in air ingestion. These results suggest that the wettability of a sealant may be a significant factor in air ingestion.

As may be observed in Figures 20 and 21, the test results from this study agree with the experimental results obtained by McGrew and McHugh (10) in the turbulent region only. Although there is not substantial proof, it is the opinion of this author that the low speeds and corresponding low pressures made an accurate pressure distribution along the seal difficult to obtain at the lower Reynolds numbers corresponding to the laminar region, where significant disagreement exists between the experimental results reported by McGrew and McHugh and those reported in this study. At low pressures the pressure distribution may be biased by two different pressure indication systems and is subject to considerable interpretation in obtaining the appropriate sealing pressure-to-effective seal length ratio.

The data in Figure 22 (runs 1 through 106) were taken using the original torque-measuring procedure, while the data in Figure 23 (runs 107 through 226) were taken using the revised procedure. The improvement is evident.

From the foregoing discussion it may be concluded that

1. The visco seal test stand presented and discussed in this study has been fabricated and operated successfully and has produced reasonable data.
2. The data discussed in this study are of the same general nature as those published by McGrew and McHugh.

3. The data obtained in the laminar region agree reasonably well with the theoretical values of the sealing coefficient and dissipation function as predicted by Equations (17) and (20), respectively.

In addition, some conclusions may be suggested concerning the visco seal in general. These conclusions are

1. The effect of eccentric operation in the laminar region is negligible, but in the turbulent region eccentric operation increases air ingestion and decreases the value of the sealing coefficient.
2. The wettability of a sealant may be a significant factor in air ingestion.

It should be noted that the general conclusions drawn regarding the visco seal are of a preliminary nature.

LIST OF REFERENCES

LIST OF REFERENCES

1. Stair, W. K. "The Visco Seal – A Survey." The University of Tennessee Report No. ME-5-62-2, March 1962.

2. Rowell, H. S., and D. Finlayson. "Screw Viscosity Pumps." Engineering, Vol. CXIV, November 17, 1922, pp. 606–07.

3. Rowell, H. S., and D. Finlayson. "Screw Viscosity Pumps." Engineering, Vol. CXXVI, August 31, 1928, pp. 249–50; Vol. CXXVI, September 28, 1928, pp. 385–87; "Discussion, Vol. CXXVI, November 23, 1928.

4. Asanuma, T. "Study on the Sealing Action by Viscous Fluids." Transactions of the Japan Society of Mechanical Engineers, Vol. XVII (Issue 60), 1951, pp. 119–25.

5. Boon, E. F., S. Honingh, and D. C. Van Rijssen. "Some Notes on Seals for Rotating Shafts." Proceedings, Fourth World Petroleum Congress, Section VII/A, Paper 1, June 10, 1955.

6. Van Hoek, P.H.F. "Overzichtsrapport over reeds verrichte onderzoekinger aan Visco-afdichtingen." Technische Hogeschool Te Delft, April 20, 1955.

7. Frössel, W. "Hydrodynamisch Wirkende Wellendichtung" (Hydrodynamic Shaft Seals). Konstruction, Vol. VIII (Issue 11), November 1965, pp. 463–66; abstract: The Engineer's Digest, Vol. 18 (Issue 1), 1957, pp. 18–20.

8. Boon, E. F., and S. E. Tal. "Hydrodynamische Dichtung für rotierende Wellen" (Hydrodynamic Seal for Rotating Shafts). Chemie-Ing. Technik, Vol. XXXI (Issue 3), January 31, 1959, pp. 202–12. Translated by R. Presser and published by United Kingdom Atomic Energy Agency as DEG Information Series 13 (CA) (1961).

9. Asanuma, T. "Studies on the Sealing Action of Viscous Fluids." Paper A3, presented at the International Conference on Fluid Sealing, April 17–19, 1961, BHRA, Harlow, Essex, England.

10. McGrew, J. M., and J. D. McHugh. "Analysis and Test of the Screw Seal in Laminar and Turbulent Operation," General Electric Advanced Technology Laboratories Report No. 63GL66, May 3, 1963.

11. Zotov, V. A. "Research on Helical Groove Seals." Machine Design and Calculation (Russia) No. 10.

12. Radzimovsky, E. I. Lubrication of Bearings. Ronald Press, New York, 1959.

13. Stair, W. K. "Analysis of the Visco Seal Part I — The Concentric Laminar Case." The University of Tennessee Report No. ME-65-587-2, January 1965.

14. Stair, W. K. "Theoretical and Experimental Studies of Visco-Type Shaft Seals," Semiannual Progress Report, October 15, 1964, to April 15, 1965. The University of Tennessee Report No. ME-65-587-3, May 21, 1965.

15. Fourman, J. F. "Distance Measurements Without Contact." Oak Ridge Recorder, Vol. VII (Issue 10), March 1962.

16. Letter from W. K. Stair to R. L. Johnson and Joseph Maltz, NASA, July 23, 1965.

APPENDIX

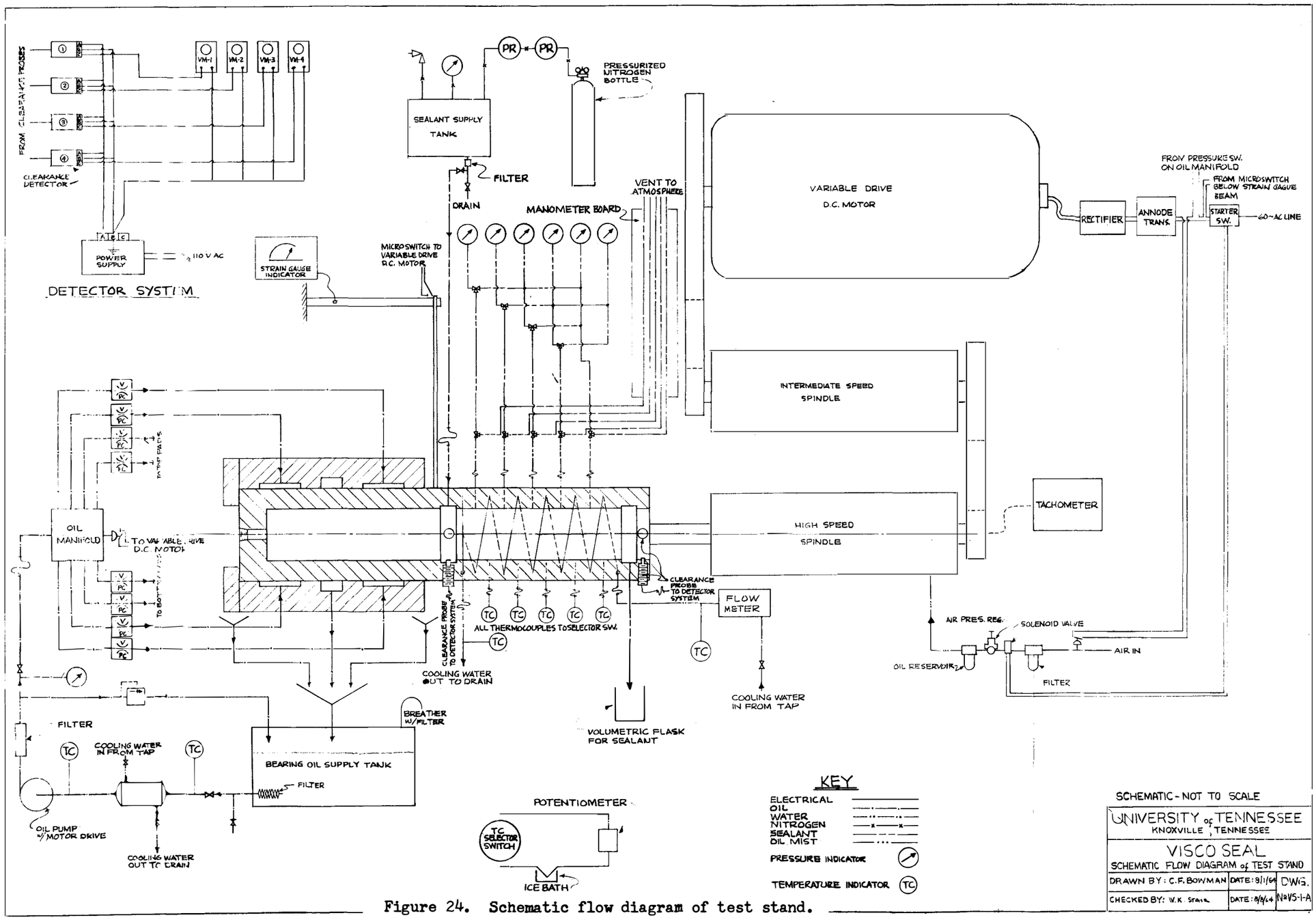

Figure 24. Schematic flow diagram of test stand.

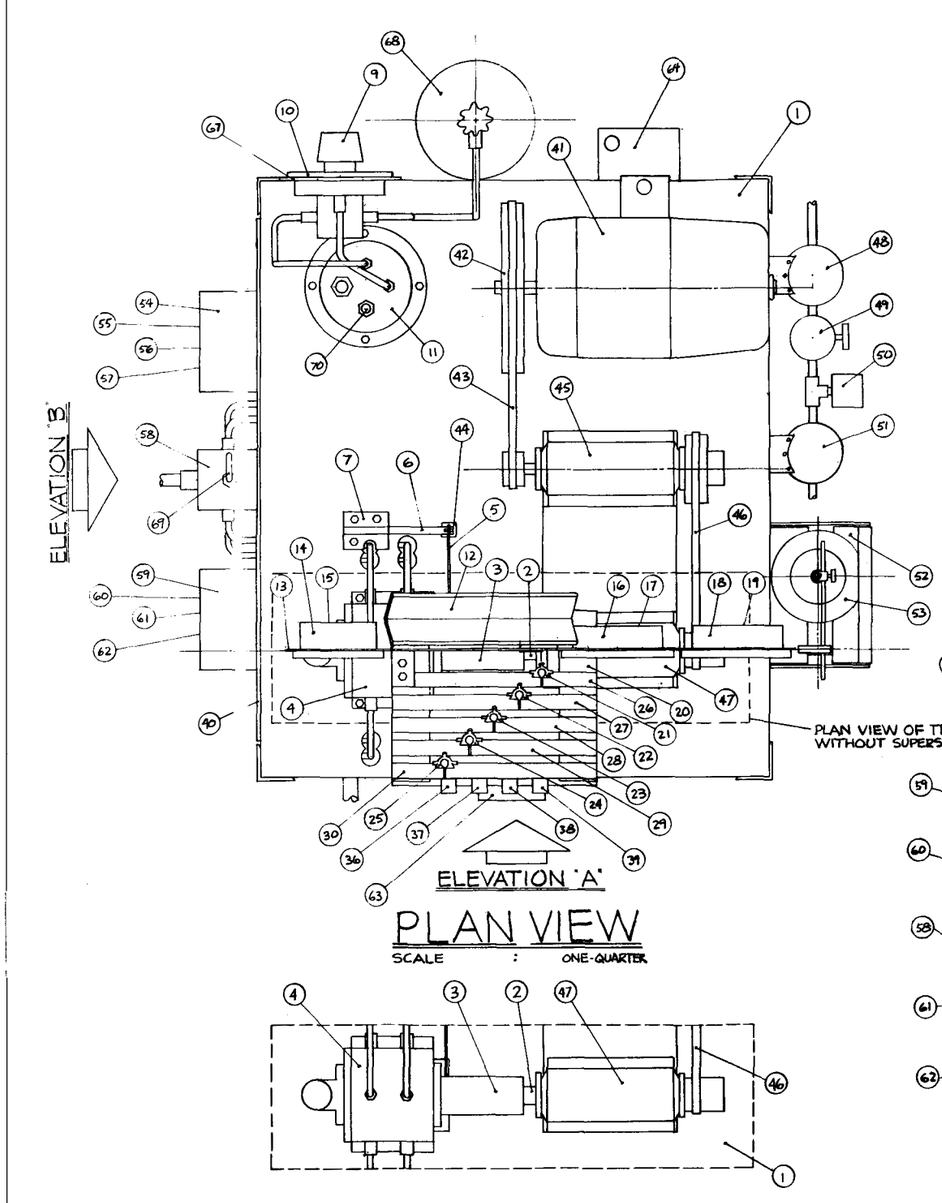

PLAN VIEW

SCALE : ONE-QUARTER

PLAN VIEW OF TEST AREA WITHOUT SUPERSTRUCTURE

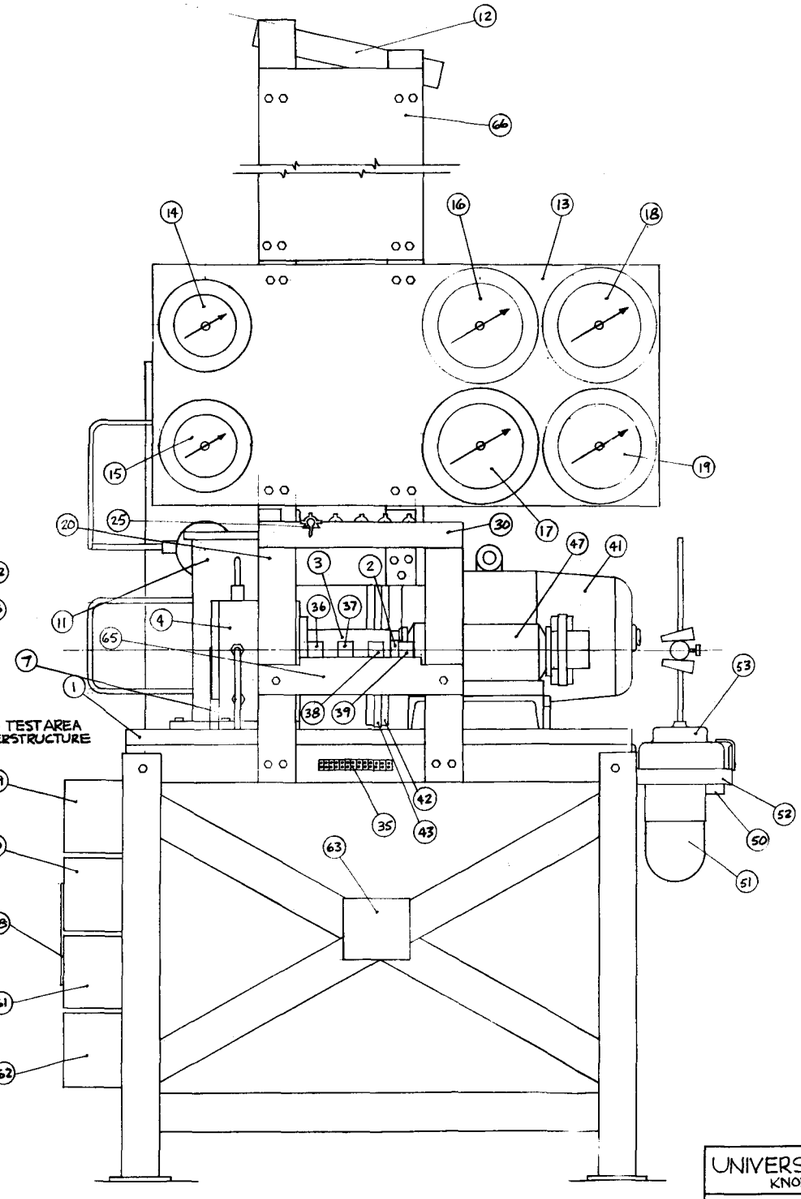

ELEVATION "A"

SCALE : ONE-QUARTER

UNIVERSITY of TENNESSEE KNOXVILLE, TENNESSEE		
VISCO SEAL TEST STAND ASSEMBLY		
DRAWN BY: C.F. BOWMAN	DATE: 11/1/61	DWG. No. 5-2A
CHECKED BY: W.R. STAHL	DATE: 12-9-61	

Figure 25. Test stand assembly.

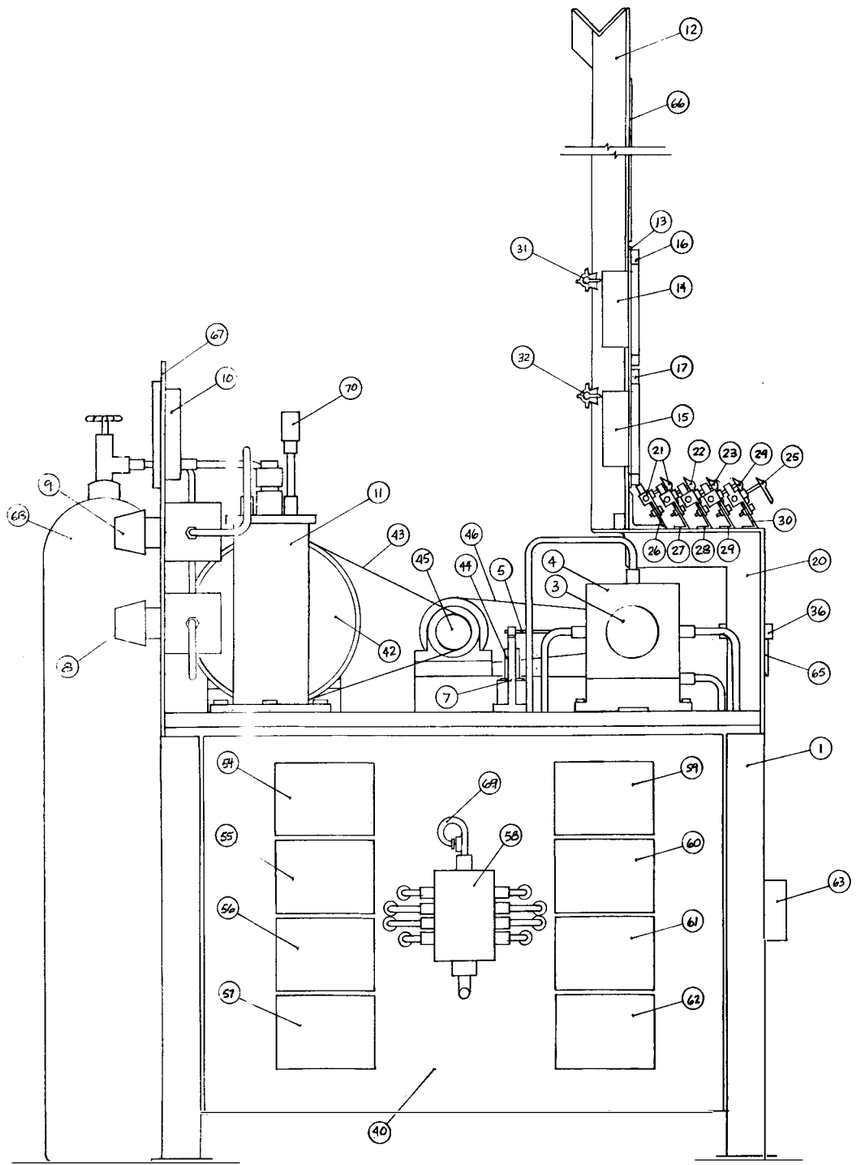

ELEVATION "B"

SCALE : ONE-QUARTER

PARTS LIST

PART Nº	DESCRIPTION	DWG. Nº
1	TEST STAND	VS-9-A
2	TEST SPINDLE	VS-9-A
3	TEST SLEEVE	VS-7-A
4	OIL PAD BEARING HOUSING	VS-6-A
5	TORQUE ARM	VS-5-A
6	STRAIN GAUGE BEAM	VS-5-A
7	STRAIN GAUGE BEAM STAND	VS-10-A
8	PRESSURE REGULATOR	CA1-1
9	PRESSURE REGULATOR	CA1-1
10	PRESSURE GAUGE	CA1-2
11	SEALANT SUPPLY TANK	VS-5-A
12	MANOMETER BOARD SUPPORT	VS-10-A
13	PRESSURE GAUGE PANEL	VS-10-A
14-15	PRESSURE GAUGE	CA1-3
16-17	PRESSURE GAUGE	CA1-4
18-19	PRESSURE GAUGE	CA1-5
20	PRESSURE TAP & SEALANT SUPPLY TUBE BRACKET	VS-5-A
21-25	3-WAY SEALANT VALVE	CA1-6
26-30	SEALANT VALVE SUPPORT	VS-10-A
31-34	3-WAY SEALANT VALVE	CA1-6
35	THERMOCOUPLE WIRE JUNCTION	CA1-7
36-39	DISTANCE DETECTOR	CA1-8
40	FLOW CONTROL VALVE PANEL	VS-5-A
41	D.C. MOTOR	CA1-9
42	D.C. MOTOR PULLEY	VS-11-A
43	HIGH SPEED BELT	CA1-10
44	MICROSWITCH	CA1-11
45	LOW SPEED SPINDLE	CA1-12

PART Nº	DESCRIPTION	DWG. Nº
46	HIGH SPEED BELT	CA1-13
47	HIGH SPEED SPINDLE	CA1-14
48	MICRO-FOG	CA1-15
49	PRESSURE REGULATOR	CA1-16
50	SOLENOID VALVE	CA1-17
51	FILTER	CA1-18
52	TACHOMETER EYE SUPPORT	VS-11-A
53	TACHOMETER EYE	CA1-19
54-57	FLOW CONTROL VALVE	CA1-20
58	MANIFOLD	VS-5-A
59-62	FLOW CONTROL VALVE	CA1-20
63	JUNCTION BOX	CA1-21
64	JUNCTION BOX	CA1-22
65	DISTANCE DETECTOR SUPPORT	VS-11-A
66	MANOMETER BOARD	VS-10-A
67	SEALANT PRESSURE REG. & INDICATOR PANEL	VS-5-A
68	NITROGEN BOTTLE	CA1-23
69	PRESSURE SWITCH	CA1-24
70	RELIEF VALVE	CA1-25
71	FILTER	CA1-26
72-73	GATE VALVE	CA1-27

NOTE
CA1- INDICATES COMMERCIALLY AVAILABLE ITEM.
FOR MAKE AND MODEL OF ITEMS LISTED, SEE TABLE V.

UNIVERSITY of TENNESSEE
KNOXVILLE, TENNESSEE

VISCO SEAL
TEST STAND ASSEMBLY

DRAWN BY: C.F. BOWMAN	DATE: 12/5/64	DWG.
CHECKED BY: W.K. STARK	DATE: 12-9-64	Nº VS-31

Figure 26. Test stand assembly.

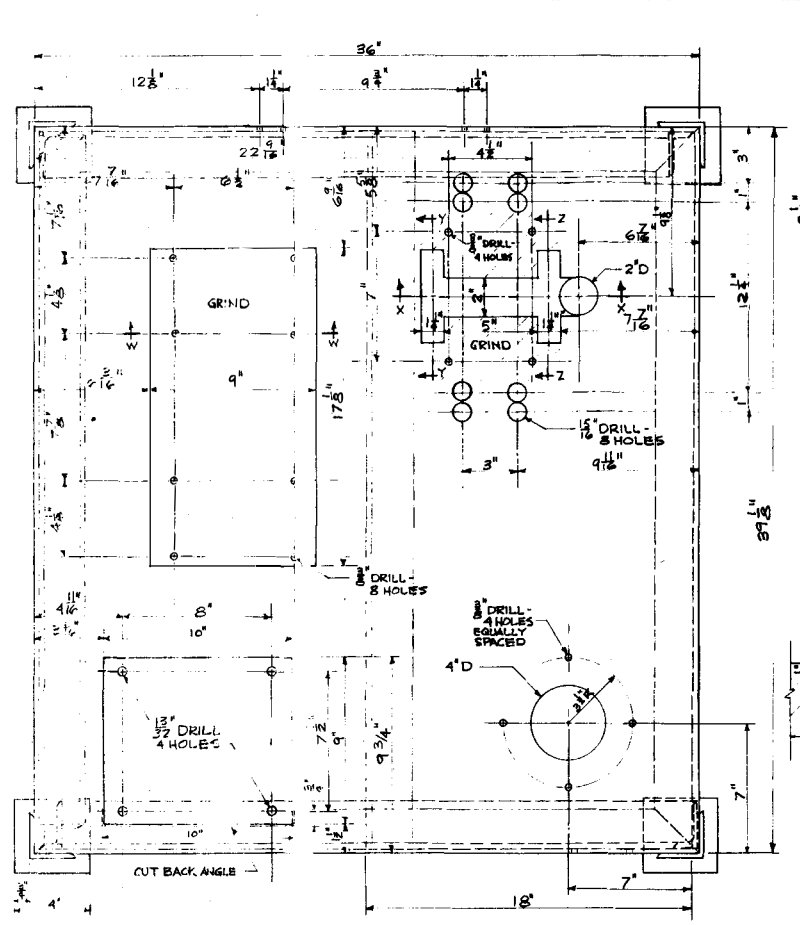

PLAN VIEW

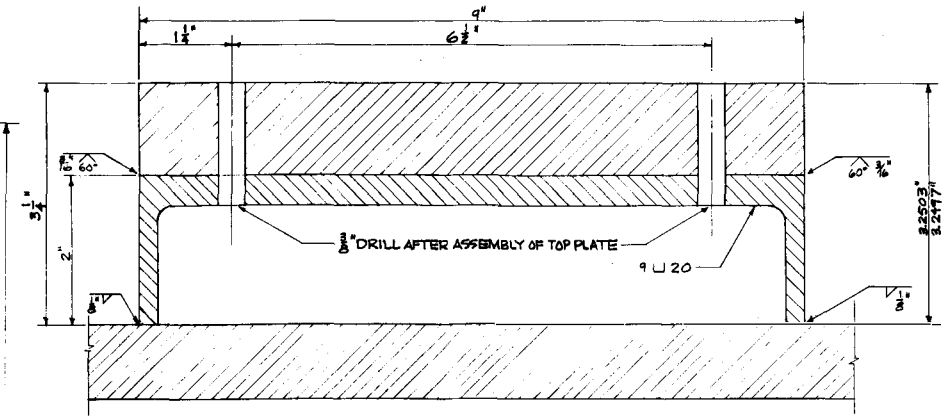

SECTION W-W
SCALE : FULL

NOTE
MILL CUTTER MAY NOT BE LARGER THAN 3 1/4" DIAMETER

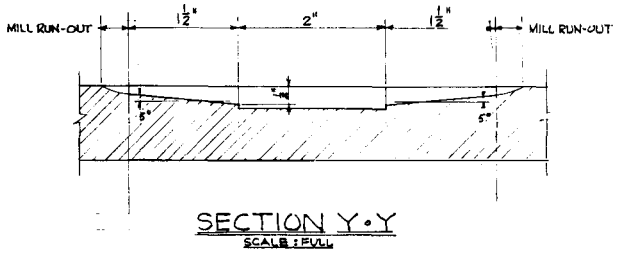

SECTION Y-Y
SCALE : FULL

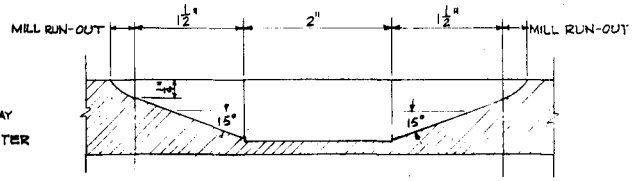

SECTION Z-Z
SCALE : FULL

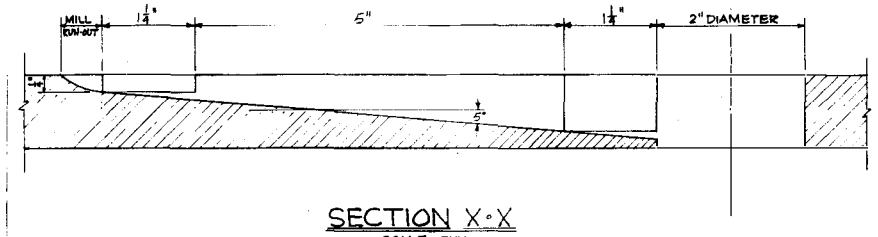

SECTION X-X
SCALE : FULL

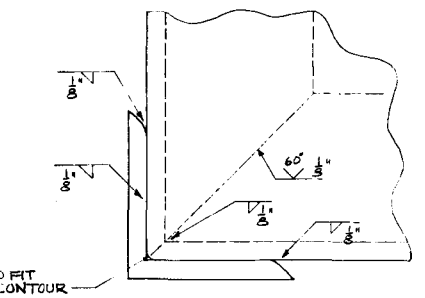

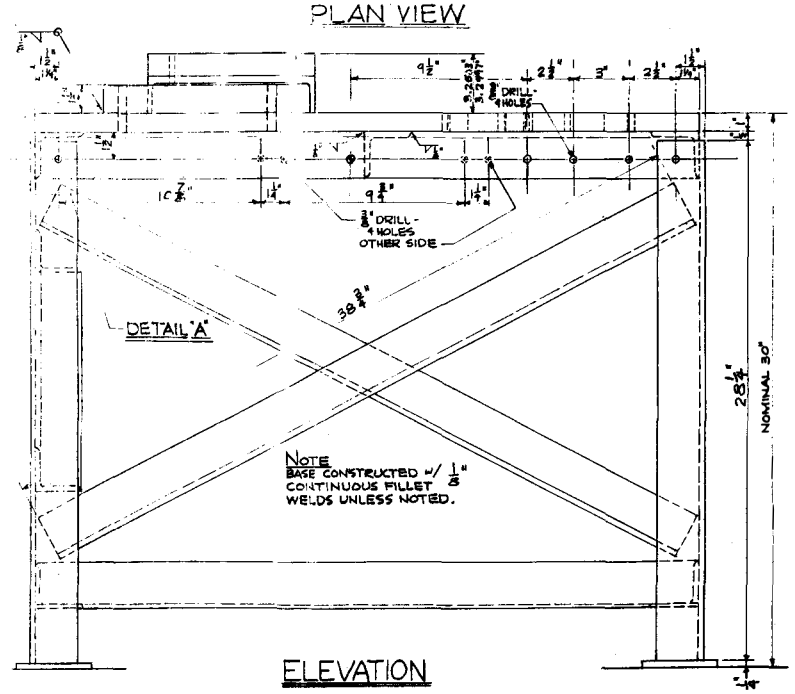

ELEVATION

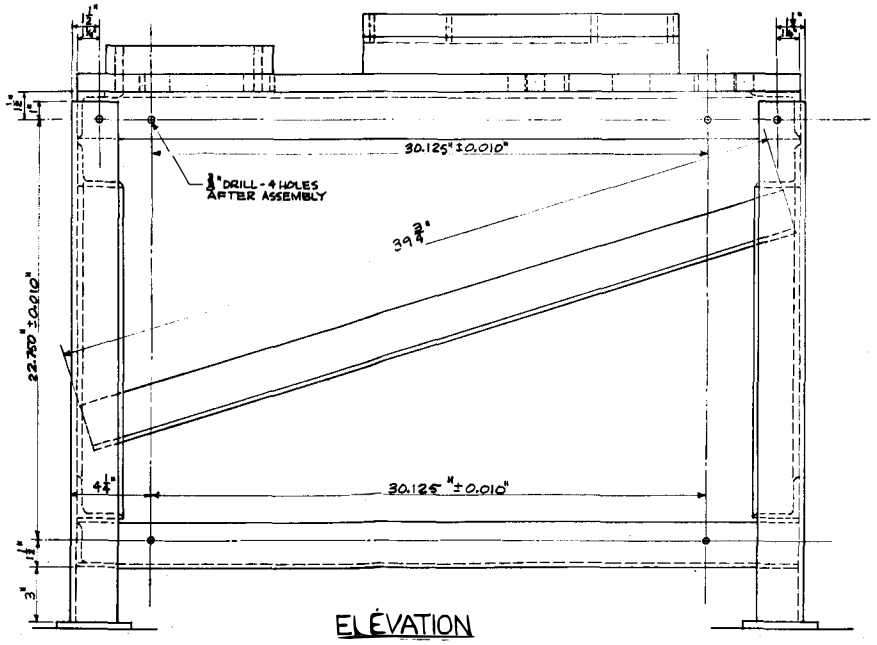

ELEVATION

NOTE
1/4" HOLE TO BE DRILLED IN TOP PLATE & BASE. MACHINE TOP PLATE & BOLT TO BASE. WELD AROUND BOLTED JOINT AS INDICATED.

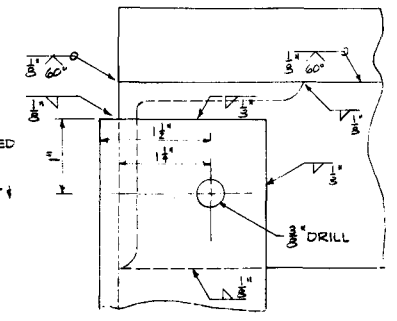

DETAIL "A"
SCALE : FULL

SCALE: 1/4" UNLESS OTHERWISE NOTED
TOLERANCES: ±1/64 UNLESS OTHERWISE NOTED

UNIVERSITY of TENNESSEE KNOXVILLE, TENNESSEE		
VISCO SEAL TEST STAND		
DRAWN BY: C.F. BOWMAN	DATE: 9/29/64	DWG.
CHECKED BY: W.K. STAIR	DATE: 9-11-64	M-VS-1A

Figure 27. Test stand.

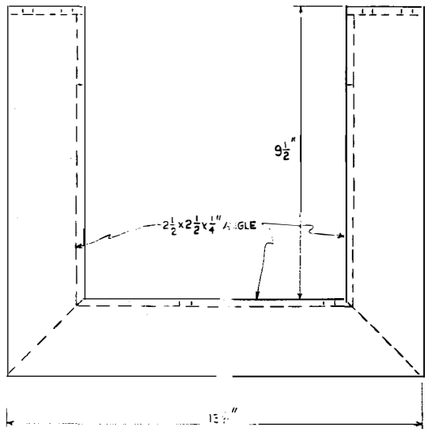

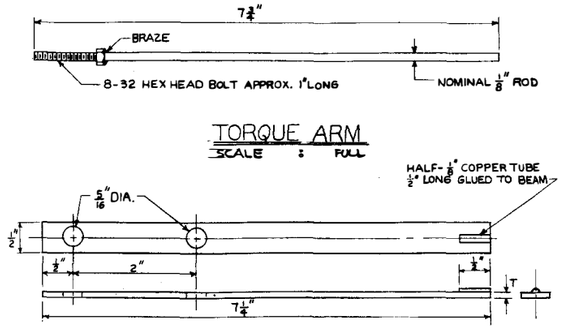

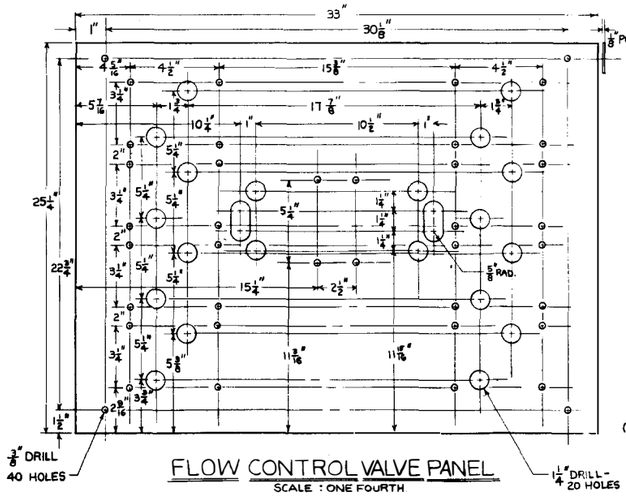

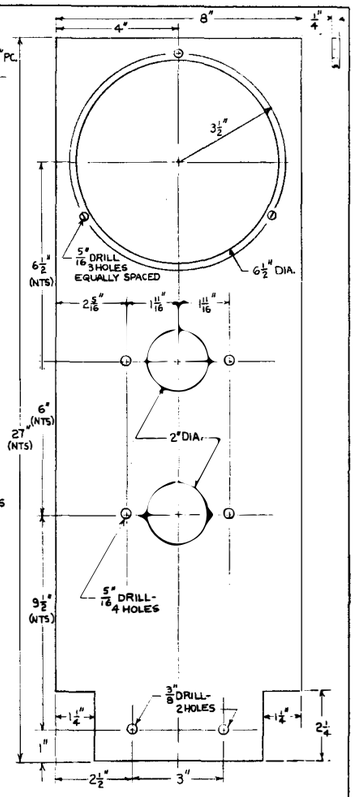

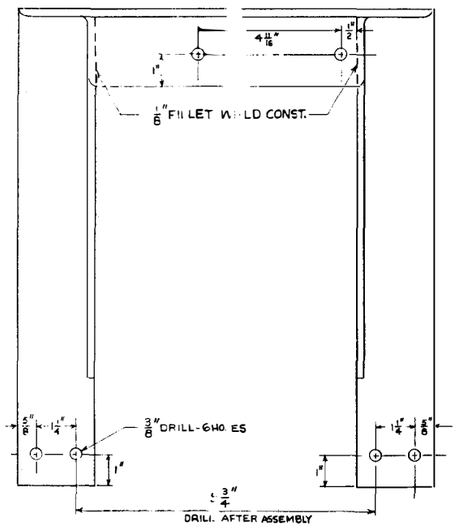

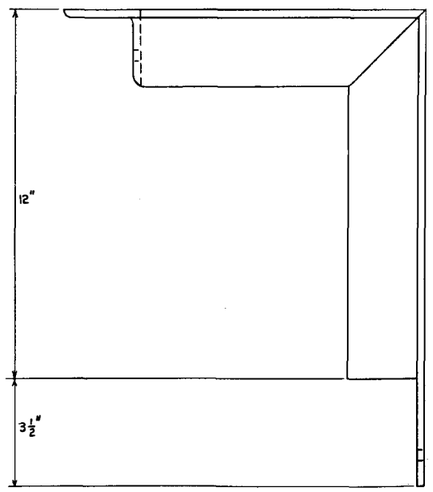

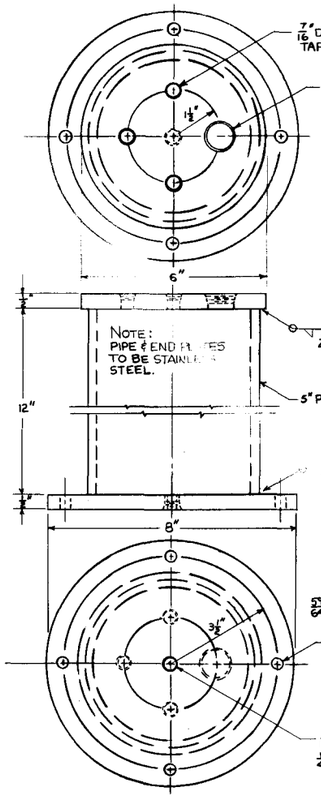

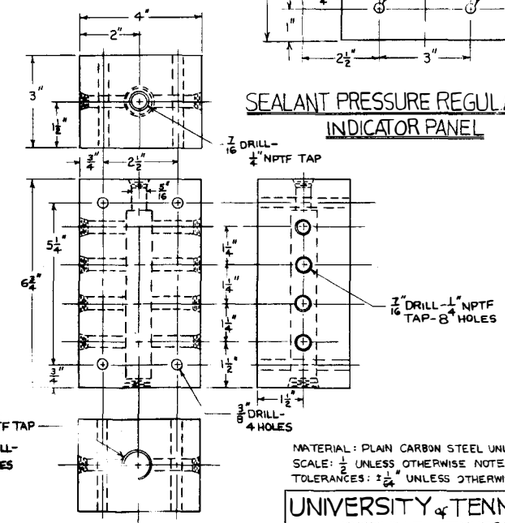

PRESSURE TAP & SEALANT SUPPLY TUBE BRACKET

MATERIAL: PLAIN CARBON STEEL UNLESS NOTED
SCALE: ½ UNLESS OTHERWISE NOTED
TOLERANCES: ± 1/64" UNLESS OTHERWISE NOTED

UNIVERSITY of TENNESSEE KNOXVILLE, TENNESSEE		
VISCO SEALS TEST STAND SUPPLEMENTARY EQUIP.		
DRAWN BY: C.F. BOWMAN	DATE: 9/11/64	DWG.
CHECKED BY: W.K. STARK	DATE: 9-17-64	Nº VF-5-A

Figure 28. Test stand supplementary equipment.

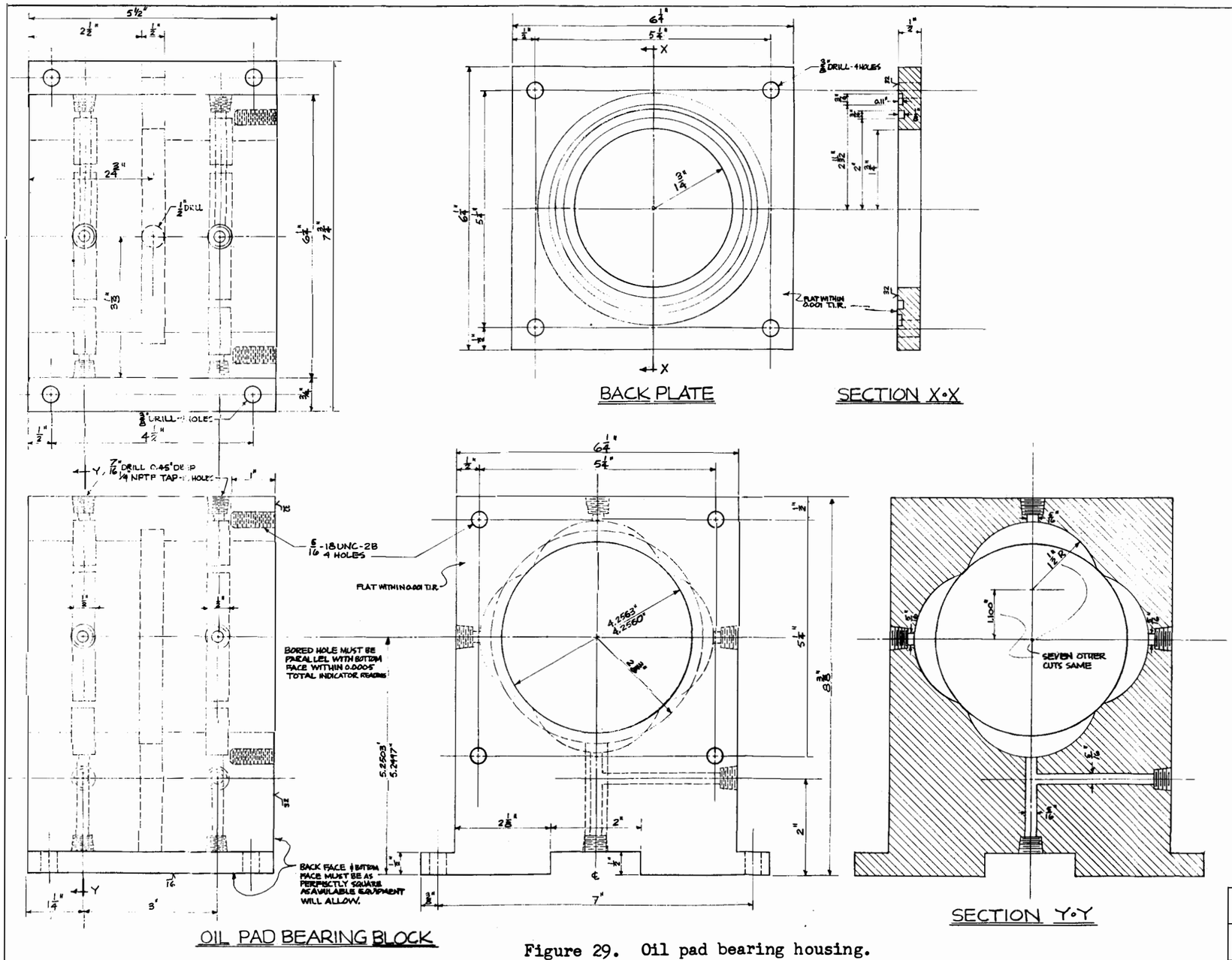

Figure 29. Oil pad bearing housing.

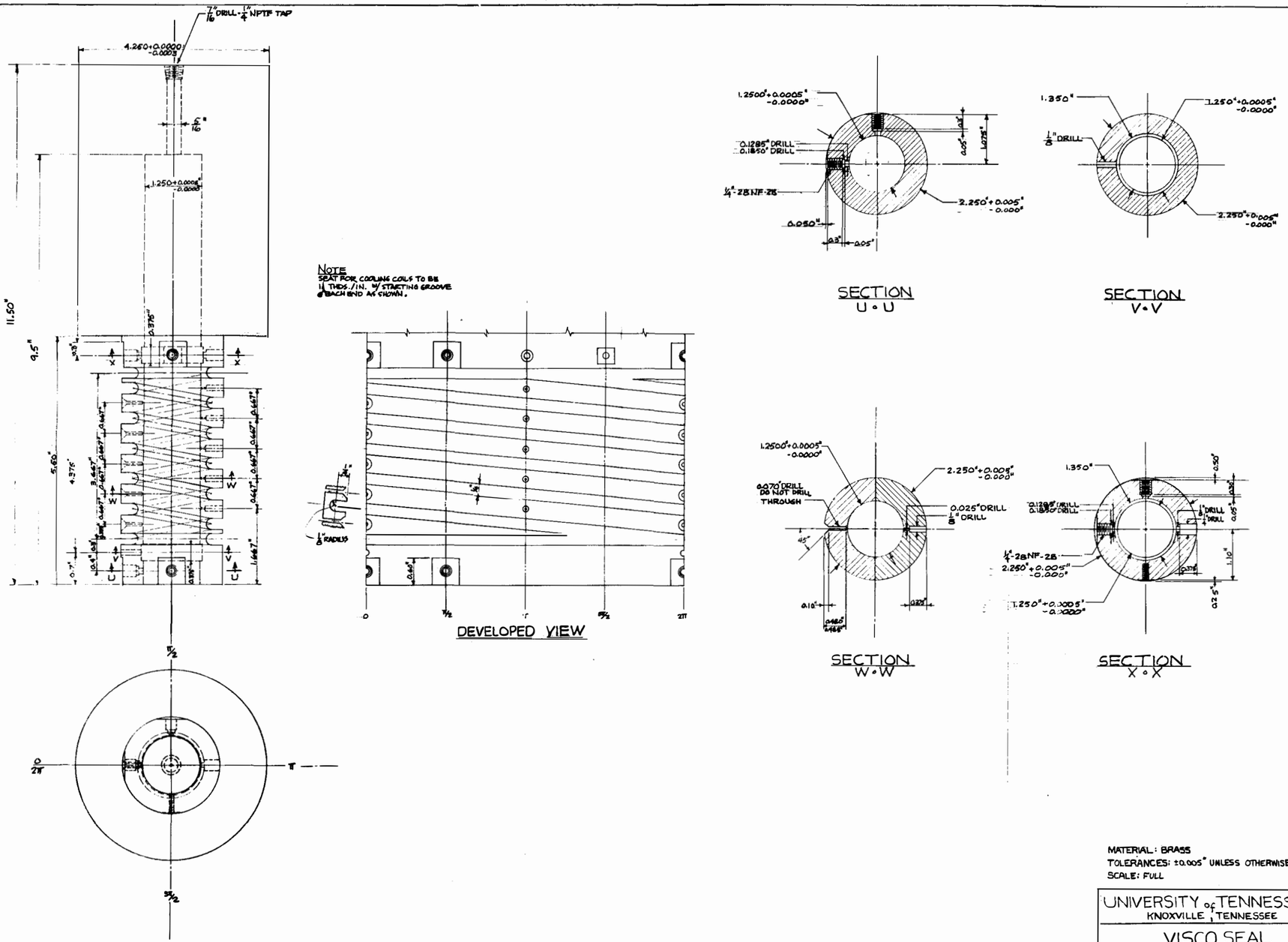

Figure 30. Test sleeve.

MATERIAL: BRASS
TOLERANCES: ±0.005" UNLESS OTHERWISE NOTED
SCALE: FULL

UNIVERSITY of TENNESSEE KNOXVILLE, TENNESSEE		
VISCO SEAL TEST SLEEVE		
DRAWN BY: C.F. BOWMAN	DATE: 8/17/64	DWG No VS-7-A
CHECKED BY: W.K. STAIR	DATE: 9-3-64	

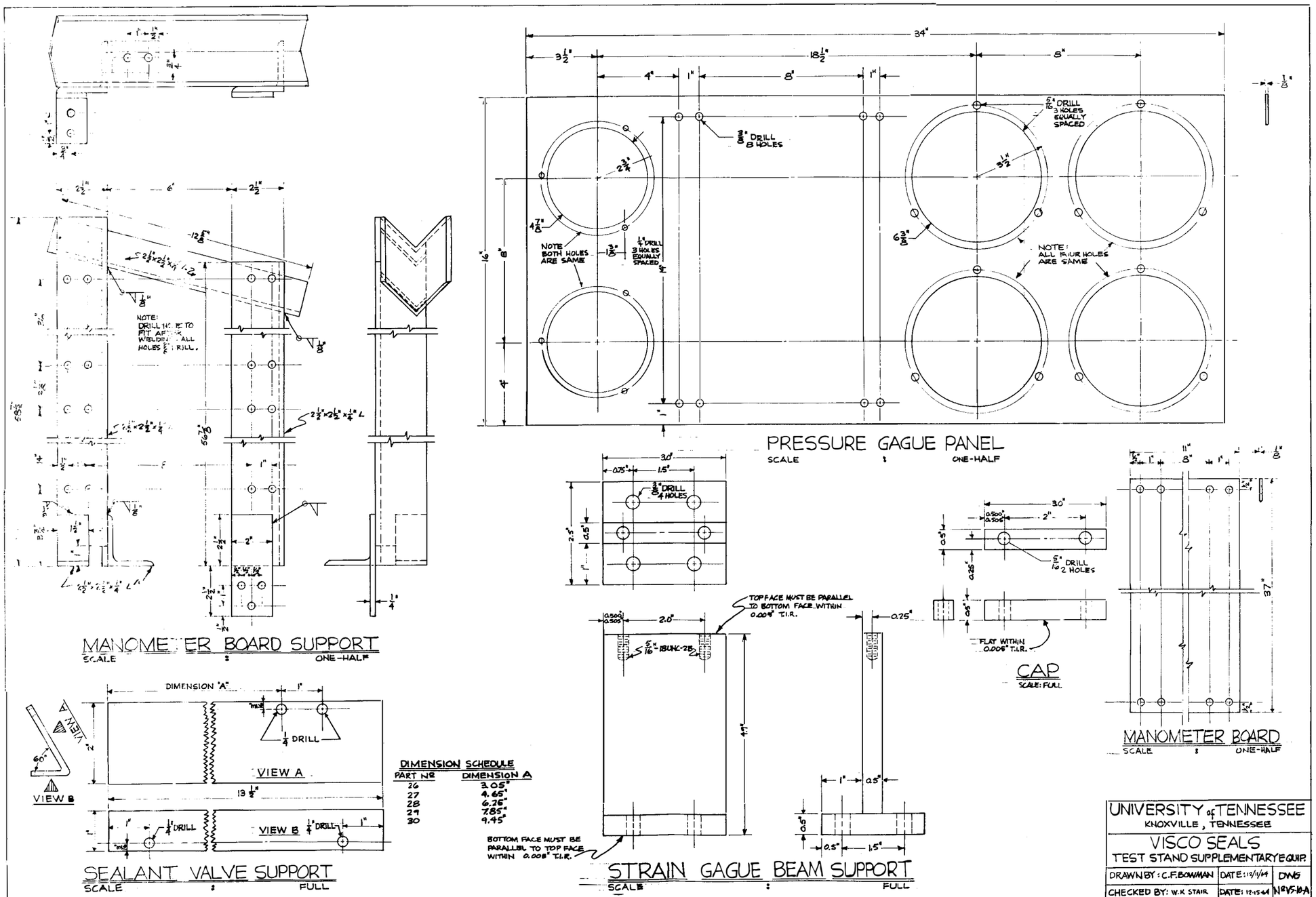

Figure 31. Test stand supplementary equipment.

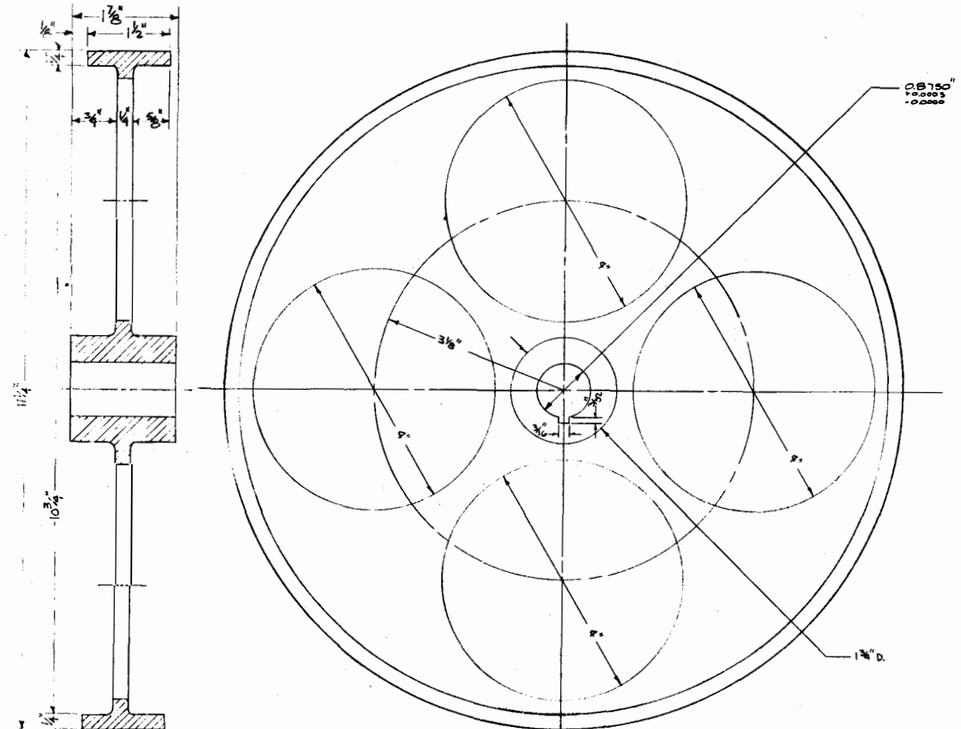

D.C. MOTOR PULLEY
SCALE : FULL

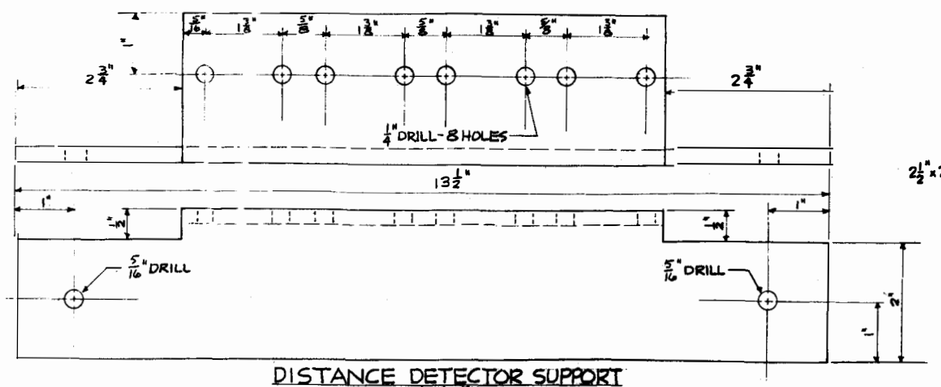

DISTANCE DETECTOR SUPPORT
SCALE : FULL

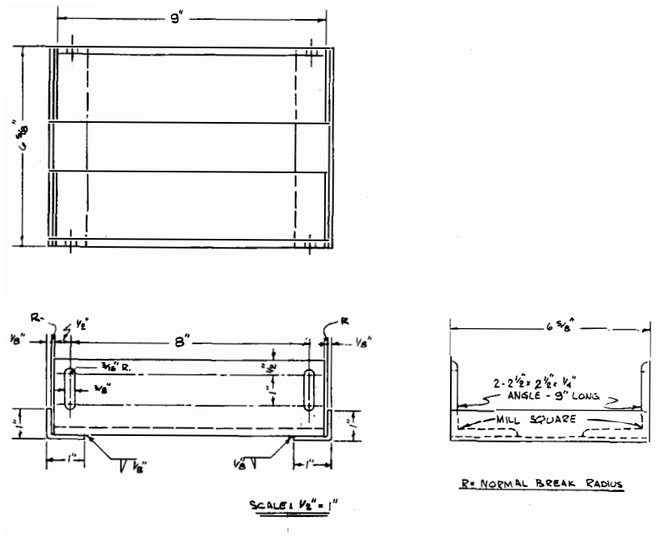

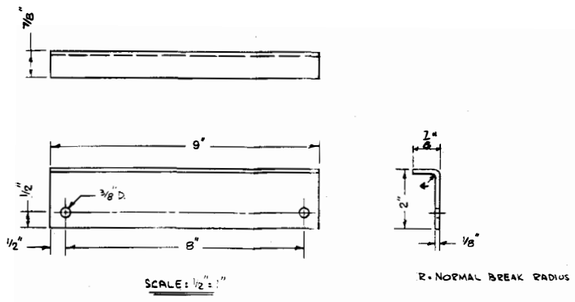

TACHOMETER EYE SUPPORT

UNIVERSITY of TENNESSEE
KNOXVILLE, TENNESSEE

VISCO SEALS
TEST STAND SUPPLEMENTARY EQUIP.

DRAWN BY: C.F. EDMAN	DATE: 12/13/64	DWG No V5114
CHECKED BY: V.K. SEAL	DATE: 12-13-64	

Figure 32. Test stand supplementary equipment.

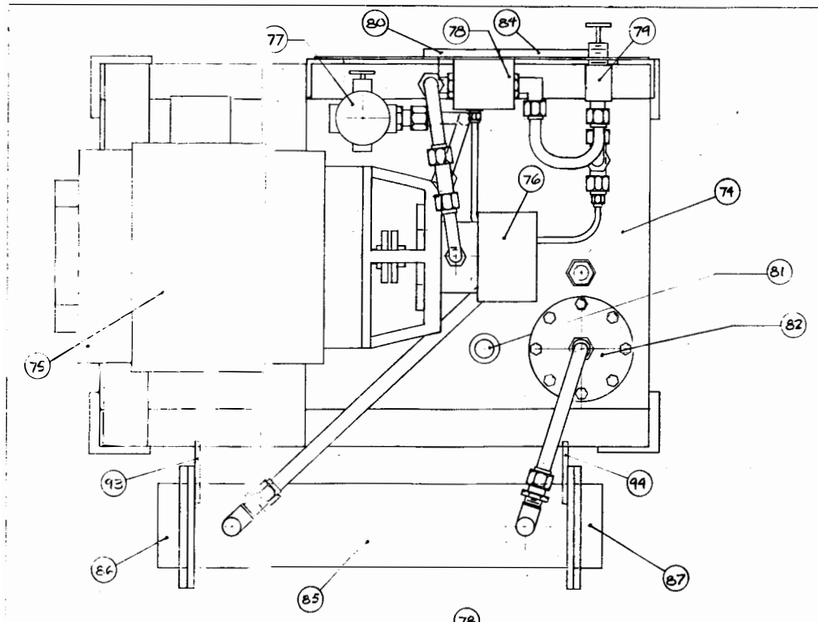

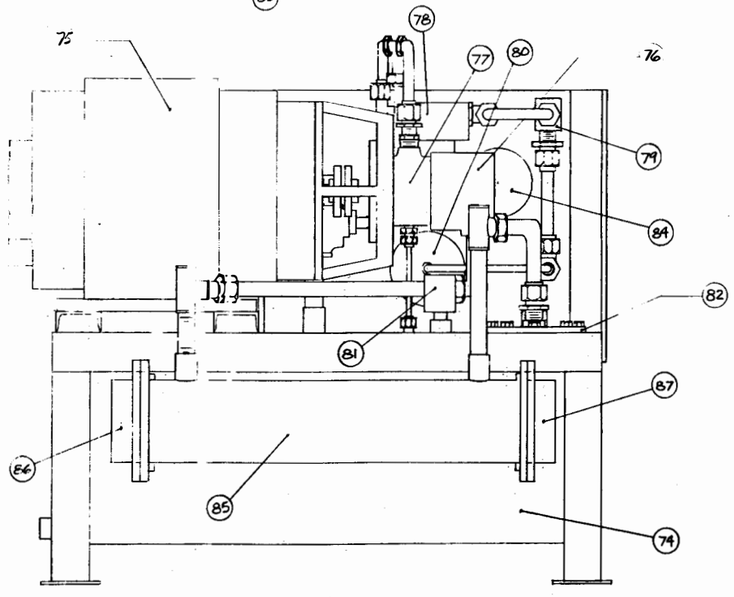

PARTS LIST

PART Nº	DESCRIPTION	DWG Nº
74	OIL STAND	VS-3-B
75	A.C. MOTOR	CAI-28
76	PUMP	CAI-29
77	RELIEF VALVE	CAI-30
78	FILTER	CAI-31
79	CONTROL VALVE	CAI-32
80	PRESSURE GAUGE	CAI-33
81	BREATHER	CAI-34
82	COVER PLATE	VS-9-B
83	PUMP MOUNTING ADAPTER	VS-9-B
84	PYROMETER	VS-2-B
85	HEAT EXCHANGER SHELL	VS-2-B
86-87	HEADER	VS-5-B
88-90	BAFFLE SHEET	VS-5-B
91-92	END TUBE SHEET	VS-5-B
93-94	HEAT EXCHANGER SUPPORT	VS-5-B

NOTE:
CAI - INDICATES COMMERCIALLY AVAILABLE ITEM. FOR MAKE AND MODEL OF ITEMS LISTED SEE TABLE IX.
FOR ASSEMBLED VIEW OF HEAT EXCHANGER SEE DWG. Nº VS-2-B

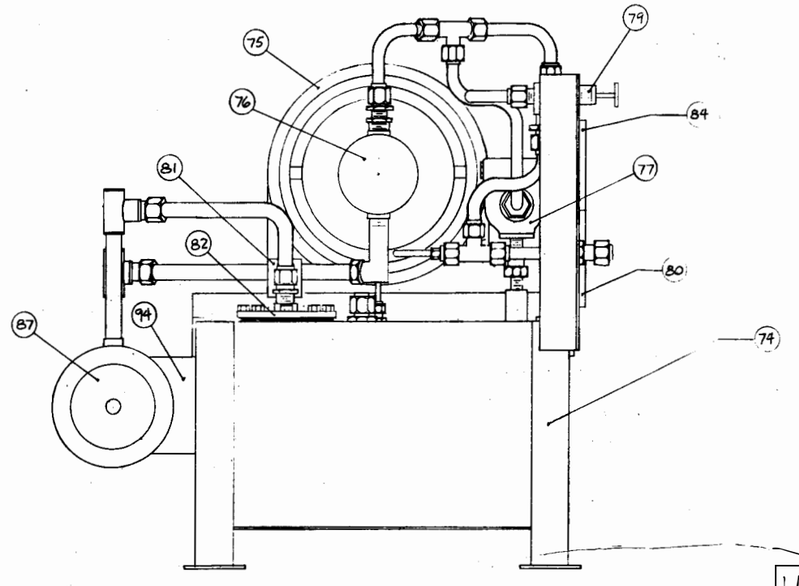

UNIVERSITY of TENNESSEE
KNOXVILLE, TENNESSEE

VISCO SEAL
OIL STAND ASSEMBLY

DRAWN BY: R.H. HALE	DATE: 5/6/64	DWG. Nº VS-1B
CHECKED BY: W.K. STAIR	DATE: 8-18-64	

Figure 33. Oil stand assembly.

NOTE
FOR PARTS LIST
SEE DWG. Nº VS-1-B

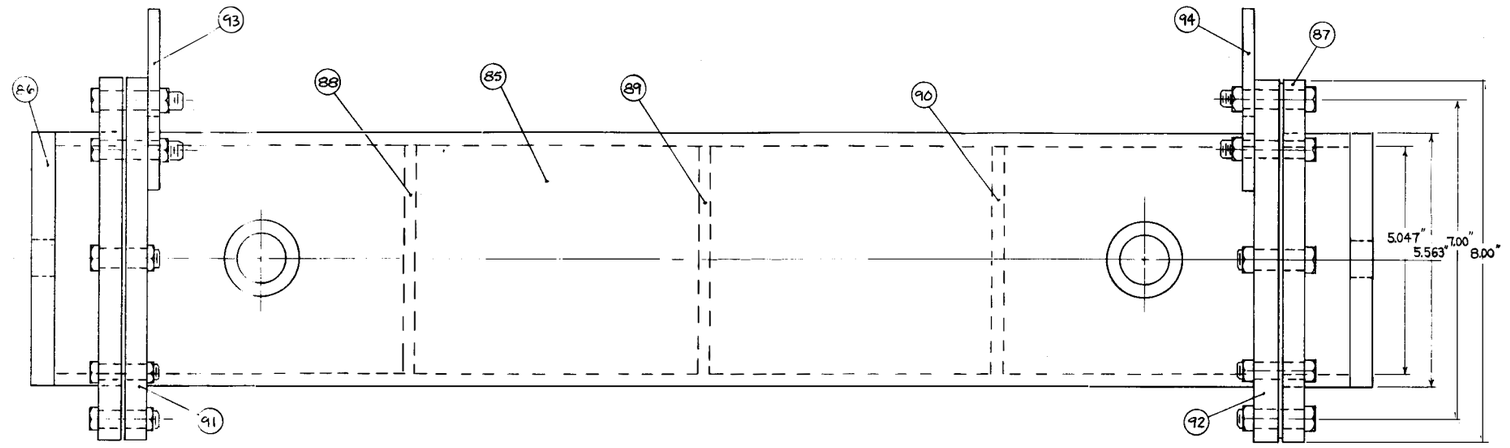

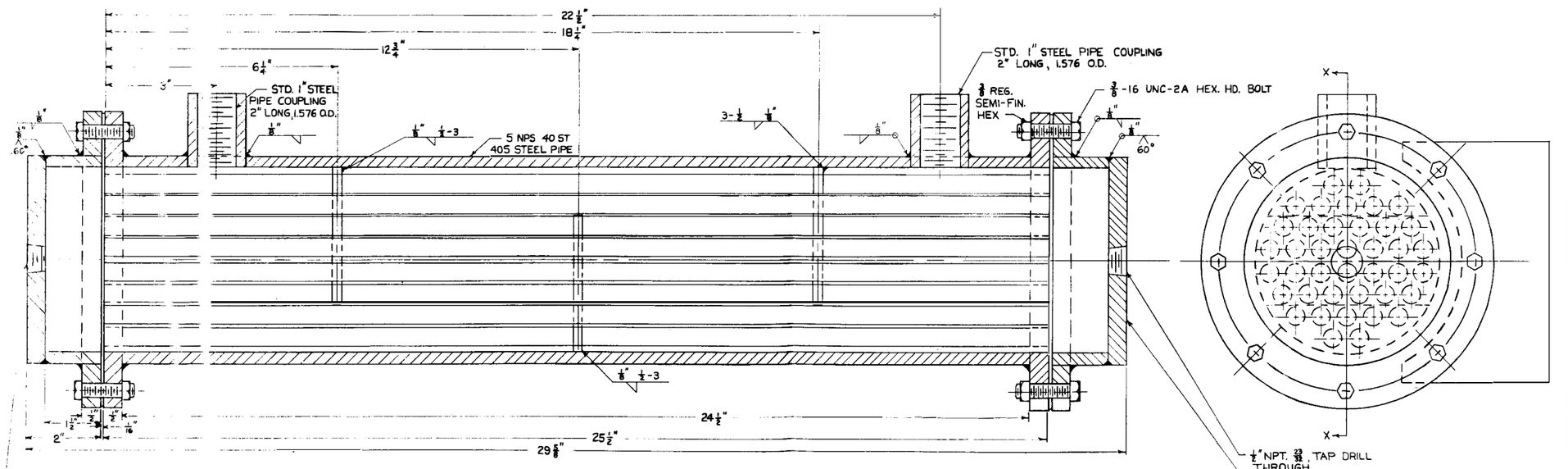

SECTION X-X

NOTE: ALL TOLERANCES ±1/64"
REQ.-10 3/8 HEX. HD. 1 1/2" LONG
6 3/8 HEX. HD. 1 3/8" LONG
MAT'L - STEEL EXCEPT WHERE NOTED
GASKETS - 1/16" RUBBER FULL FACE
8" O.D., 5" I.D.

UNIVERSITY OF TENNESSEE
KNOXVILLE, TENNESSEE

VISCO SEAL
HEAT EXCHANGER ASSEMBLY

DRAWN BY: R.H. HALE	DATE: 7/15/54	DWG. Nº VS-2-B
CHECKED BY: W.K. STAIR	DATE: 8-13-54	

Figure 34. Heat exchanger assembly.

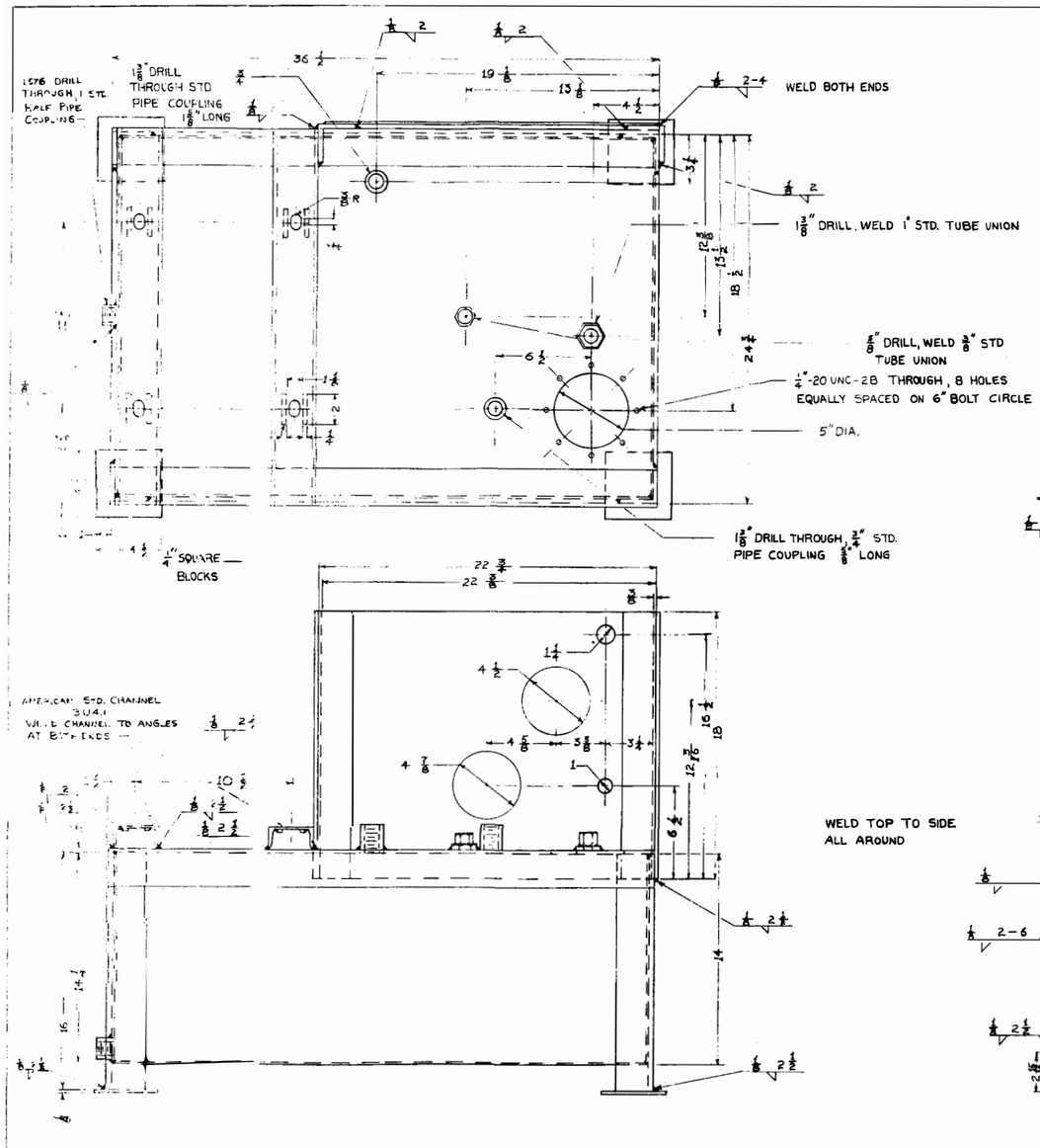

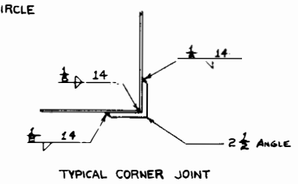

ASSEMBLY INSTRUCTIONS

1. WELD SIDES AND BOTTOM OF TANK WATER TIGHT
2. CLEAN INSIDE SURFACES OF TANK & TOP PLATE
3. OIL INSIDE SURFACES TO PREVENT RUST
4. DRILL HOLES & WELD COUPLINGS IN PLACE ON TOP PLATE
5. WELD TOP IN PLACE ALL AROUND, AIR TIGHT
6. WELD CORNER ANGLES IN PLACE
7. WELD TOP SIDE ANGLES IN PLACE
8. PUT 4, ⅝" AMERICAN STD. SQUARE HEAVY BOLT 2" LONG THROUGH UNDER SIDE OF CHANNEL
9. WELD CHANNELS AT BOTH ENDS TO TOP SIDE ANGLES
10. WELD SUPPORT ANGLES FOR BACK PANEL IN PLACE
11. DRILL HOLES IN BACK PANEL
12. WELD BACK PANEL IN PLACE

NOTE:
ALL TOLERANCES ± 1/64" UNLESS OTHERWISE NOTED
MAT'L: ⅛" STEEL SHEET - SIDES, FOOT PADS, & BOTTOM OF TANK
¼" SHEET STEEL - TOP
ALL TUBE UNIONS J.I.C. STD. 37° FLARE ANGLE

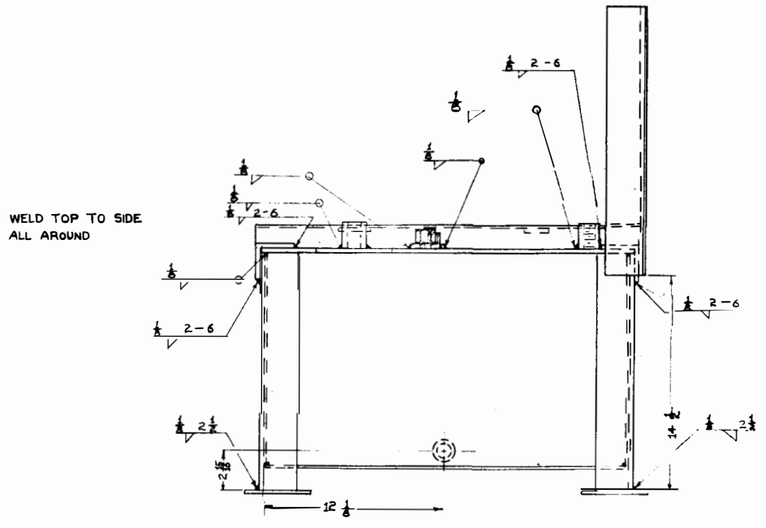

SCALE: 1" = ¼"

UNIVERSITY of TENNESSEE KNOXVILLE, TENNESSEE		
VISCO SEAL OIL STAND		
DRAWN BY: R.H. HALE	DATE: 6/27/64	DWG.
CHECKED BY: W.K. STAIR	DATE: 8/20/64	NO. 5-3B

Figure 35. Oil stand.

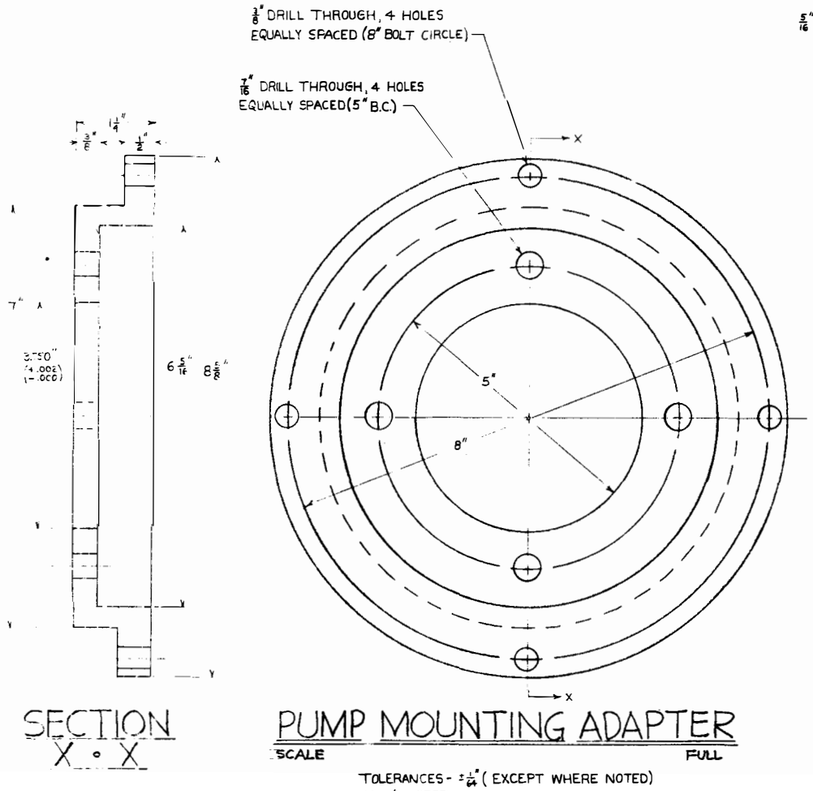

PUMP MOUNTING ADAPTER

SCALE FULL

TOLERANCES - ±1/64" (EXCEPT WHERE NOTED)
MAT'L - STEEL
ALL RIGHT ANGLES ± 30 MIN.

SECTION X - X

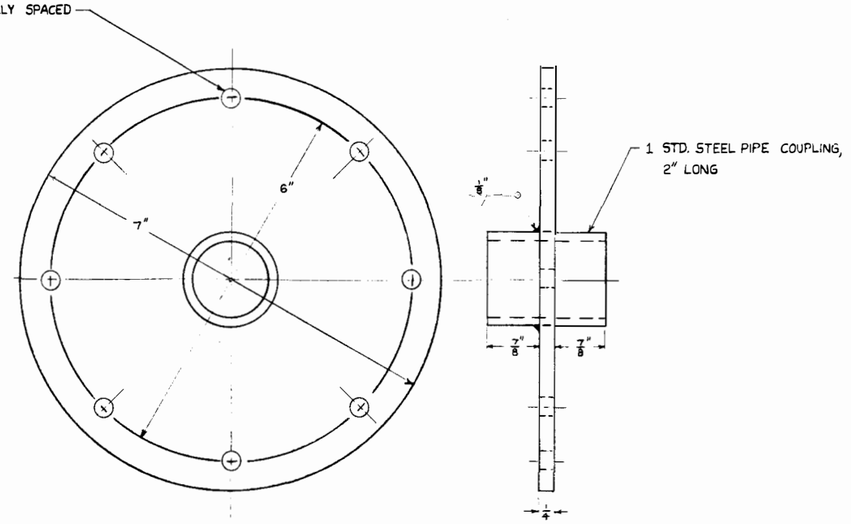

COVER PLATE

SCALE FULL

NOTE:
ALL TOLERANCES ± 1/64" EXCEPT WHERE NOTED
MATERIAL - STEEL

UNIVERSITY of TENNESSEE KNOXVILLE, TENNESSEE		
VISCO SEAL OILSTAND SUPPLEMENTARY EQUIPMENT		
DRAWN BY: R.H. HALE	DATE: 8/19/64	DWG.
CHECKED BY: W.K. STAIR	DATE: 8-20-64	N° VS-4B

Figure 36. Oil stand supplementary equipment.

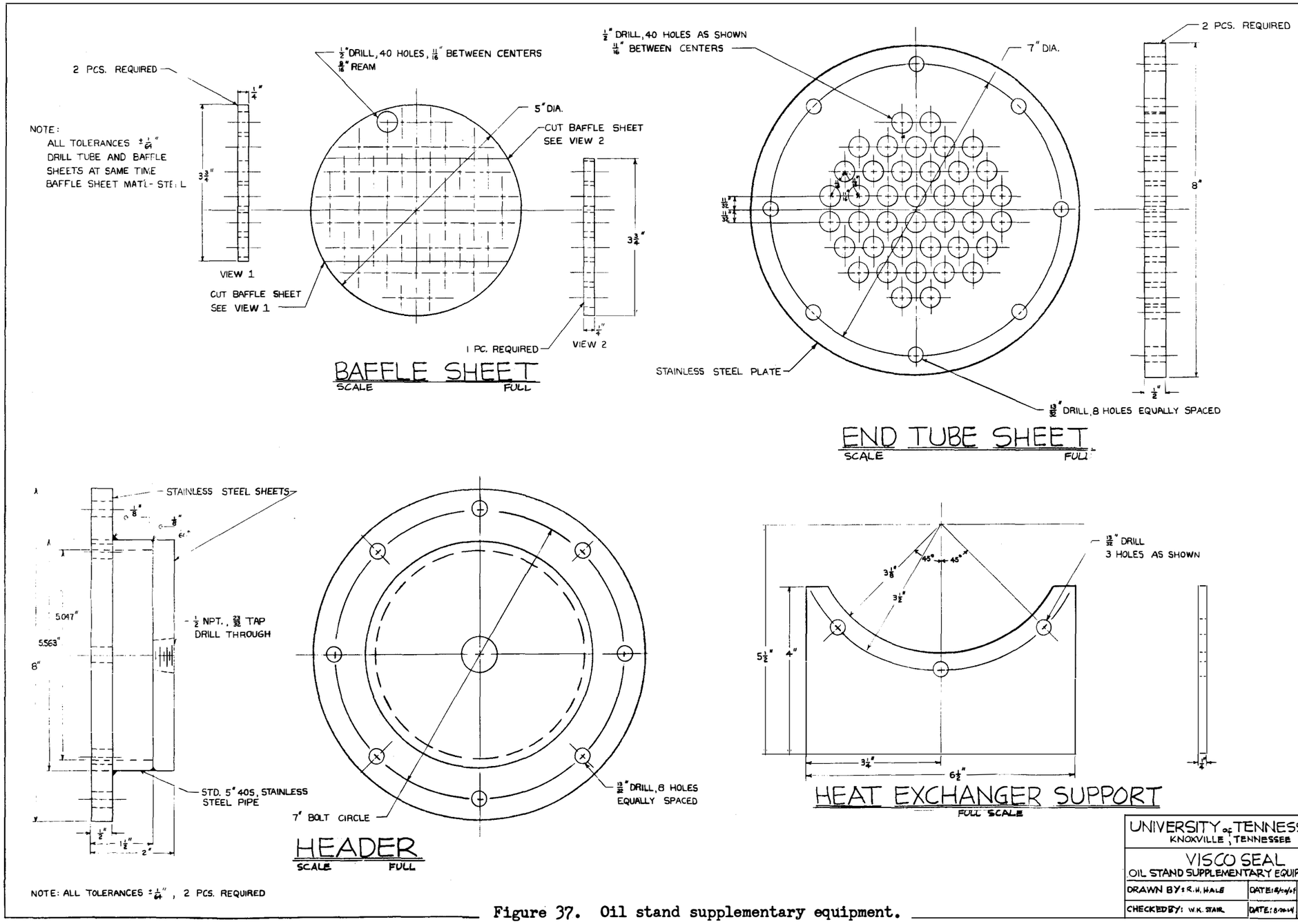

Figure 37. Oil stand supplementary equipment.

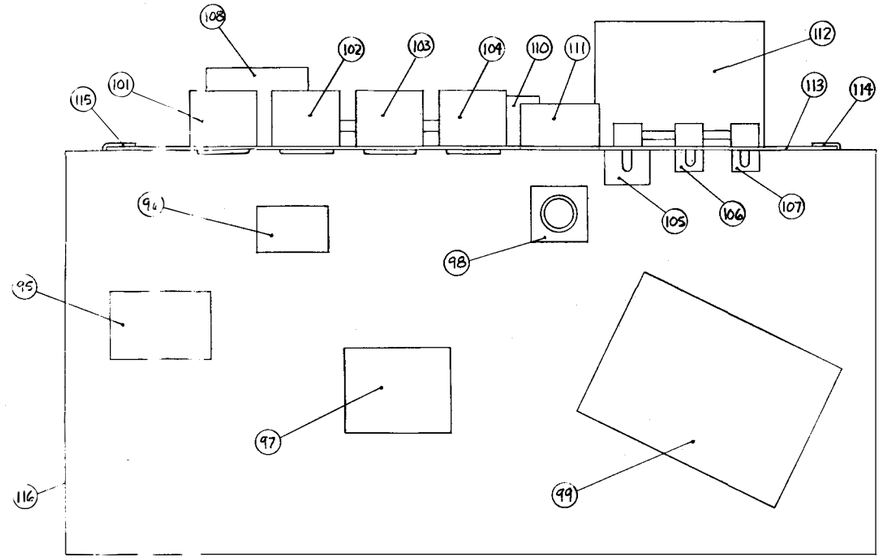

PLAN VIEW

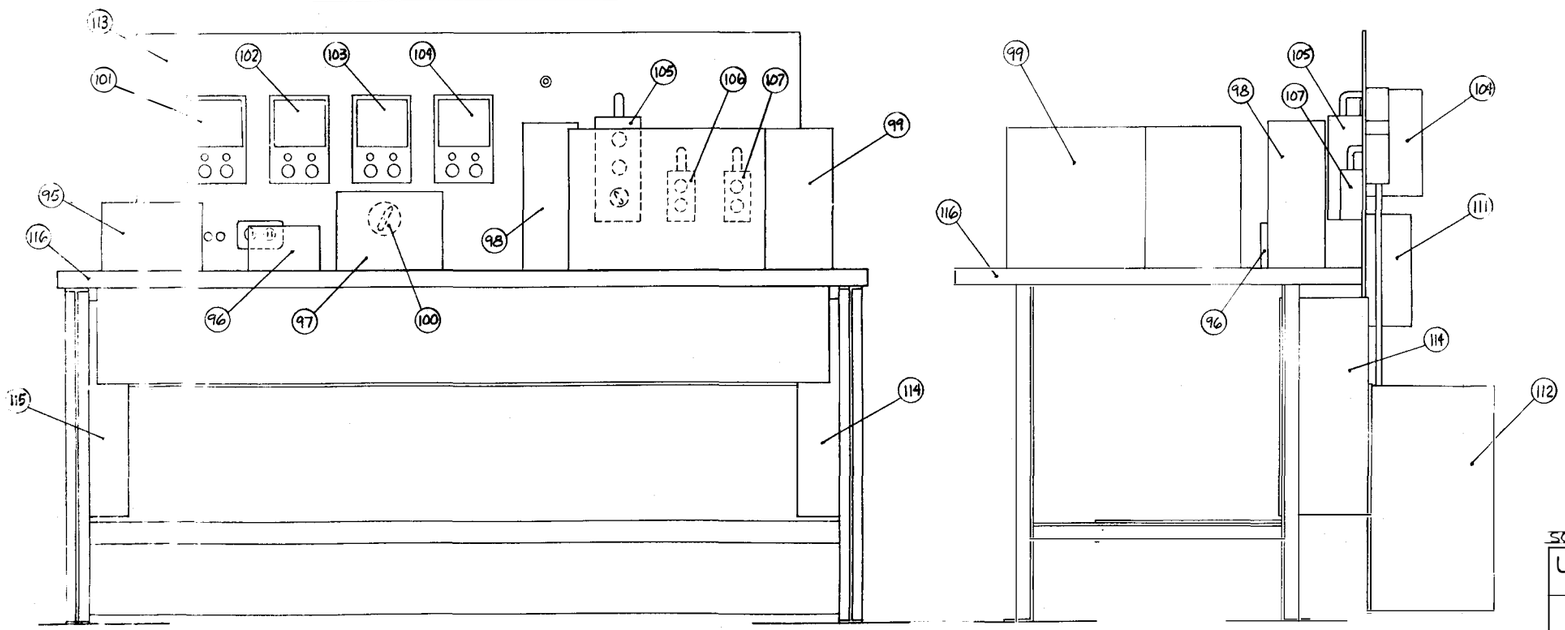

PARTS LIST

PART Nº	DESCRIPTION	DWG. Nº
95	STRAIN INDICATOR	CAI-35
96	DISTANCE DETECTOR ENERGIZER	CAI-36
97	POTENTIOMETER	CAI-37
98	ICE BATH	CAI-38
99	ELECTRONIC COUNTER	CAI-39
100	SELECTOR SWITCH	CAI-40
101-104	ELECTRONIC VOLTMETER	CAI-41
105	START-STOP SWITCH & SPEED REGULATOR	CAI-42
106	START-STOP SWITCH	CAI-43
107	START-STOP SWITCH	CAI-44

PART Nº	DESCRIPTION	DWG Nº
108	STARTER	CAI-45
109	TRANSFORMER	CAI-46
110	TRANSFORMER	CAI-47
111	STARTER	CAI-48
112	RECTIFIER	CAI-49
113	INSTRUMENTATION PANEL	VS-2-C
114	PANEL SUPPORT	VS-2-C
115	PANEL SUPPORT	VS-2-C
116	TABLE	CAI-50

NOTE:
CAI- INDICATES COMMERCIALLY AVAILABLE ITEM.
FOR MAKE AND MODEL OF ITEMS LISTED SEE TABLE V.

SCALE: THREE SIXTEENTHS

UNIVERSITY of TENNESSEE KNOXVILLE, TENNESSEE		
VISCO SEAL CONTROL STAND		
DRAWN BY: C.F. BOWMAN	DATE: 11/64	DWG. Nº 15-10
CHECKED BY: W.K. STAIR	DATE: 12-1864	

Figure 38. Control stand.

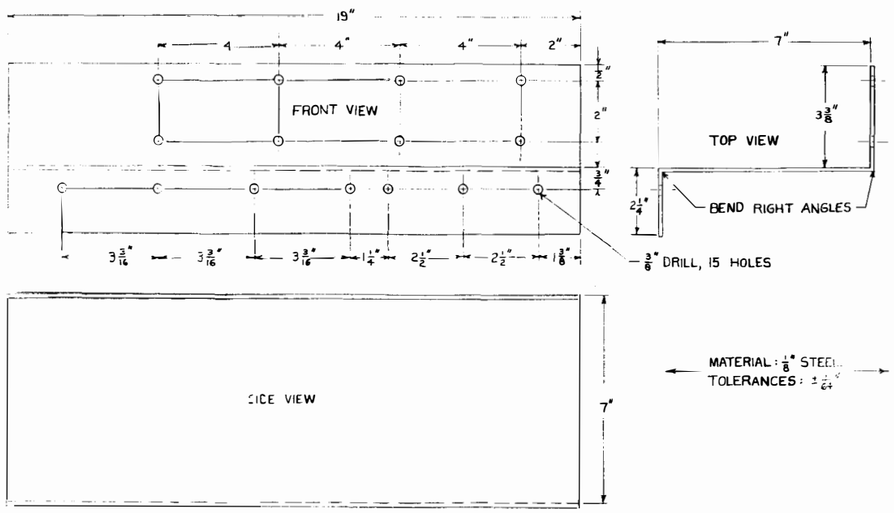

PANEL SUPPORT
SCALE HALF

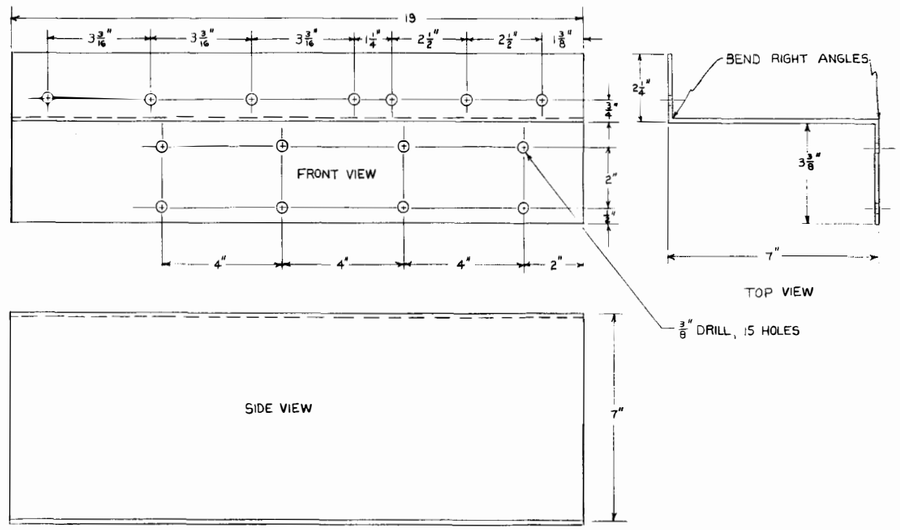

PANEL SUPPORT
SCALE HALF

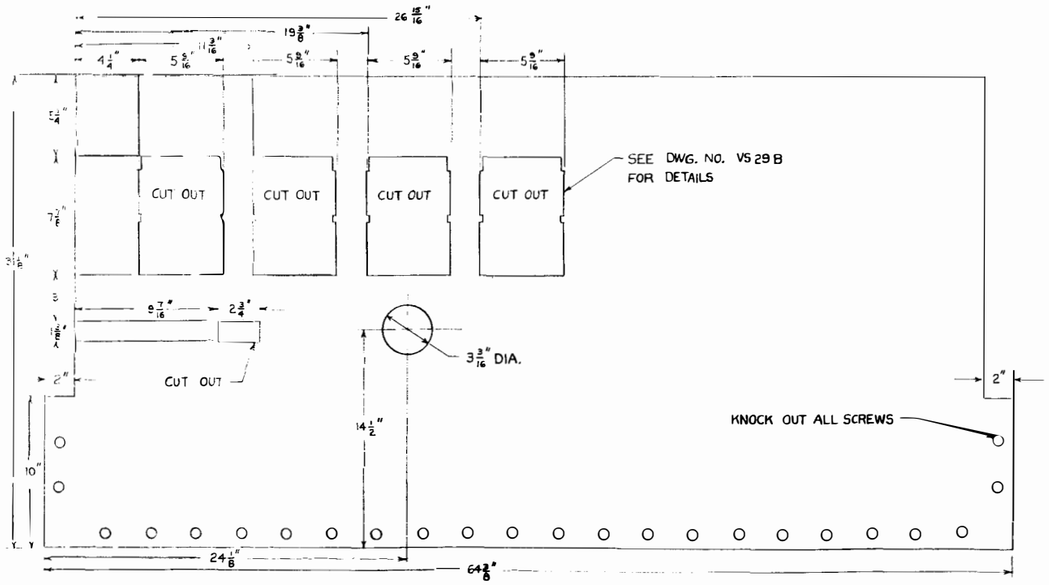

NOTE: PAINT ALL SURFACES MACHINE GRAY
ALL TOLERANCES ±1/64"

INSTRUMENTATION PANEL
SCALE ONE-FOUR

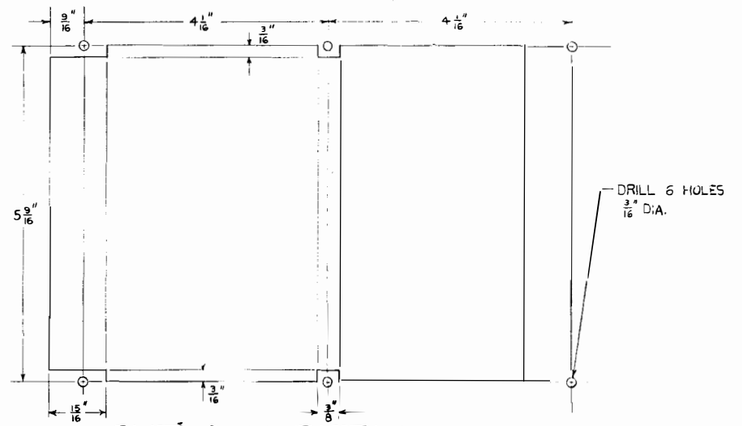

CUT OUT DETAIL
SCALE FULL

Figure 39. Control stand supplementary equipment.

UNIVERSITY of TENNESSEE KNOXVILLE, TENNESSEE	
VISCO SEAL CONTROL STAND SUPPLIMENTARY EQUIP.	
DRAWN BY: R. H. HALE	DATE: 10/1961
CHECKED BY: W. K. STAIR	DATE: 11-18-64

DWG. No. VS-2C

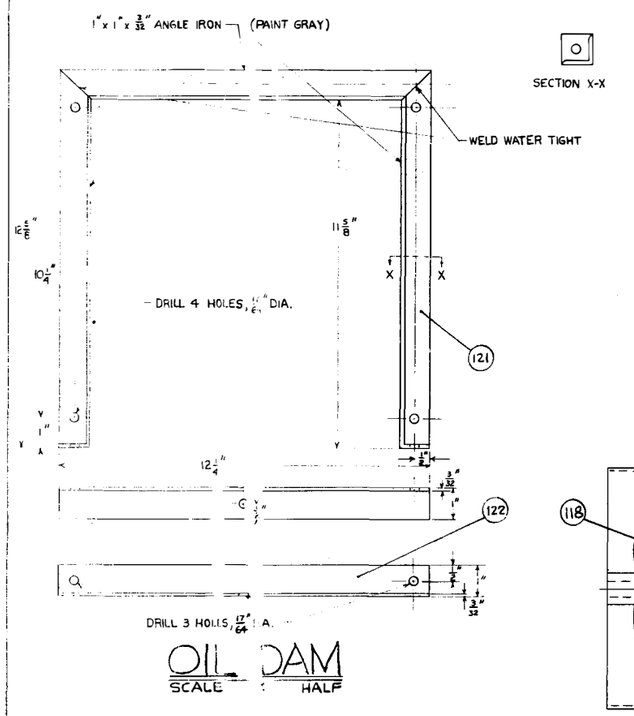

OIL DAM
SCALE : HALF

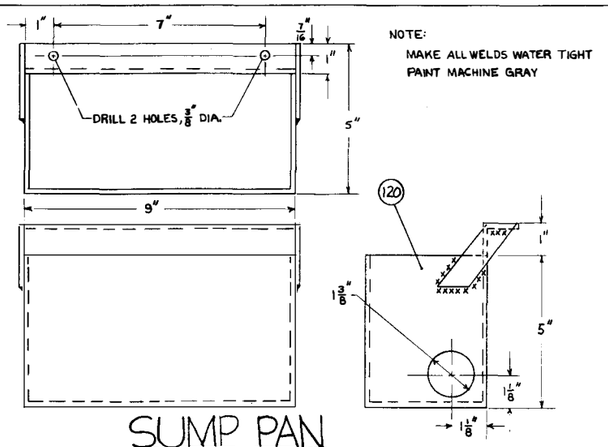

SUMP PAN
SCALE : HALF

NOTE:
MAKE ALL WELDS WATER TIGHT
PAINT MACHINE GRAY

PARTS LIST

PART Nº	DESCRIPTION	DWG. Nº
117	A.C. MOTOR	CAI-51
118	PADDLE PUMP	CAI-52
119	GATE VALVE	CAI-53
120	SUMP TANK	VS-1-R
121	OIL DAM (3 SIDES)	VS-1-R
122	OIL DAM (1 SIDE)	VS-1-R
123	UNISTRUT STAND	CAI-54
124-125	PRESSURE GAGUE	CAI-4
126	PRESSURE GAGUE	CAI-5
127-130	MANOMETER	CAI-55
131-132	MANOMETER	CAI-56
133	BRACKET	CAI-57

NOTE:
CAI-INDICATES COMMERCIALLY AVAILABLE ITEM. FOR MAKE AND MODEL OF ITEMS LISTED SEE TABLE V.

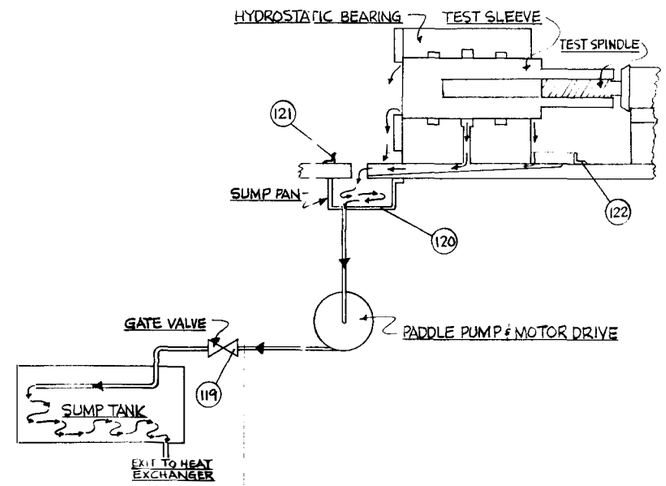

REVISED BEARING OIL RETURN LINE
NOT TO SCALE

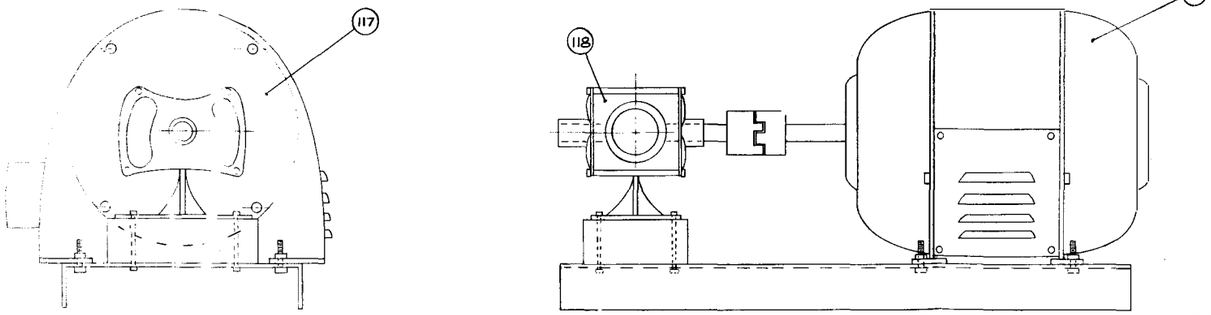

PADDLE PUMP & MOTOR DRIVE ASSEMBLY
SCALE HALF

UNIVERSITY of TENNESSEE KNOXVILLE, TENNESSEE		
VISCO SEAL HYDROSTATIC BEARING SYSTEM REVISIONS		
DRAWN BY: C.F. BOWMAN	DATE: 3/65	DWG.
CHECKED BY: W.K. STAIR	DATE: 3-1765	Nº VS-R

Figure 40. Hydrostatic bearing system revisions.

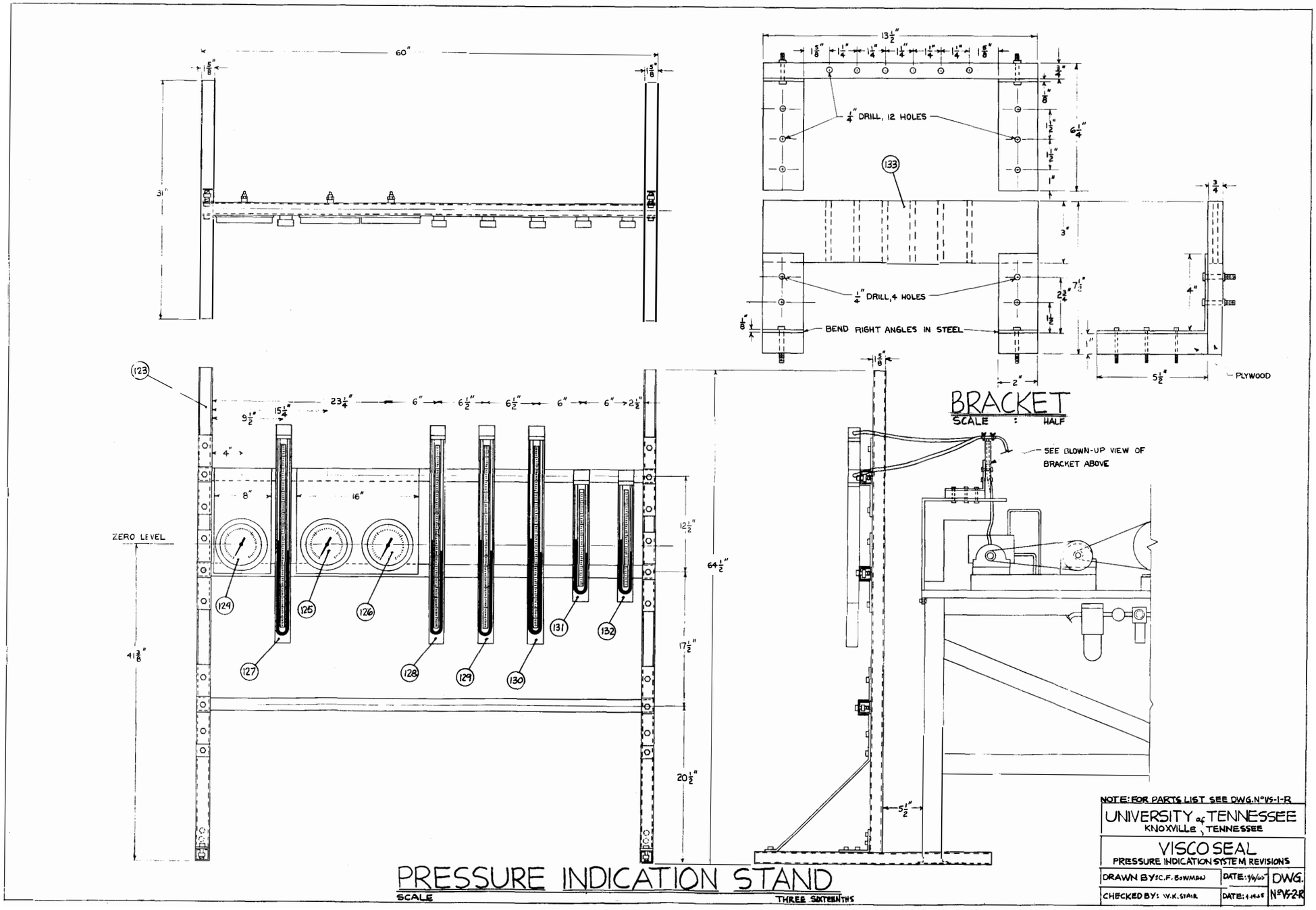

Figure 41. Pressure indication system revisions.